COMPOSITE ANALYSIS OF EL-NIÑO SOUTHERN OSCILLATION TELECONNECTIONS IN ANTARCTICA

by

Lee J. Welhouse

A THESIS SUBMITTED IN PARTIAL FULFILLMENT OF THE REQUIREMENTS FOR THE DEGREE OF

Master of Science
(Atmospheric and Oceanic Sciences)

at the

UNIVERSITY OF WISCONSIN-MADISON

2011

Abstract

Significant work has been done on identifying and understanding upper level height anomalies associated with El Niño Southern Oscillation (ENSO) throughout Antarctica. The Amundsen-Bellingshausen Sea (ABS) region is a primary region of exploration. This is still an active region of study, and while this region is of primary importance there remains the potential for other regions to show effects of these teleconnections.

This work focuses on the effect these teleconnections have on the Antarctic continent and adjacent Southern Ocean. Composites of Southern Hemisphere upper level heights, and surface variables have been created using the ERA-40, and ERA-Interim (European Centre for Medium-range Weather Forecasting Reanalysis) from the years 1979-2010. The basis for these composites consist of monthly averaged data compiled using the Oceanic Niño Index (ONI), the Multivariate ENSO Index (MEI), and the Southern Oscillation Index (SOI). To ensure the accuracy of these findings regions with sufficient ground based observations, from automatic weather stations (AWS) managed by the University of Wisconsin-Madison, are compared with the reanalysis products.

The focus of this analysis has been determining differences between the phases of ENSO events, as well as the seasonality of these differences. A secondary goal has been ensuring the accuracy of reanalysis products at high southern latitudes. Analysis has indicated the reanalysis products adequately capture surface temperature and pressure variability. There also exists a bias within the reanalysis products temperature fields. The composite analysis has indicated strong seasonal differences between austral summer, and austral spring. Further, strong differences exist in the effect of the phases of ENSO, particularly during austral summer. This indicates both new regions in need of examination, and further examination of the mechanism of these teleconnections.

Acknowledgements

First, I would like to thank the Antarctic Meteorological Research Center, Dr. Matthew Lazzara, Linda Keller, Jonathan Thom, and George Weidner, for the opportunity to work on this project, as well as the opportunity to assist in the installation of Automatic Weather Stations in Antarctica. I would particularly like to thank Matthew and Linda for their patience with my constant questions and assisting me in constantly improving this study. I would like to thank George and Linda for laying much of the ground work for this project, and for helping me to understand the underlying mechanisms in Antarctic climate. I would also like to thank Jonathan and Matthew for putting up with me while on the ice.

I also would like to thank Dr. Gregory Tripoli for assisting me in focusing this topic. Throughout this work Greg forced me to always be prepared to defend my statements and to be as clear as possible. I would also like to thank my readers Dr. Dan Vimont, and Dr. Matthew Hitchman, for their comments and critiques as they improved this document greatly. Dan's assistance with the statistical techniques used throughout this document was invaluable. Dr.

Michael Morgan also deserves thanks, as without his recommendation I likely would not have had the opportunity to attend UW-Madison.

Finally, I would like to thank my friends and family. My thanks go to Patrick O'Connell, Erin Reilly, Melissa Budde, Ben Dittmann, and Kelsey Roy, because I wouldn't have been able to make it through the more stressful aspects of this process without good friends to rely on. To my parents, and my brother and sister thanks for putting up with my incessant ramblings about statistics and climate.

Table of Contents

1. Introduction:

Antarctica is among the harshest climates on the planet. The extreme cold, high wind speed, and months of darkness make comprehensive manned station observations all but impossible. This difficulty in obtaining data provides a unique challenge in determining how Antarctica interacts with various major climate events. Despite the difficulty, research into Antarctic climate has provided a unique view of both how events around the world affect this largely untouched continent, and how Antarctica affects the rest of the world. Considerable effort has gone into determining links between major climate events, such as the El Niño Southern Oscillation (ENSO), the Southern Annular Mode (SAM), and this continent. This analysis expands, and improves upon previous methods used in analyzing ENSO events and their effect on Antarctica.

This project involves a number of separate sections, each necessary for the conclusions drawn. The project began by applying various statistical analyses to automatic weather station (AWS) data throughout Antarctica to determine the effects of ENSO on the Antarctic surface. It was determined that this method lacked the resolution necessary to show large scale effects

adequately so the reanalysis data was incorporated to determine large scale features. This reanalysis data was validated against AWS data in point comparisons during times when the AWS data was assimilated, and during periods when it was not assimilated. Throughout the remainder of this document periods when AWS data was assimilated are referred to as periods of usage, while periods when AWS data was not assimilated are referred to as periods of non-usage. The large scale analysis was performed in a manner to differentiate the phases of ENSO, and their effects.

This research has been broken up into various chapters, each representing a step along the path to the conclusions reached. Chapter 1 introduced the research and indicates some of the unique challenges in working on this topic and how they were met. Chapter 2 provides definitions and a literature review for various terms used ENSO; SAM; teleconnection. Chapter 3 provides information regarding the various data sets used, and how they were validated, how this data was utilized to form composites, how these composites differ from prior attempts within the literature. Chapter 4 will provide a discussion of the validation analysis and composite analysis. Chapter 5 will provide conclusions as well as potential future work.

2. Background Literature:

The mechanism of atmospheric ENSO teleconnections is the focus of this section, for a more complete review of interactions between ENSO and Antarctica see Turner (2004). Understanding of ENSO, and its effects, has changed substantially since it was initially viewed as warm water off the Pacific coast of equatorial South America. ENSO is now understood to be among the dominant cycles of both the atmosphere and ocean on decadal and sub-decadal time scales, with effects found throughout the globe, rather than simply in the Pacific where it has its origin (Diaz and Markgraf, 1992; Trenberth, 1975; 1976; Mo and White, 1985). ENSO has been described as a coupled system linking an oceanic segment and an atmospheric segment, El Niño and the Southern Oscillation respectively (Philander and Rasmusson, 1985). The oceanic segment has been defined as significant anomalies in sea surface temperatures throughout the equatorial Pacific, stretching from approximately 80 degrees west to 180 degrees. The Southern Oscillation has been defined as the surface pressure variations between the equatorial Western and Eastern Pacific, which is generally measured by the Southern Oscillation Index (SOI) which will be specifically

defined in the following section. As El Niño (La Niña) is defined as anomalously warm (cool) conditions in the central and eastern, tropical Pacific, care must be taken when discussing the oceanic segment of ENSO to avoid confusion. Throughout this section when considering the oceanic component of ENSO, it will be referred to as the oceanic component. When discussing either warm or cold events of the full ENSO pattern they will be referred to as El Niño or La Niña, respectively. The definition of El Niño (La Niña) used predominantly in the literature is that of greater (less) than 0.4 (-0.4) degrees Celsius variation of sea surface temperatures for 6 months or longer within the Niño 3.4 region (150-90 degrees W and 5 degrees north to 5 degrees south). This definition indicates that El Niños occur 31% of the time, La Niñas occur 23% of the time, while neutral events account for 56% of the time (Trenberth 1997). A similar definition is used in subsequent sections as the basis for the Oceanic Niño Index (ONI) as this index is based upon the Niño 3.4 region sea surface temperatures.

Considerable work has gone into determining mechanisms for transmission of a signal to explain the teleconnections found throughout the Southern Hemisphere. Hoskins and Karoly (1981) found that an area of deep convection near the equator can act to create Rossby waves, which then

propagate to high latitudes. It was then indicated that these Rossby waves can have a further effect on mid and high latitude storm tracks in turn allowing larger effects at high latitudes from smaller changes in tropical sea surface temperatures (Held 1989). Such wave trains are known as the Pacific North America (PNA) pattern in the Northern Hemisphere, and the Pacific South America (PSA) pattern in the Southern Hemisphere (Karoly, 1989). Though there was initially less evidence to support this designation, further investigation into the PSA pattern has indicated it has effects throughout the Southern Hemisphere. (Harangozo, 2000; Mo and Higgins, 1998) While much of the literature focuses on the Amundsen Bellingshausen Sea (ABS) region and much of West Antarctica, there is a distinct signal throughout East Antarctica (Houseago-Stokes, 2000). More recently mechanisms for variability in ENSO signals have been explored. Of particular interest for this study are investigations into the timing, and extent of teleconnection patterns. Recent work suggests the Southern Hemisphere response leads ENSO by approximately one season (Jin, 2009).

The Southern Annular Mode (SAM) has also been referred to as the Antarctic Oscillation (AO), and is generally considered the difference in the zonally averaged mean sea level pressure at 40 and 65 degrees South (Gong,

1999; Thompson, 2000). The SAM has been found to interact with the propagation of the Rossby wave train to higher latitudes (Fogt, 2006). More specifically, SAM was found to constructively (destructively) interfere when in (out) of phase with ENSO events. Positive (negative) SAM index indicates an in phase occurrence with La Niña (El Niño). It has also been determined that there are significant trends in recent decades toward a positive phase of SAM, particularly during austral summer months, December through February. Austral spring months, September through November, showed no significant trends (Marshall, 2003). This indicates an increasing austral summer teleconnection during La Niña, and a decreasing one during El Niño. The teleconnection during austral spring months should remain relatively similar during both El Niño and La Niña.

3. Data and Methods:

The data sets used throughout this project are categorized and explained here. The methods used to determine the reanalysis accuracy with respect to the AWS observation network are discussed. The European Center for Medium Range Weather Forecasting (ECMWF) Reanalysis 40 (ERA-40) and the ECMWF Reanalysis Interim (ERA-Interim) have been evaluated during periods of both AWS assimilation and non-assimilation to determine how the reanalysis performs (Kallberg, 2004). The AWS network was selected as it provides surface observations in otherwise remote locations, and the ECMWF reanalysis products were chosen as they are considered relatively accurate, as well as easily obtained. The ECMWF ERA-40 and ERA-Interim data used in this study have been obtained from the ECMWF Data Server.

3.1 ERA-40

The ERA-40 is a reanalysis product consisting of 2.5x2.5 degree resolution. The focus of this analysis, for comparison with AWS

observation, is placed entirely on surface based observation. The 2 meter temperatures and the surface pressure are used for this comparison. As this resolution is not well suited to point comparisons with observational data, we have used the four nearest points to interpolate to the points of observations in the AWS network. This interpolation is done with simple weighted averaging based on latitude and longitude. This does not account for changes in elevation, though this seems to have no detrimental effect. Through this interpolation we are able to achieve some expectation of the model value at the location of AWS observations. Recent research has shown that surface winds within the model show significant biases and inaccuracies when compared with observational data from manned stations (Lejiang, 2010). As such, composites and further analysis of winds has not been performed. For this study the period of 1979-2002 was used, as this extends throughout the period of accurate global satellite coverage, which marks the period of reanalysis data lacking large, anomalous trends. The ERA-40 is generally considered among the most reliable data sets for long term atmospheric variables in high Southern latitudes throughout this time period (Bromwich, 2004). For this analysis we have used the monthly average of daily averages. These daily averages are computed from a 6 hour

model run performed at 00Z, 06Z, 12Z, and 18Z. These values were used to determine how direct observations had an affect on the accuracy of the model on monthly time scales.

3.2 ERA-Interim

The ERA-Interim has yet to be fully validated at high southern latitudes, but is considered in this analysis as an extension of the ERA-40. The ERA-Interim has an increased resolution of 1.5X1.5 degrees, which remains relatively coarse, but may account for improved performance seen. It also extends the time of analysis to the period 1989-2010, allowing an extended overlap to compare with the ERA-40 as well as a period extending well beyond to compare how their differing assimilation schemes affect accuracy. While formal documentation has not been released as to the assimilation of observations in Antarctica, the ERA-Interim dataset seems to have followed a similar assimilation scheme to the ERA-40 through approximately 2000. After this point, the reanalysis moves to an assimilation scheme similar to the operational arm of ECMWF, indicating it is likely that they have similar periods of time where AWS data was not

used, but after 2003 it seems likely that many stations have been assimilated (personal communication Paul Poli, 2010). Similar to the ERA-40 analysis, interpolation of the four nearest points has been performed to make point comparisons to a variety of AWS locations comparing two meter temperature, and surface pressure.

3.3 AWS Network

The AWS network began in 1980, and has been utilized as a resource for Antarctic meteorological studies since this point. As there are relatively few manned stations throughout the Antarctic continent, these stations were originally used as a supplement to these manned stations, and were placed in regions of ongoing study. As research increased, the coverage of this network also increased with currently approximately 120 automatic weather stations located throughout the continent, with approximately 60 being operated by the University of Wisconsin-Madison and the rest being operated by numerous other countries and groups. Antarctica is among the most hostile environments on the planet; as such, the data these sites provide must be monitored to ensure it is as accurate as possible. In the interest of

ensuring temporally accurate monthly averages, any month containing less that 50% of the expected observations has not been used. This is due to the tendency for such months to have the available observations clumped to the beginning or end of the month.

A subset of the full AWS observation network has been utilized for this analysis with stations in the Ross Ice Shelf, West Antarctica, and Wilkes Land as these are primary areas of interest for the study (Figure 1). By choosing these regions, a good categorization of accuracy throughout the major regions of the continent can be evaluated. In each region, stations have been selected, which have been in for a long enough period to make reasonable comparisons for monthly time scales (See Table 1). Throughout this process, the various reanalysis products are compared with the observational network (Figure 2) during times when the data has been assimilated, and kept, and when the data has not been assimilated.

As some of the reanalysis products discontinued using AWS station data in 1998, a period of 44 months remains available in the ERA-40 data set that we are able to compare with, and a more substantial period of time remains in the ERA-Interim. Dome C is used fully by both the ERA-40, while Dome C II goes unused. All other stations analyzed in this document

stop being used in 1998, though based on the ERA archive it is not possible to determine what specific month data is no longer assimilated from these stations. Elaine, due to on site problems with the station, is unavailable after 2002. Byrd and Gill both have records after 2002. As such, a reasonable comparison of periods of both data being assimilated, as well as periods of no data being assimilated, is available. Our choices of AWS generally vary from near manned stations to far from manned stations. This is primarily due to restrictions of the number of stations available for long enough time periods. It is uncertain whether the summer manned stations are utilized by either the ERA-40 or the ERA-Interim. Thus, the information from the Byrd summer station may play no role, and the Byrd AWS is the only source of surface data in the region. A similar conclusion can be reached for Dome C station prior to 2005 when the Concordia station became a year round site. It is also uncertain what data is utilized by the ERA-Interim, but based on the ERA-40 it seems likely that year round, manned, stations are utilized.

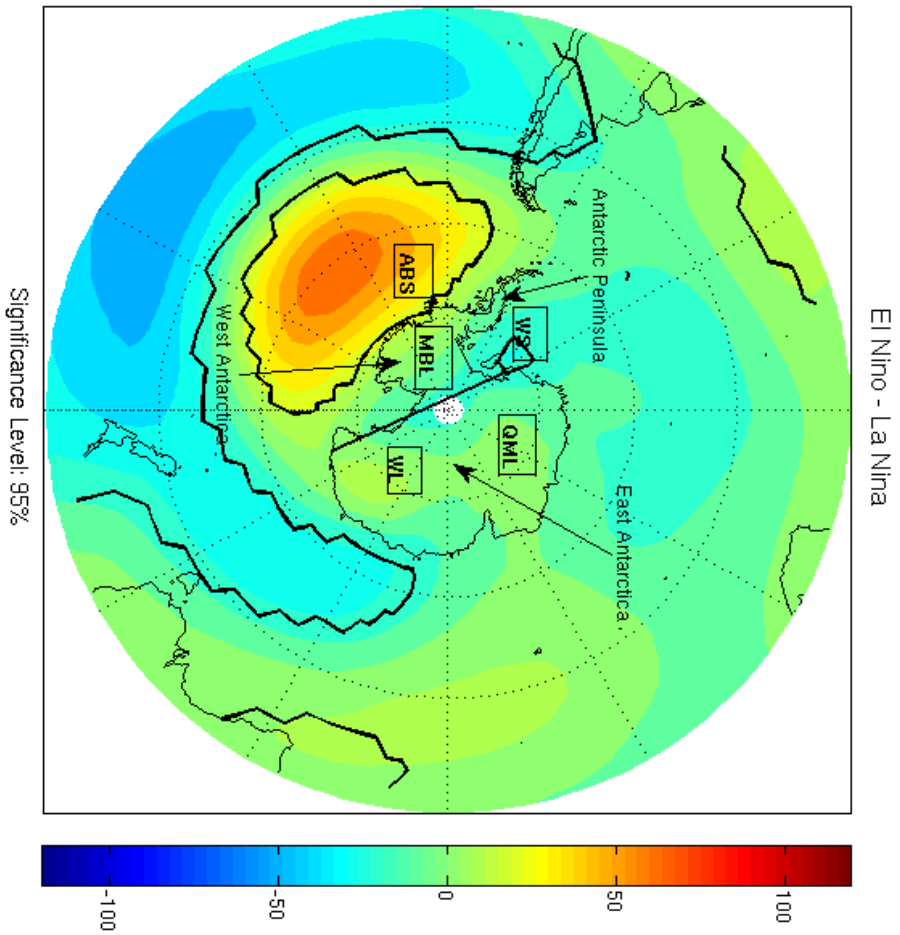

Figure 1: Year long composite of El Nino – La Nina events using MEI for 500 hPA. Black lines enclose regions of significance. The line separating West and East Antarctica is indicated, as are the Ross Ice Shelf (RIS), Marie Byrd Land (MBL), Wilkes Land (WL), Queen Maud Land (QML), ABS region, and WS region.

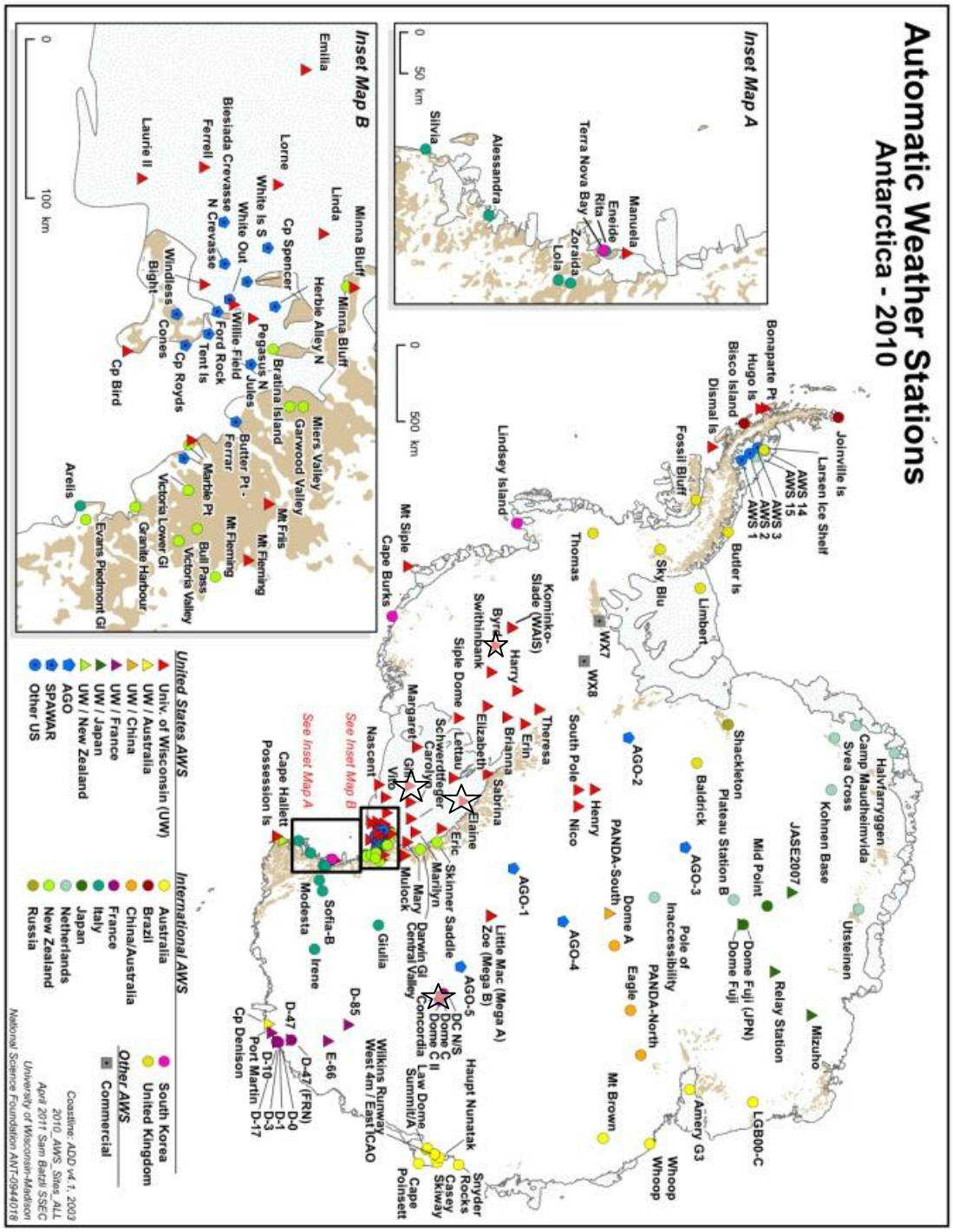

Figure 2: Recent Map of AWS stations located in Antarctica. Gill, Elaine, Byrd, and Dome C have been used in this analysis.

Station Name	**Region**	**Data Coverage**
Dome C	Wilkes Land	1980-1995
Dome C II	Wilkes Land	1995-2010
Gill	Ross Ice Shelf	1985-1988, 1992-2010
Byrd	Marie Byrd Land	1980-1988, 1991-2003 2006-2008, 2009-2010
Elaine	Ross Ice Shelf	1986-2002

Table 1: Stations data coverage, during some years only partial coverage is available

3.4 ENSO Indices

There are many separate indices available to describe ENSO events; throughout this study three have been used. These three indices are the Multivariate ENSO Index (MEI), the Southern Oscillation Index (SOI), and the Oceanic Niño Index (ONI). This has been done as in prior work to form composites of ENSO events. SOI and ONI have been used as means for determining the basis for the composites, and as this study adapts these methods, limiting the study to these indices ensures a more valid

comparison. In the interest of determining a full affect of both the atmospheric and oceanic aspects of ENSO, the MEI has been utilized as equatorial Pacific variables of both the atmosphere and ocean go into the formation of this index (Wolter, 1998).

The ONI, obtained from the Climate Prediction Center (CPC, available at http://www.cpc.ncep.noaa.gov) consists of 3 month running mean of sea surface temperature anomalies in the Niño 3.4 region (5^{o}N-5^{o}S, 120^{o}-170^{o}W). Anomalies have been based on the 1971-2000 base period. For historical purposes, cold and warm episodes are defined when the threshold is met for a minimum of 5 consecutive over-lapping seasons. Events are listed in table 2.

The SOI consists of the difference between standardized pressure measured at Tahiti, and the standardized pressure measured at Darwin Australia. This data set was obtained from the Climate and Global Dynamics (CGD) group at the National Center for Atmospheric Research (NCAR) (available online at http://www.cgd.ucar.edu/). Anomalies are calculated from the base period of 1951 to 1980, with negative (positive) index values representing warm (cool) ENSO events (Table 3).

The MEI is computed in a much more complex manner which is

described in Wolter 1998. These values have been obtained from the Earth Systems Research Laboratory Physical Science Division (available online at http://www.esrl.noaa.gov/psd/enso/mei/). A basic description of the index is the first, unrotated principle component of sea-level pressure, zonal and meridional components of the surface wind, sea surface temperature, surface air temperature, and total cloudiness fraction of the sky over the tropical Pacific Ocean. As these values incorporate those used in the ONI and SOI, and these indices correlate relatively well, we expect similar results. Events are listed in table 4.

El Nino ONI Events	**La Nina ONI Events**
1982 SON – 1983 DJF	1984 SON – 1985 DJF
1986 SON – 1987 DJF	1988 SON – 1989 DJF
1987 SON – 1988 DJF	1995 SON – 1996 DJF
1991 SON – 1992 DJF	1998 SON – 1999 DJF
1994 SON – 1995 DJF	1999 SON – 2000DJF
1997 SON – 1998 DJF	2000 SON – 2001 DJF
2002 SON – 2003 DJF	2007 SON – 2008 DJF
2004 SON – 2005 DJF	2010 SON – 2011 DJF
2006 SON – 2007 DJF	
2009 SON – 2010 DJF	

Table 2: ONI ENSO events listed during the austral spring through austral summer. Events are 3 month seasons of greater than (less than) 0.5 degree difference for 5 months or more in the Nino 3.4 region.

El Nino SOI Events	**La Nina SOI Events**
December 1979	February 1979
September 1982 – February 1983	September, December 1981; January 1982
February 1986	September 1983, February 1984
November 1986 – February 1987	February 1985
September 1987, February 1988	January, October 1986
February 1990	September 1988 – February 1989
September 1991 – February 1992	September, October 1989
October 1992 – February 1993	January 1991
November 1993	January 1996
September, October, December 1994	September, October December 1996 – February 1997
September 1997 – February 1998	September 1998 – February 1999
December 2001	October 1999 – February 2000
December 2002, February 2003	September 2000 – February 2001
January 2004	November 2001; January, February 2002
November, December 2004; February 2005	December 2003, February 2004
October 2006, January 2007	September, October 2005; January 2006
October 2009 – February 2010	October 2007 – February 2008
	September 2008 - February 2009
	September 2010 – January 2011

Table 3: SOI ENSO events, with events defined as single month values greater than (less than) 0.5 standard deviations from 1979-2010 mean.

El Nino MEI Events	**La Nina MEI events**
September, October 1979; November 1979 – February 1980	January – February 1984
September 1982 – February 1983	November 1984 – February 1985
SO 1986, November 1986 – February 1987	September 1988 – February 1989
September 1987 – February 1988	December 1995 – February 1996
January, February 1990	January-February 1997
September 1991 – February 1992	September – November 1998; December 1998 – February 1999
September, October 1992 December 1992 – February 1993	September 1999 – February 2000
September, October 1993	December 2000 – February 2001
September 1994 – February 1995	September 2007 – February 2008
September 1997 – February 1998	September – October 2008; December 2008 – February 2009
September 2002 – February 2003	September 2010 – January 2011
September, October 2003	
January, February 2005	
September - November 2006; December 2006 - February 2007	
September 2009 – February 2010	

Table 4: MEI ENSO events, with events defined as single month values greater than (less than) 0.5 standard deviations from 1979-2010 mean.

3.5 Anomaly Creation

In the interest of isolating the differences between the reanalysis data sets and the AWS network, each data set has been converted into two data sets - the first consisting of the annual cycle, and the second consisting of

anomalies. To ensure a comparison over similar time periods, the data sets have been formatted to ensure only months, and days, where both the reanalysis and the observations are available. To separate the anomalies and the annual cycle, 3 harmonics were fitted to each data set, at the 12 month, 6 month, and 4 month time periods. Through removal of these harmonics, we are left with anomalies for each station, as the harmonics are considered the annual cycle.

In each depiction of the annual cycle we note a kernlose or “coreless” winter (Stearns and Wendler, 1988), which is described as a lack of observed minimum temperature in any specific winter month. This feature becomes more pronounced as you move from the coast. The presence of this feature is a good indicator that the annual cycle created is a relatively accurate depiction. Similar anomalies have been created in the process of creating the composites discussed in the next section. In this case, only the reanalysis data anomalies for monthly averages have been created, the annual cycle has been calculated by taking the average of each month separately. Again this produces the expected kernlose winter.

3.6 Data Validity

For this analysis, a set of representative stations were chosen, as they resided within areas of interest for the composite analysis, had long periods of uninterrupted observation, and were noted in the ERA-40 archive for both high usage percentages, and a distinct end point in usage. These stations are Byrd, Elaine, and Dome C I and II. These sites were analyzed throughout their observation period, during times when they were being assimilated and used, during times where they were not being used, and finally during the ERA-interim period when archival data has not yet been released so usage is uncertain.

3.7 Composite Methods

There are a number of steps necessary to form composites of any given phenomenon. The first step is choosing a basis for the analysis, more specifically a positive and negative basis must be chosen. In prior work on ENSO composite analysis, generally the positive basis is used to describe El Niño events, and the negative basis is used to describe La Niña events. In

this study, a different basis has been applied to the various indices. For the ONI, the basis used is the same used to determine events, or a five month period of overlapping three month seasons with an anomaly of greater than 0.4 degrees Celsius. For the MEI and SOI, a value of greater than 0.5 standard deviations from the mean is used for the basis. Initially a basis of 1 standard deviation was used, but in the interest of achieving a complete period of ENSO events in each month, it was relaxed. Different time scales are used for composites depending on the index as well. Specifically, the MEI uses two month seasons, the ONI uses three month seasons, and the SOI is used for monthly composites. This is due to how these indices are computed, and how events are determined. This study differs from prior work, by using the mean of non-event months as the negative basis. For example, in composites of December, the negative basis will consist of all December months where there was no event, in the case of ONI, or where the index was within 0.5 standard deviations of the mean, in the case of the SOI or MEI. It is expected that by including the non-events as the negative basis differences between El Niño and La Niña events can be discerned. After the basis is formed, and events chosen, these events are then averaged, and the positive and negative averaged events are subtracted from one

another. Finally, statistical significance is determined by using a two tailed student-t test, and for the cases evaluated, the confidence interval has been set at 0.95.

4. Results and Discussion:

Throughout this section, the results of the data validation and composite processes are examined in depth. As the importance of the composite analysis cannot be examined without first ensuring the accuracy of the data used, the validity will be discussed first. This is followed directly by the new composite analysis technique.

4.1 Validation Analysis

As the prior section indicated, four stations have been chosen in areas of importance for ensuring composite validity. These stations are Byrd, Elaine, Dome C, and Gill. The focus of this evaluation has been placed on AWS locations because recent analysis presented by Lejiang et al (2010) indicates for surface pressure and temperature the manned stations are relatively well represented and match quite well with the reanalysis. As this is the case, there is some concern that for these stations there is potential for contamination from the near-by manned stations as Byrd station is located near the summer station of the same name, and Dome C is located near

Concordia which was a summer station from 1992 through 2005 and then became a year round station. There is some uncertainty as to whether summer station data has been included in the reanalysis. Elaine is not located near a summer or year round station, nor is Gill Station. Both of these stations are away from manned stations and are within the Ross Ice Shelf region, which is an area of primary importance for the expected effects of ENSO events as seen in prior literature (Karoly 1989). All stations evaluated have good correlations, between .8 and .87 with little discernible difference on monthly time scales between periods of use and periods where the data was not assimilated (Table 5).

This analysis includes monthly values, as the composite analysis is on tri-monthly, bi-monthly, and monthly time scales. The method of performing the annual cycle removal contains what bias the location has. The bias is important to know from a validation standpoint, but for composite analysis so long as the bias remains consistent it will not negatively impact the findings of the composite analysis. This is due to the bias having the same effect on both the positive basis and negative basis thus being removed in the process of comparison. The important aspect for ensuring validity for the composites is the correlation between the AWS data

and the reanalysis interpolated to this point. A high correlation will confirm that the variability of the location is captured accurately, which indicates the variability associated with ENSO events will also be captured accurately.

Station Name	**ERA-40 Use**	**ERA-40 Non-Use**	**ERA-Interim**
Gill	0.9	0.95	0.95
Byrd	0.92	0.92	0.92
Dome C	0.87	Unavailable	Unavailable
Dome C II	Unavailable	0.8	0.93
Elaine	0.9	0.93	0.95

Table 5: Correlation values between locations and ERA-40. Non-use indicates periods where observations were not assimilated.

4.1.1 Byrd Station

Byrd station was installed in 1980 and has been in use through the present. It is located at 80.00S and 120.00W, which is very near a summer station of the same name which has data assimilated throughout the austral summer. Based on the analysis of the annual cycle within the ERA-40

reanalysis, we can note a slight warm bias within the reanalysis. This lines up with prior validation of the reanalysis, as most locations indicate a warm bias (Lejiang, 2010). The correlation, which is more important for ensuring accurate composites, is quite high at 0.93. It is worth noting that the correlation after 1997, when this station stopped being assimilated, seems highly dependent on seasonality which is to be expected given the presence of the field camp, though correlation still seems high enough to provide useful information. Simply from visual inspection of the reanalysis data and the AWS data it is apparent that the data sets largely agree (Figures 3.1; 3.2).

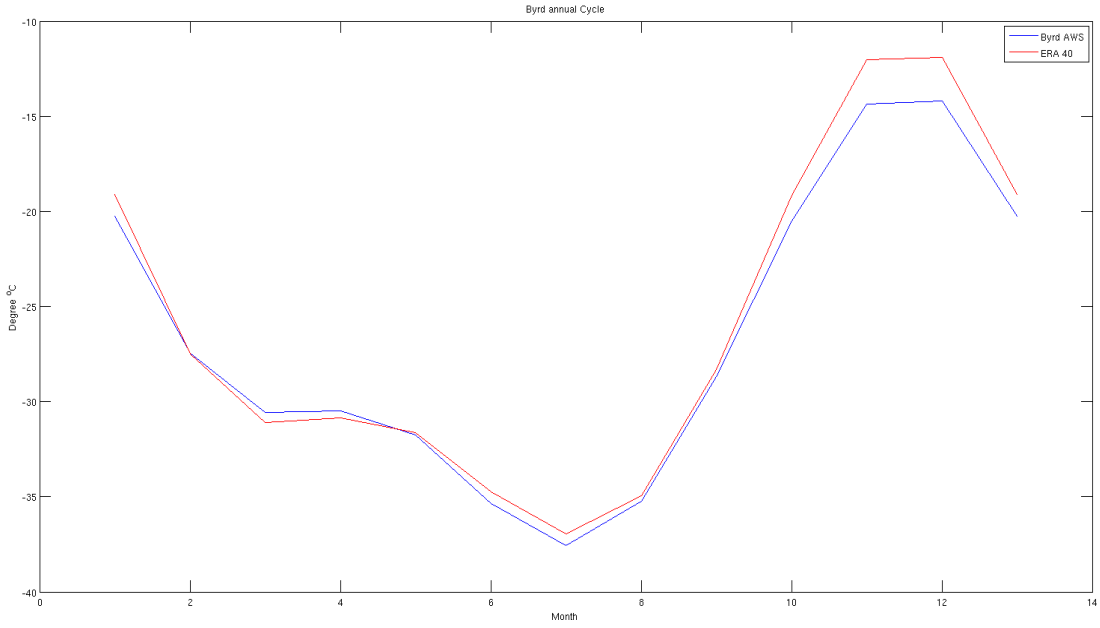

Figure 3.1: Comparison of Gill Station (blue) to ERA-40 (red) analysis of annual cycle.

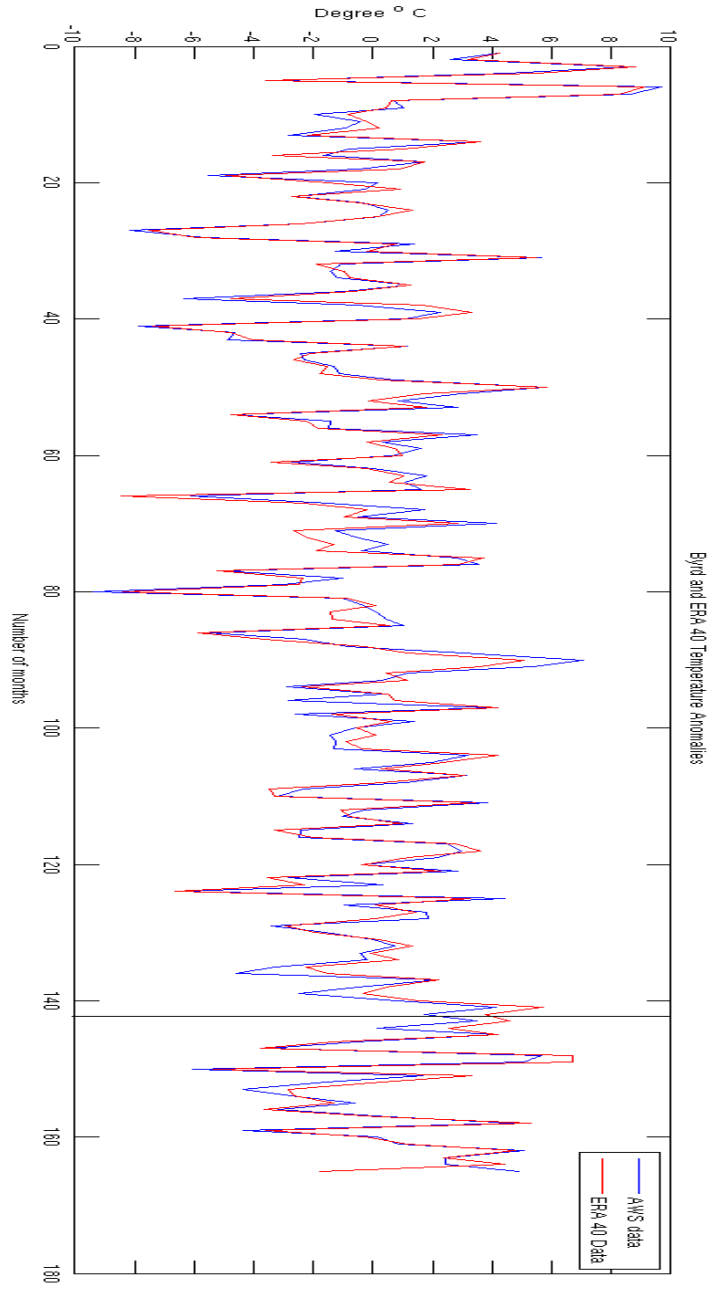

Figure 3.2: Comparison of Gill Station (blue) to ERA-40 (red) analysis of annual cycle. Black line indicates the cutoff of data being assimilated

4.1.2 Elaine Station

Elaine station is located at 83.15S and 174.46E, placing it on the southern edge of the Ross Ice Shelf near the Transantarctic Mountain range. The annual cycle (Figure 4) indicates a mild warm bias in the model primarily focused during winter months. The correlation is high at .90 throughout the time period with oddly increased correlation after data assimilation of this station has stopped. The lowest correlation is during the year 1993 this seems to correspond to a decreased number of data points assimilated according to the ERA archive. Specifically there are approximately 2700 observations assimilated in 1993 as opposed to the approximately 2900 observations in other years of full data coverage (Kallberg 2004). The data was similarly compared with the ERA-interim data to determine if the model continued to do well during the years 1998-2002 as these years showed an unexpected increase in correlation despite no data assimilation. Correlation values were much higher in general for the ERA-interim throughout the period analyzed, 1993-2002. This comparison shows a similar low correlation during 1993, and a minor decline after 1997, which coincides with the period the ERA-40 stopped assimilating the

station. This station has not been compared with the interim reanalysis after the 2002 period because the station had insufficient data due to issues with the station.

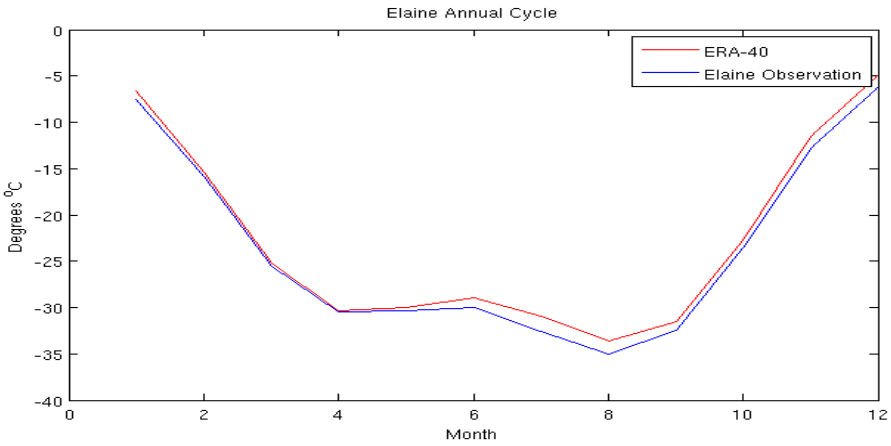

Figure 4: Comparison of the Elaine station data (blue) and ERA-40 data (red) for the annual cycle

4.1.3 Dome C stations

The Dome C station analysis has been separated by the year 1995, as this is the final year of operation of the original station, with 1996 being the first year of a new station installed in close proximity, but not at the exact same location. There is a manned station located nearby, operating as a summer station from 1992-2004, and as a year round station from 2005-2011. Again, a warm bias is noted in the annual cycle for this station in both

the interim and the 40, though during different seasons. (Figure 5). Correlation for the ERA-interim is high for these stations at .93 for Dome C 2 station, which has been in place from 1996-2010. For the ERA-40 the correlation is .87 for the first station, years 1980-1995, and .80 for the second station, 1996-2002. This drop in correlation is somewhat expected as the second station was not assimilated by the ERA-40. Despite this drop off a correlation of .8 is still acceptable for our purposes.

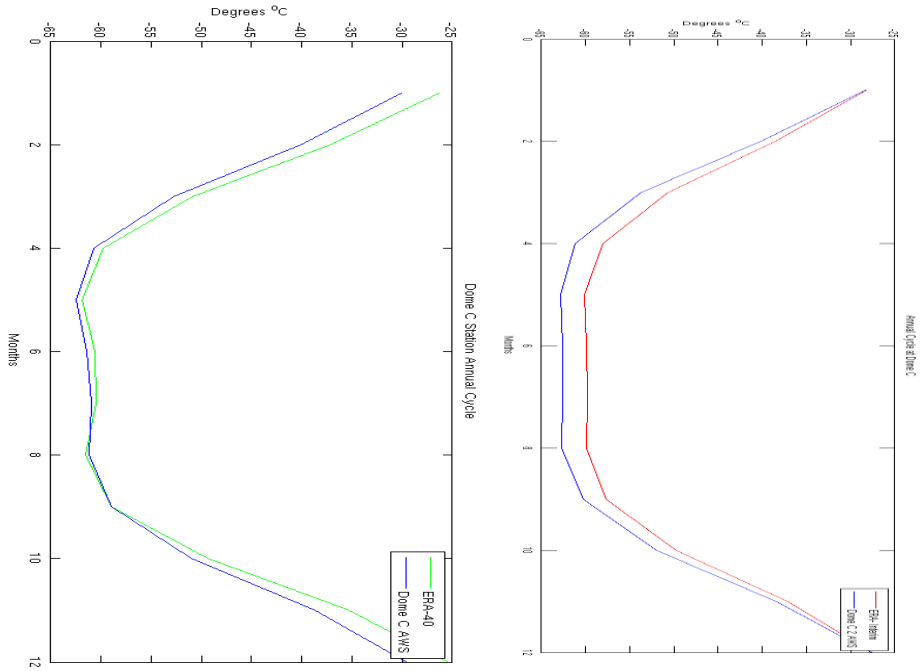

Figure 5: Comparison of annual cycles between (left) Dome C (blue) and ERA-40 (green), (right) Dome C II (blue) and ERA-Interim (red).

4.1.4 Gill Station

The Gill station is located on the Ross Ice Shelf, further from the Transantarctic Mountains at 80S and 179W. Similar to other stations, a warm bias is observed in the annual cycle. The overall correlation throughout the period is quite good, at 0.9 with the ERA-40 and .95 with the ERA-interim. Similar to Elaine station, a noticeable drop in accuracy is found during the year 1993. Again, fewer observations have been assimilated during this year than many other years, but a lack of observations can't fully explain this drop as years after 1997 show an increased correlation despite the archive indicating no observations being assimilated (Figure 6.1; 6.2).

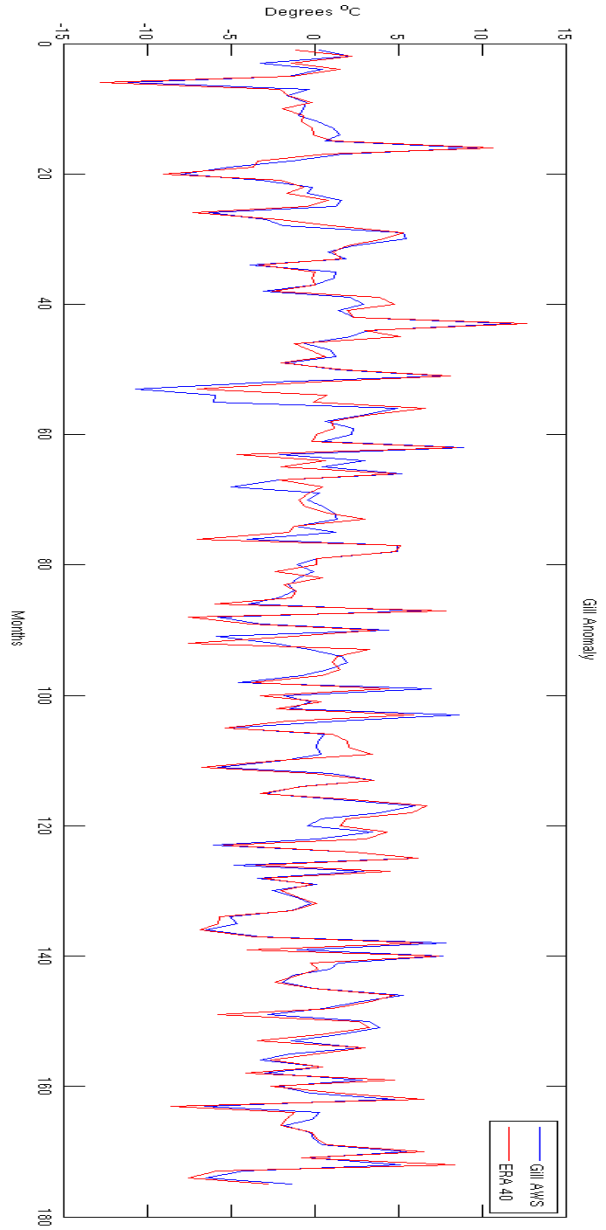

Figure 6.1: Anomalies as seen in Gill AWS (blue) and ERA-40 (red)

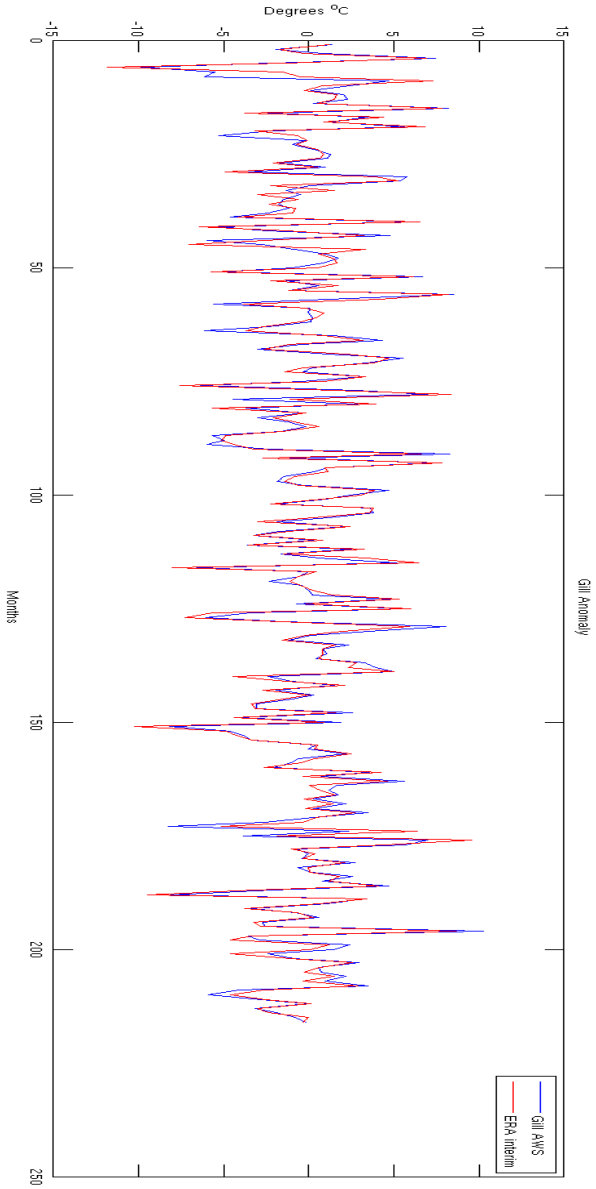

Figure 6.2: Comparison of Anomalies between Gill AWS (blue) and ERA-Interim (red)

4.2 Composite Analysis

Given that the reanalysis data is considered a reliable reconstruction of the variability of the three regions of analysis, Wilkes Land, Marie Byrd Land, and the Ross Ice Shelf, composite analysis of these regions can be viewed as realistic depictions of these regions during ENSO events. Throughout this section comparisons between indices have been performed, and effort has gone to understanding whether the change in basis or change in the time period observed is the source of differences in the observations. As each index represents a different length of time this is possibly also a source of discrepancy, and as such effort, has been taken to determine how the indices agree and disagree. This work has focused on the months September through February, as these are the months of peak ENSO activity (Turner 2004). These months also tend to have greater agreement than other time periods, indicating more robust ENSO events, as opposed to temporary variations in the various indices. This analysis has been separated by reanalysis type as they each represent different periods of time.

4.2.1 ERA-40

General similarities exist between the MEI analysis and the ONI analysis in both pattern and regions of significance, with some differences noticed, while the SOI analysis has relatively large differences in regions of significance, and in some instances in the patterns created. This is somewhat expected as the ONI and MEI measure in relatively the same region, the equatorial Pacific somewhat closer to central and eastern Pacific, while the SOI measurements are across the full equatorial pacific, and based on only two locations of measurement. As the mean sea level pressure seems to mirror the 500 hecto-pascal (hPa) height anomalies, and the surface temperature generally seems to be a function of the expected changes in advection associated with these changes in sea level pressure, surface pressure will not be shown.

4.2.1.A El Niño

4.2.1.A.1 ONI

Beginning with the ONI in September, October, and November(SON)

for El Niño events, the ABS teleconnection is highly noticeable in the 500 hPa height plot. Also notable are the alternating highs and lows associated with the PSA that has been posited as a means of transmitting the ENSO signal from the tropics to polar latitudes (Figure 7). Specifically, this teleconnection weakens (strengthening) the ABS low (Weddell Sea low) during El Niño events. These changes have the effect of warming the ABS region, with this warm surface air spreading only slightly onto the Ross Ice Shelf. The Antarctic Peninsula cools, as the Peninsula lies between the weakened ABS low and the amplified Weddell Sea (WS) low which acts to advect cooler, more southerly air from West Antarctica into the Peninsula (Figure 8). As the time period moves to the months of October-December (OND), the ABS low teleconnection has become stronger and moved more onto the continent. In turn the WS low amplification has moved to more northern latitude. Also, there are regions of significant positive 500 hPa height anomalies throughout East Antarctica (Figure 9). This pattern induces more warming on the Ross Ice Shelf and West Antarctica, while the cooling seen in the Peninsula has shifted to more northern latitudes, while still remaining on the Peninsula. There is a warming signal in East Antarctica associated with the upper level height anomalies (Figure 10).

Moving forward to austral summer beginning with November-January (NDJ), the ABS low teleconnection has moved further toward the Antarctic Peninsula, with the WS low amplification moving further north. This has the effect of reducing the effect on surface temperature, with only mild warming in West Antarctica (Figure 11; 12). This period seems to be a distinct peak before the system begins to reverse in later periods. Moving forward to December-February (DJF), the teleconnection begins to deform and stretch further away from the continent. The surface temperature seems to remain similar in Marie Byrd Land, but has changed considerably in the Ross Ice Shelf, as cooling has begun along the Transantarctic Mountains (Figure 13; 14). The timing of this cooling is interesting, but as it is distant from the upper level forcing it is unclear precisely how this feature comes about.

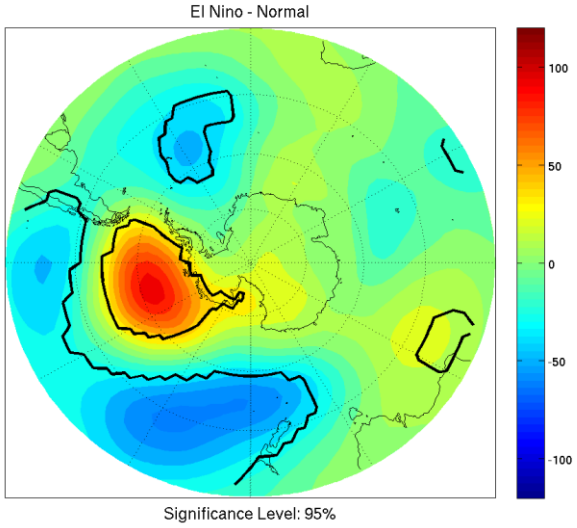

Figure 7: 500 hPa height anomalies for ONI during SON of El Niño. Black Lines enclose regions of statistical significance at 0.95.

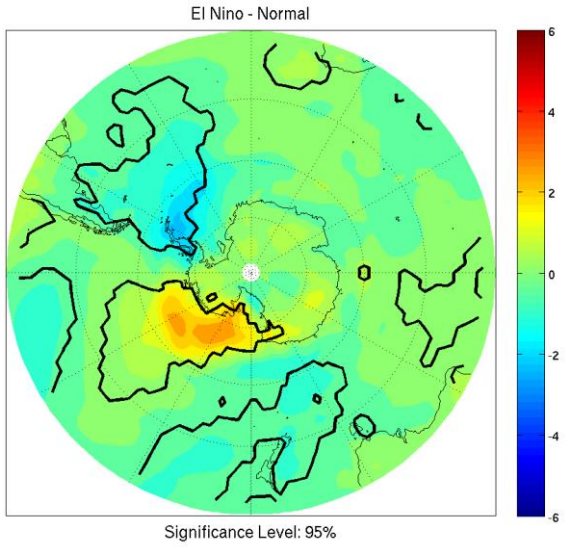

Figure 8: 2 meter temperature anomalies for ONI during SON of El Niño. Contours are every .5 degrees Celsius.

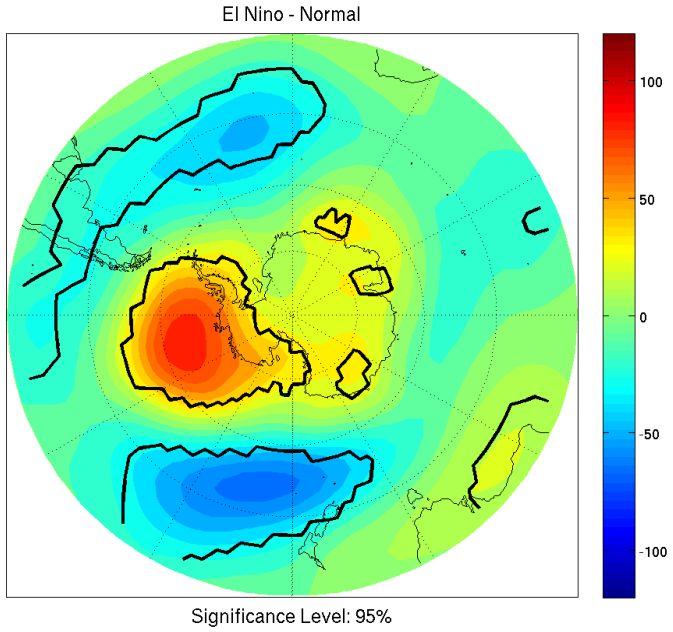

Figure 9: 500 hPa height anomalies for ONI during OND of El Niño.

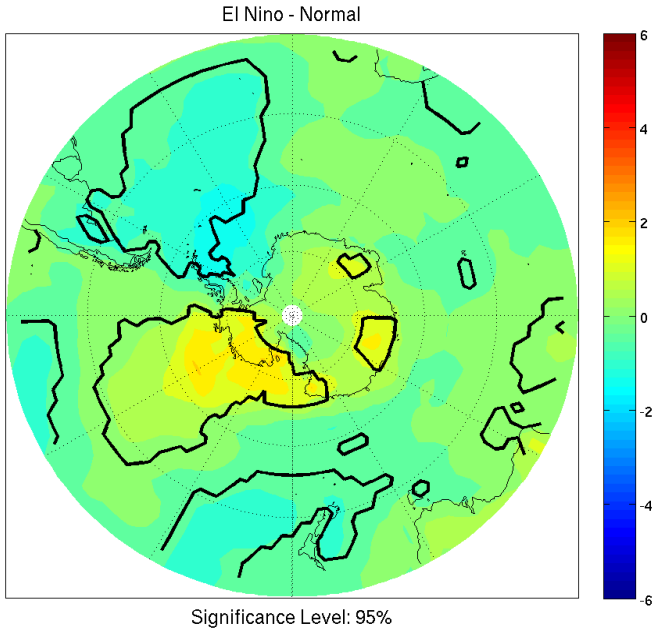

Figure 10: 2 meter temperature anomalies for ONI during OND of El Niño.

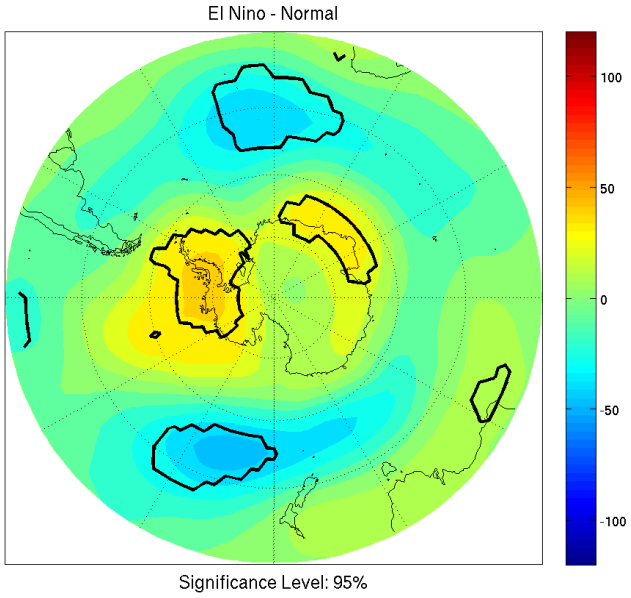

Figure 11: 500 hPa height anomalies for ONI during NDJ of El Niño.

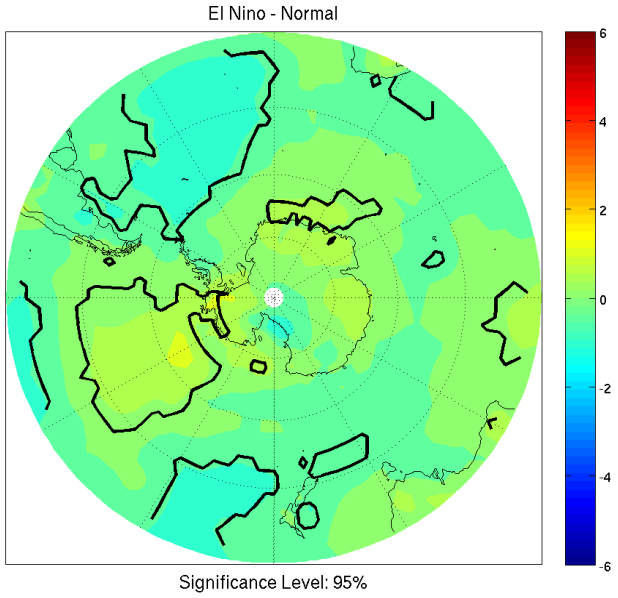

Figure 12: 2 meter temperature anomalies for ONI during NDJ of El Niño.

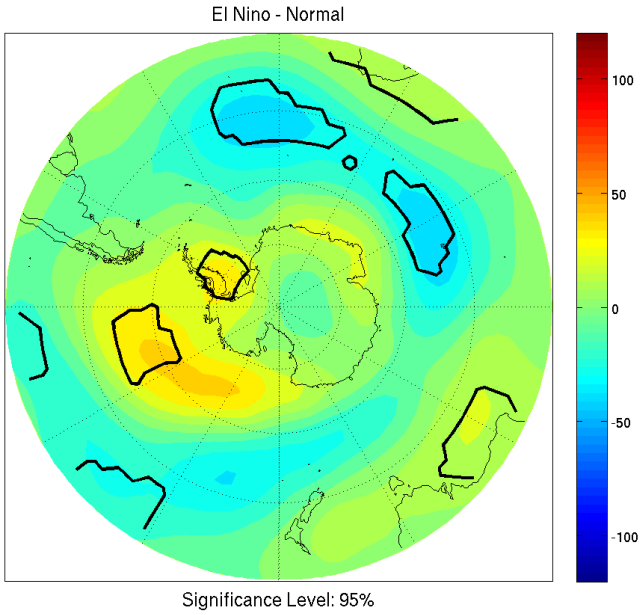

Figure 13: 500 hPa height anomalies for ONI during DJF of El Niño.

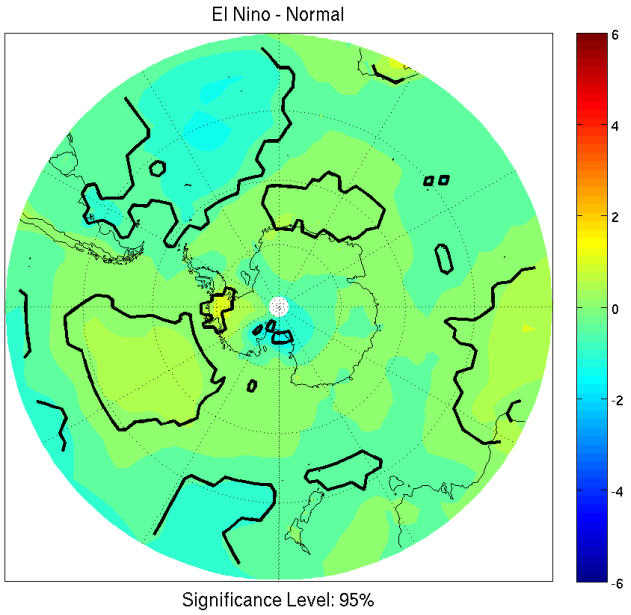

Figure 14: 2 meter temperature anomalies for ONI during DJF of El Niño.

4.2.1.A.2 MEI

Beginning in September-October (SO), we note the distinct pattern of weakened ABS low and amplified WS low in the MEI composites (Figure 15). This leads to strong warming in the ABS, and cooling throughout the Peninsula and WS (Figure 16). October-November (ON) has less of the distinct teleconnection pattern with the ABS low weakening extending through the Ross Ice Shelf and into East Antarctica. The WS low amplification is not significant during this time period (Figure 17). These features extend to the surface, inciting warming throughout Marie Byrd Land, and the Ross Ice Shelf (Figure 18). During the November-December (ND) time period, the ABS teleconnection remains quite strong, though rather than extending into the Ross Ice Shelf and Wilkes Land, the positive height anomaly extends into the WS. This indicates a weakening of the WS low (Figure 19). Despite the strength and extent of the teleconnections onto the continent, surface temperature is generally weakly affected, with Marie Byrd Land having only small warming (Figure 20).

December-January (DJ) shows the teleconnection splitting into two lobes of positive height anomaly, with one over the Peninsula, and the other

located near the Ross Ice Shelf. A third region of significance is located off the coast of Queen Maud Land (Figure 21). This has a similar effect as the ND period, with the region of warming shifted toward the Peninsula, mirroring the shift of the upper level feature (Figure 22). For January-February (JF), there is a distinct return of the ABS low teleconnection though it is shifted toward the Ross Ice Shelf, while the WS low is still mildly weakened rather than the expected strengthening (Figure 23). The warming throughout Marie Byrd Land is still distinguishable, with additional regions of cooling found in the Transantarctic Mountains bordering the southern Ross Ice Shelf, and within Queen Maud Land bordering the Wilkes Sea (Figure 24). These regions of cooling are removed from an upper level signal, making the cause difficult to determine, but it does agree with similar timing of cooling within this region found in the earlier ONI analysis. The cooling seen along the Transantarctic Mountains seems to agree with the timing and location of cooling seen by the return trip from the South Pole that claimed the lives of Robert Falcon Scott and his expedition.

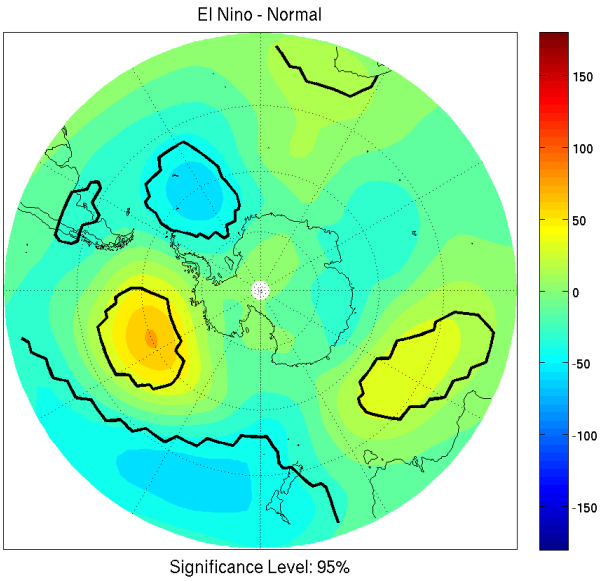

Figure 15: 500 hPa height anomalies for MEI during SO of El Niño.

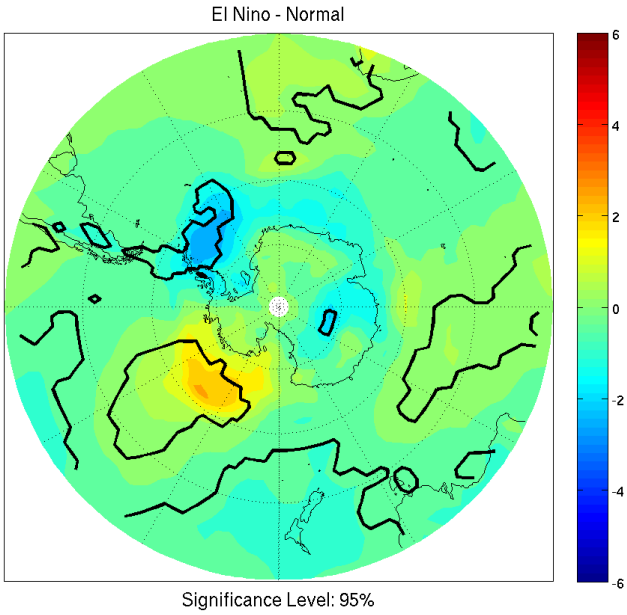

Figure 16: 2 meter temperature anomalies for MEI during SO of El Niño.

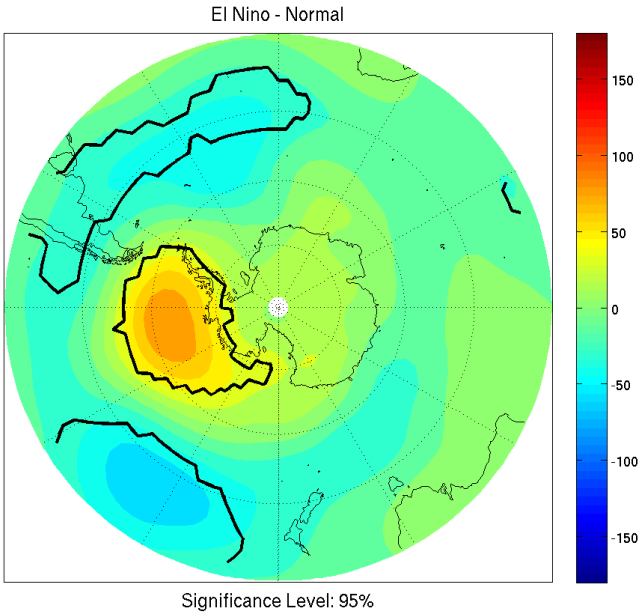

Figure 17: 500 hPa height anomalies for MEI during ON of El Niño.

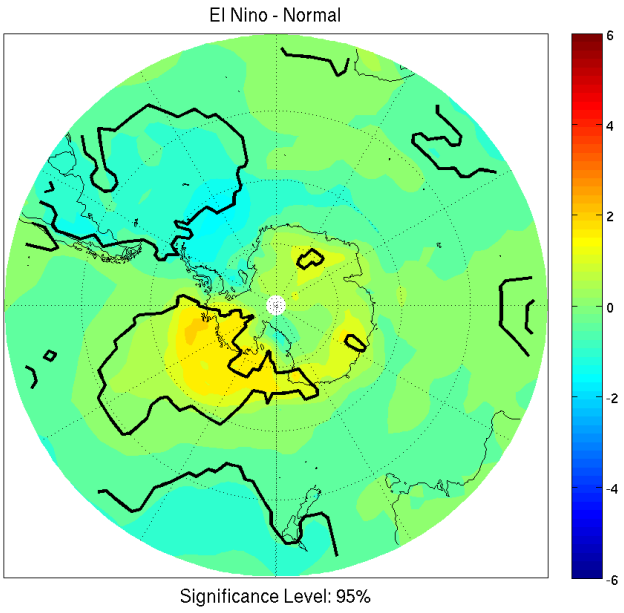

Figure 18: 2 meter temperature anomalies for MEI during ON of El Niño.

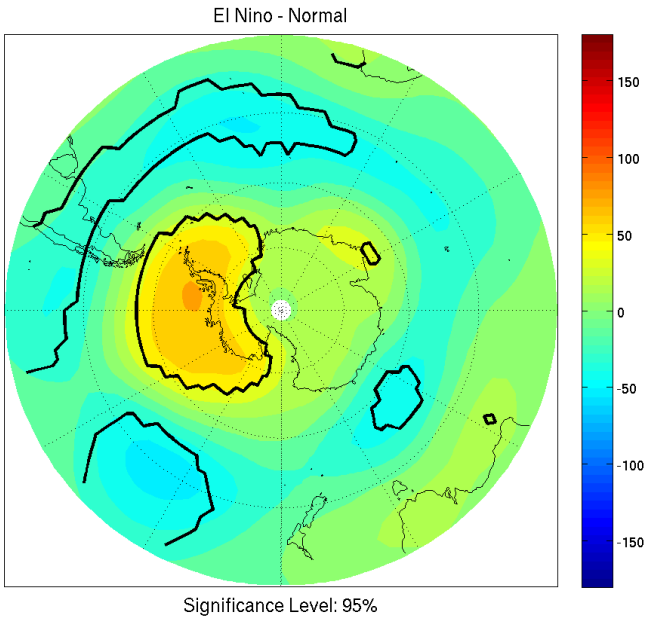

Figure 19: 500 hPa height anomalies for MEI during ND of El Niño.

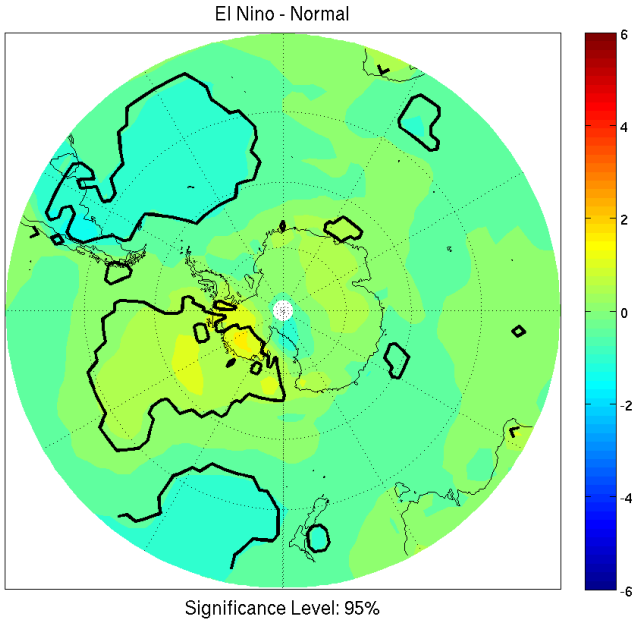

Figure 20: 2 meter temperature anomalies for MEI during ND of El Niño.

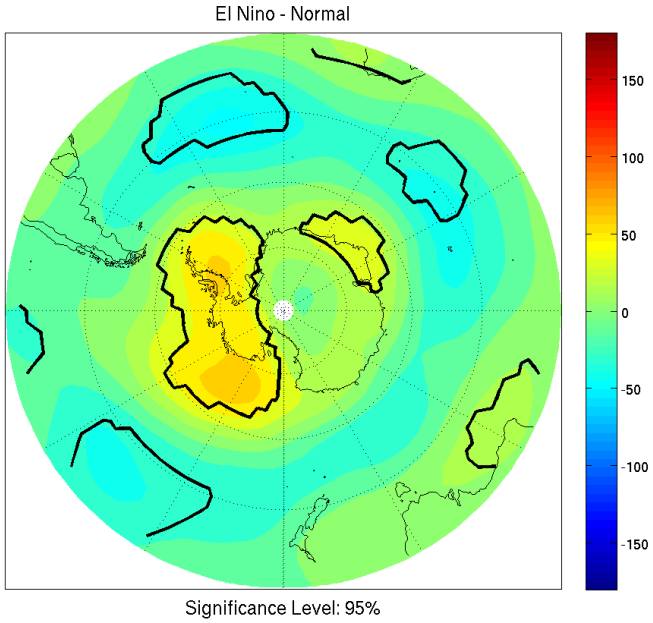

Figure 21: 500 hPa height anomalies for MEI during DJ of El Niño.

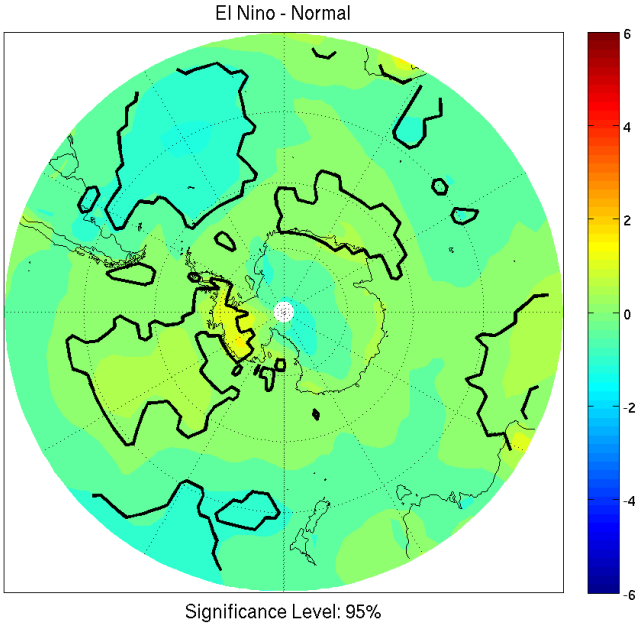

Figure 22: 2 meter temperature anomalies for MEI during DJ of El Niño.

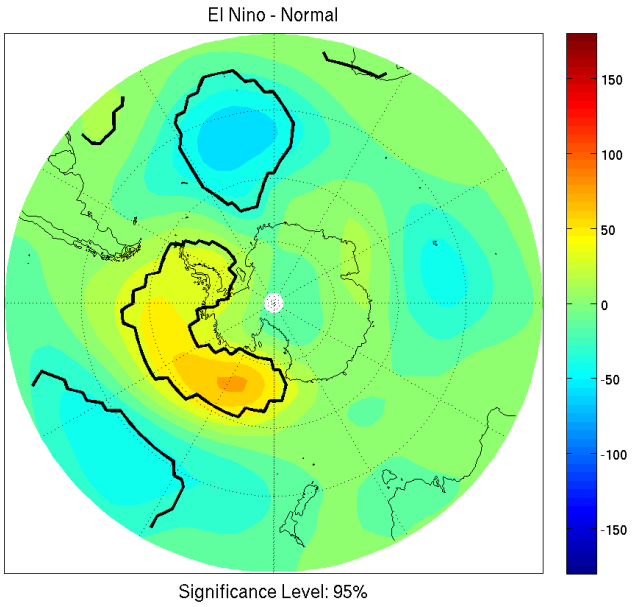

Figure 23: 500 hPa height anomalies for MEI during JF of El Niño.

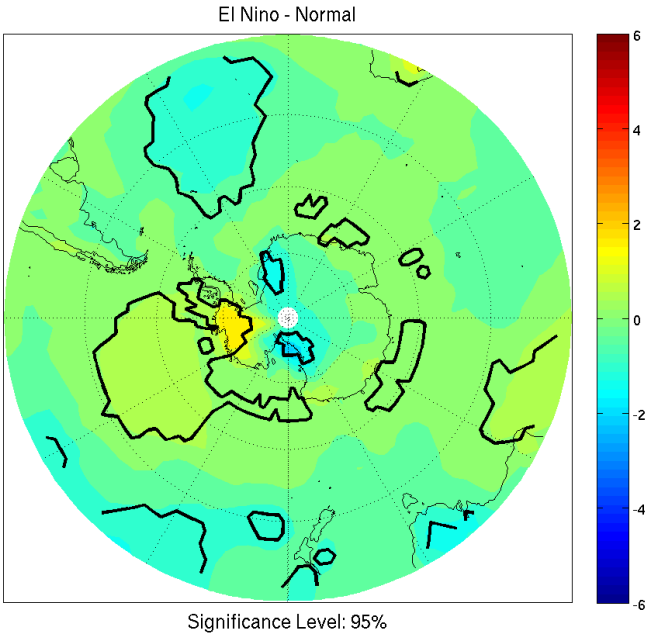

Figure 24: 2 meter temperature anomalies for MEI during JF of El Niño.

4.2.1.A.3 SOI

The SOI significance is more difficult to establish as the bi-monthly composites and tri-monthly composites non-event variance is diminished. This allows the effect of El Niño to be more distinguishable. The month of September shows little significant signal at upper levels, but the general pattern at this level is that of the expected teleconnection pattern (Figure 25). At the surface we see mild, but significant, warming in Queen Maud Land that seems associated with the WS low, as well as mild warming offshore of the Ross Ice Shelf associated with the ABS low weakening (Figure 26). October has a distinct positive upper level height anomaly in the ABS, as well as in Queen Maud Land and a smaller feature within Wilkes Land. The anomaly that would account for WS low amplification remains not significant, and in this period has become removed further removed from the WS (Figure 27). Distinct warming is seen at the surface throughout these regions (Figure 28). November has a similar ABS low weakening, though the height anomaly does not extend on continent significantly (Figure 29). As the features do not extend inland, the surface sees little significant temperature effect, but there is some cooling throughout the northernmost

reaches of the Peninsula (Figure 30).

December, January, and February all show distinctly less of the expected patterns associated with the teleconnections at upper levels, with little to no significant anomalies detected in either the upper levels or the surface temperatures. December and January both show the positive height anomaly moving toward the Ross Ice Shelf and weakening, whereas for the February period, the pattern lacks all statistical significance near Antarctica (Figures 31; 32; 33). Interestingly, cooling is noted in the southern region of the Ross Ice Shelf during February (Figure 34). This lines up with both the MEI and ONI analyses. But again, this is removed from a distinguishable upper level pattern.

Of note is that the ABS region seems to be the primary affected region for El Niño months. This is the expectation based on the prior literature, and while the lack of effect within the WS region isn't entirely unexpected as it is generally a weaker feature, the lack of significance in all but one time period indicates that the feature may be focused in La Niña or a different seasonal period of ENSO events.

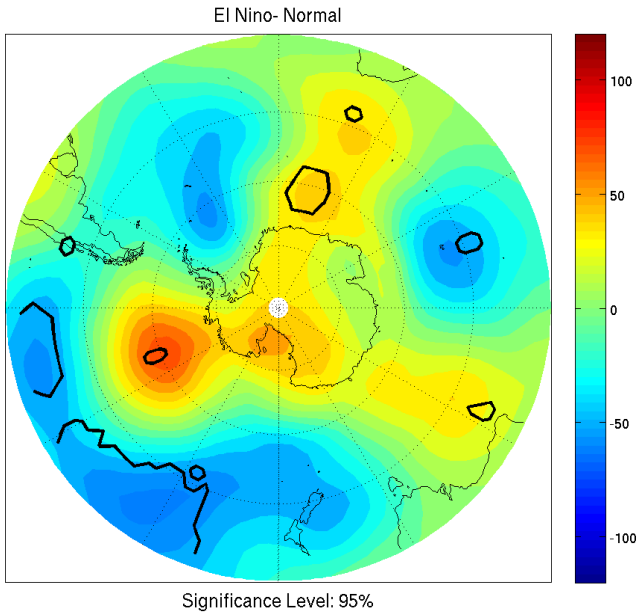

Figure 25: 500 hPa height anomalies for SOI during September of El Niño.

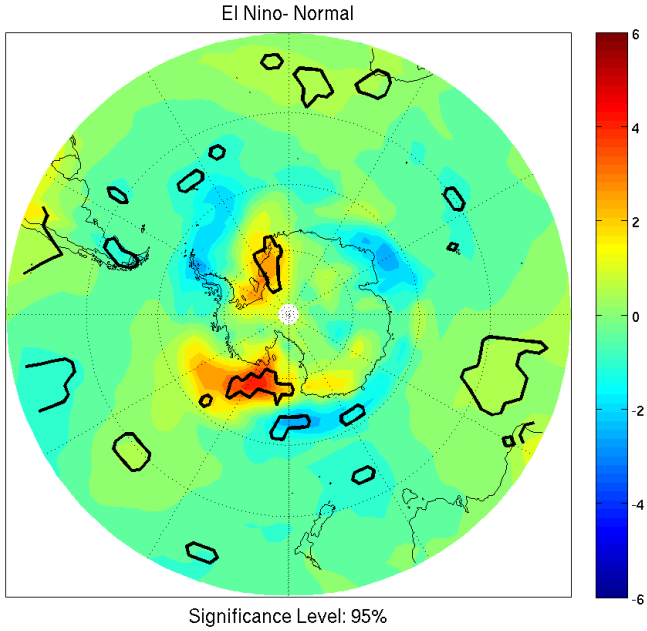

Figure 26: 2 meter temperature anomalies for SOI during September of El Niño.

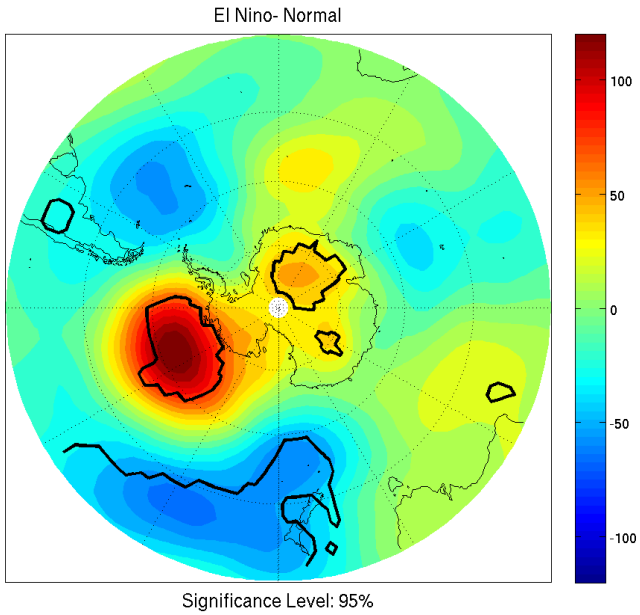

Figure 27: 500 hPa height anomalies for SOI during October of El Niño.

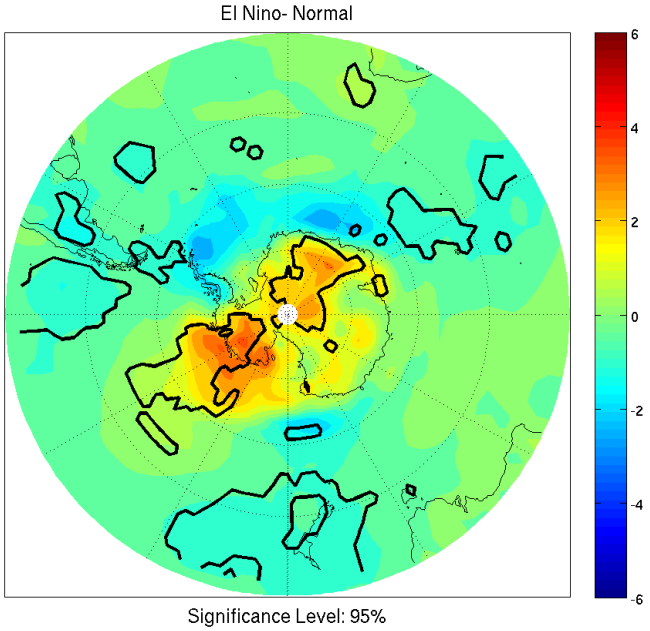

Figure 28: 2 meter temperature anomalies for SOI during October of El Niño.

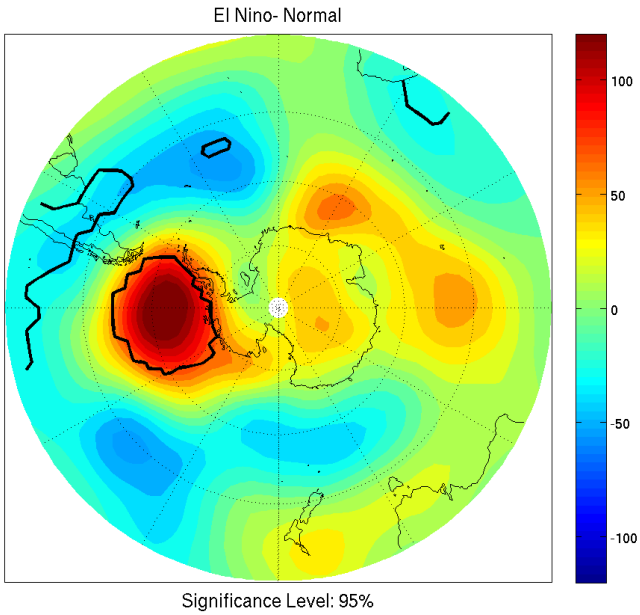

Figure 29: 500 hPa height anomalies for SOI during November of El Niño.

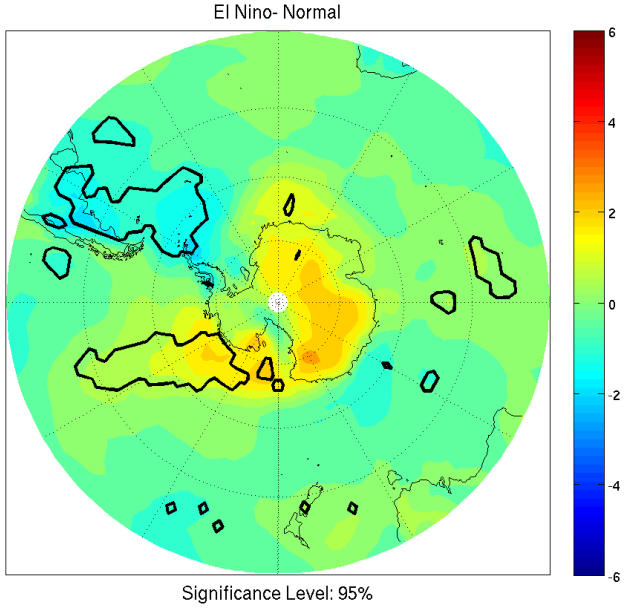

Figure 30: 2 meter temperature anomalies for SOI during November of El Niño.

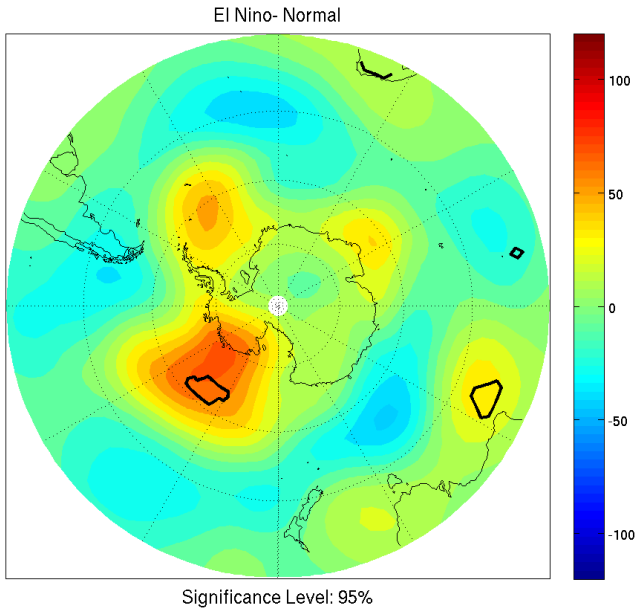

Figure 31: 500 hPa height anomalies for SOI during December of El Niño.

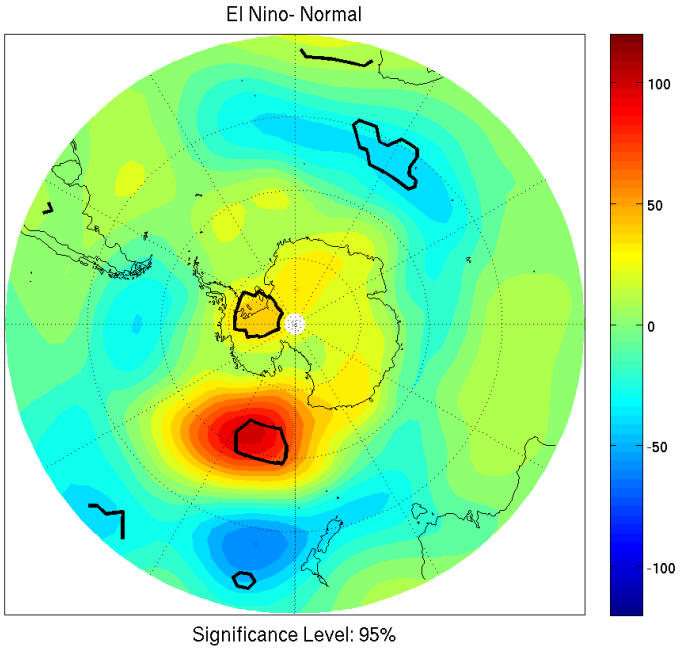

Figure 32: 500 hPa height anomalies for SOI during January of El Niño.

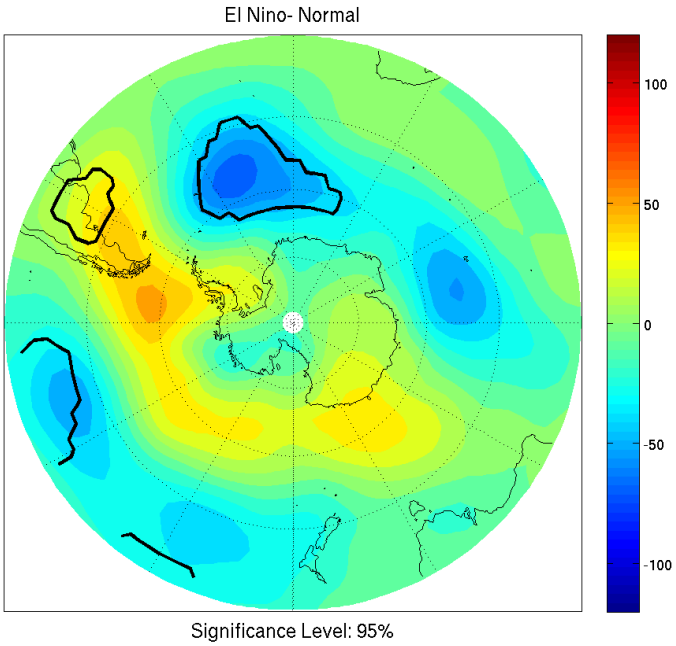

Figure 33: 500 hPa height anomalies for SOI during February of El Niño.

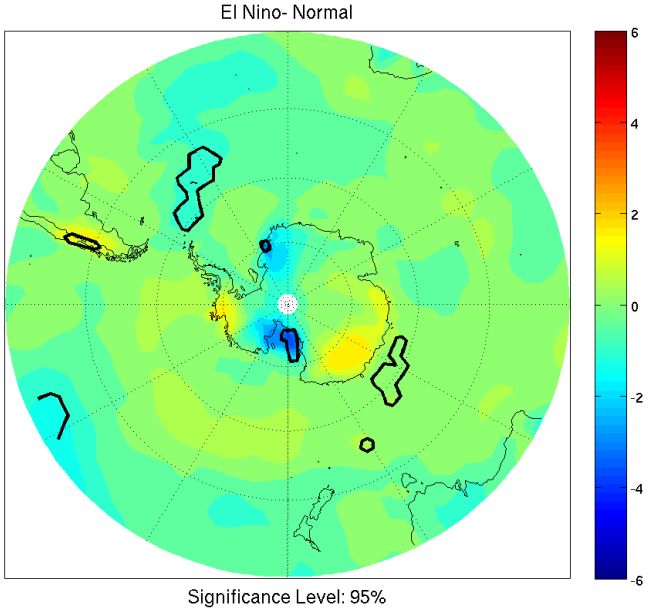

Figure 34: 2 meter temperature anomalies for SOI during February of El Niño.

4.2.1.B La Niña

4.2.1.B.1 ONI

Returning to the ONI to analyze the effects of La Niña, we note that in the SON period the expected alternating highs and lows act to weaken both the ABS low and the WS low. Also the presence of an upper level significant positive height anomaly is noted over the Ross Ice Shelf (Figure 35). This induces warming throughout West Antarctica, though the variability creates regions of significance rather than one large contiguous region of significant warming (Figure 36). For the OND period, the ABS low lacks much of the expected amplification, but rather has mild weakening near the Peninsula, while the majority of the focus of the teleconnection is in the weakening of the WS low (Figure 37). This translates to surface cooling in Queen Maud Land stretching to approximately the South Pole (Figure 38).

During the NDJ period, we note that the negative upper level height anomaly that remained relatively far off coast in prior periods has moved in to the ABS region though closer to the Ross Sea. The areas of significance still remain relatively far off the coast. A weakening of the WS low is noted,

but not significant (Figure 39). The surface temperature field shows a region of cooling in the Queen Maud Land region, which seems associated with the non-significant upper level height anomalies in the region, while the significant features associated with other features remain off coast (Figure 40). Again, we see a reduction in the regions of significance during the DJF period, though in this case the significant feature seems to be the negative height anomaly over the Wilkes Land region. There is an amplification of the ABS low, though it is not statistically significant (Figure 41). Both of these features seem associated with the surface pressure field, since cooling would expect from advection noted in West Antarctica and also cooling throughout East Antarctica (Figure 42).

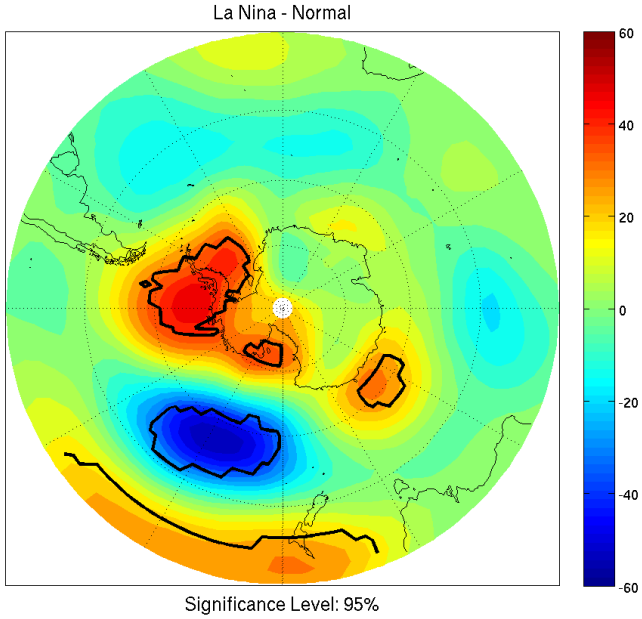

Figure 35: 500 hPa height anomalies for ONI during SON of La Niña.

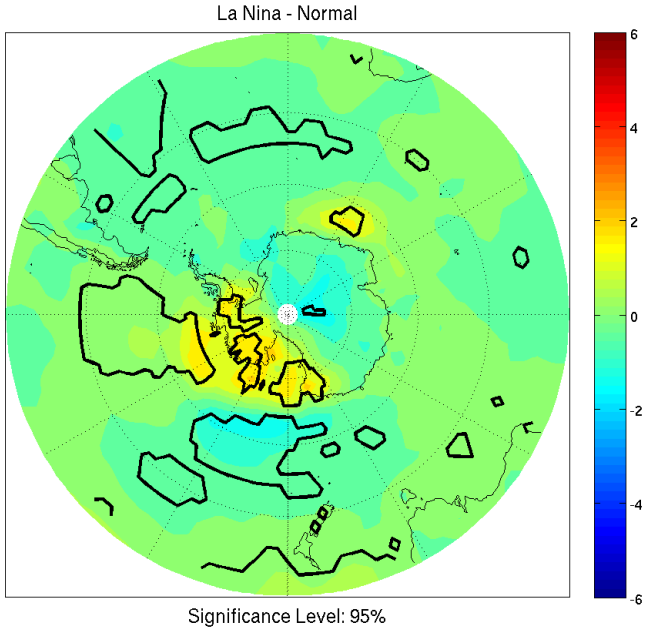

Figure 36: 2 meter temperature anomalies for ONI during SON of La Niña.

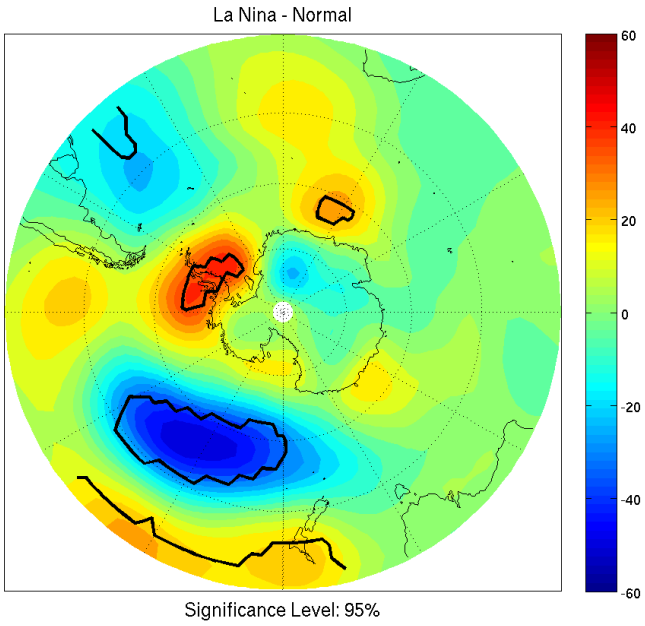

Figure 37: 500 hPa height anomalies for ONI during OND of La Niña.

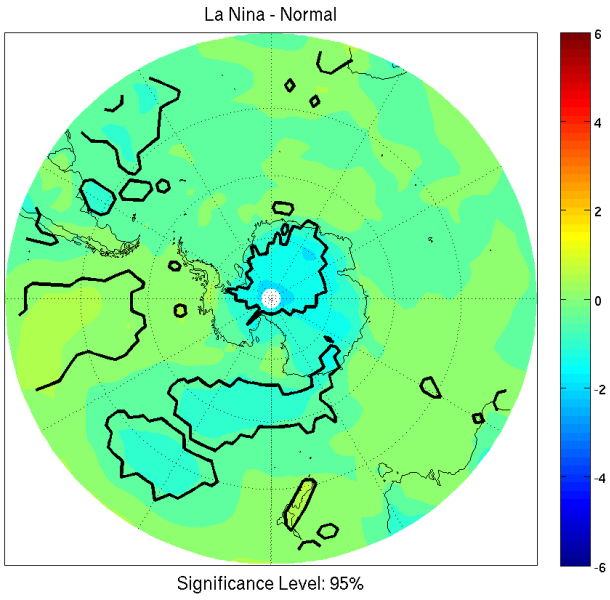

Figure 38: 2 meter temperature anomalies for ONI during OND of La Niña.

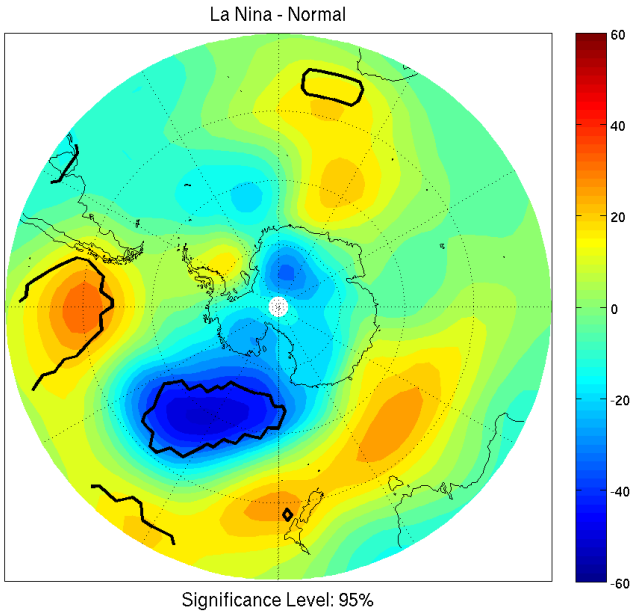

Figure 39: 500 hPa height anomalies for ONI during NDJ of La Niña.

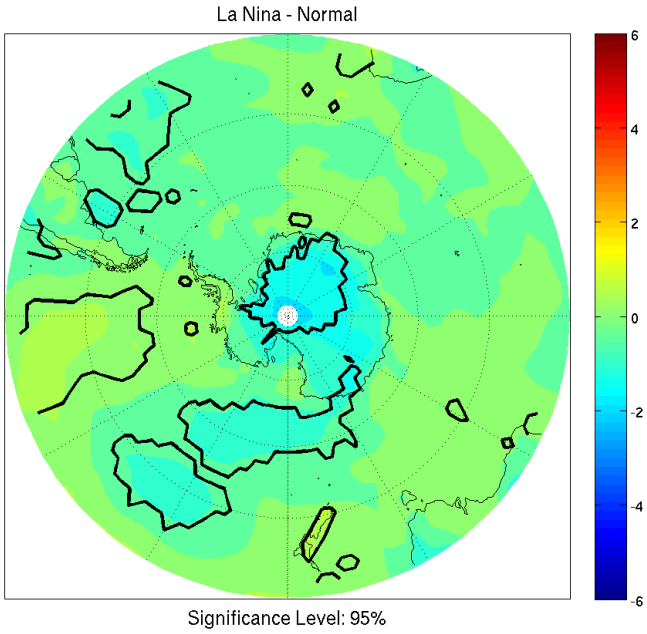

Figure 40: 2 meter temperature anomalies for ONI during NDJ of La Niña.

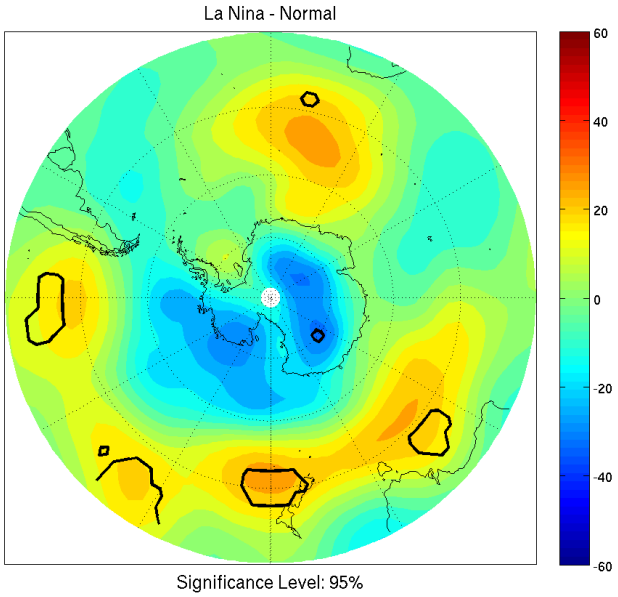

Figure 41: 500 hPa height anomalies for ONI during DJF of La Niña.

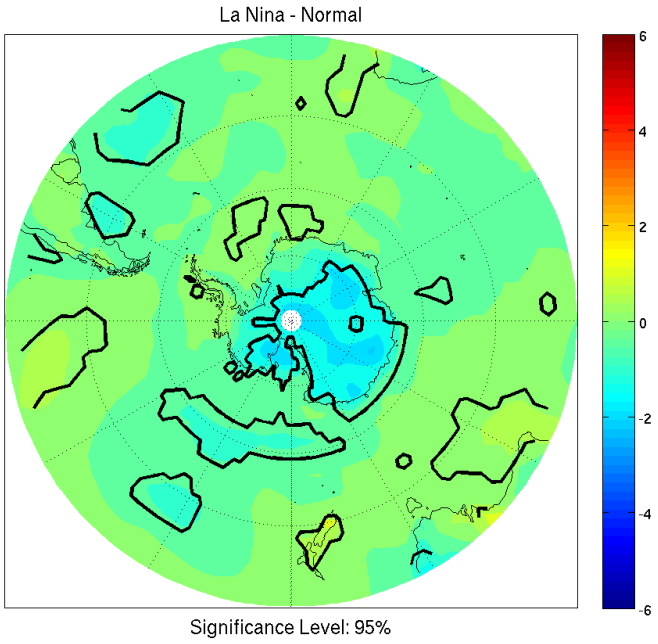

Figure 42: 2 meter temperature anomalies for ONI during DJF of La Niña.

4.2.1.B.2 MEI

The MEI composites present similar patterns for the La Niña teleconnections. Beginning in SO, a pattern with a negative anomaly far offshore and positive anomaly throughout the Ross Ice Shelf is present (Figure 43). The positive anomaly, though not significant, extends through Marie Byrd Land into the WS. When analyzing the surface features, warming is noted throughout West Antarctica, the Peninsula, and the WS. There is also cooling observed in Wilkes Land, though this is separate from upper level features (Figure 44). The ON ABS low aspect of the teleconnection is not significant, while the WS weakening is distinct though the upper level anomaly does extend slightly over the Peninsula (Figure 45). Consequently, Marie Byrd Land experiences significant warming, likely associated with advection by the upper level feature (Figure 46).

The ND, DJ, and JF periods show a lack of significant upper level features. The negative height anomaly remains well off shore, and while a positive height anomaly exists in the WS region it is not significant. Throughout this period a negative height anomaly, though it remains statistically insignificant, grows in East Antarctica (Figure 47; 48; 49). As

expected with this lack of strong upper level signal, there is no significant surface signal throughout West Antarctica. The DJ and JF periods both indicate significant cooling within East Antarctica within the regions of negative height anomaly. This is of note due to the similar timing of cooling in this region indicated in the ONI composites (Figure 50; 51).

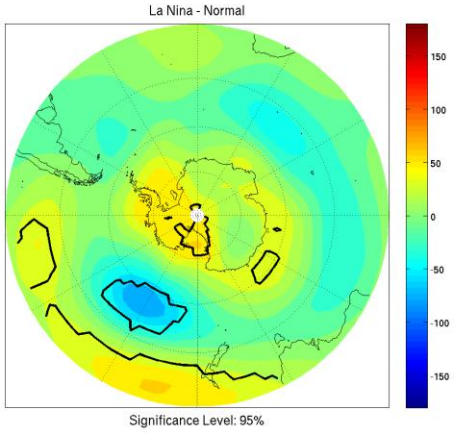

Figure 43: 500 hPa height anomalies for MEI during SO of La Niña.

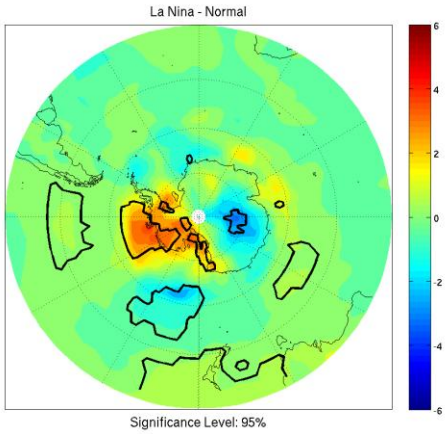

Figure 44: 2 meter temperature anomalies for MEI during SO of La Niña.

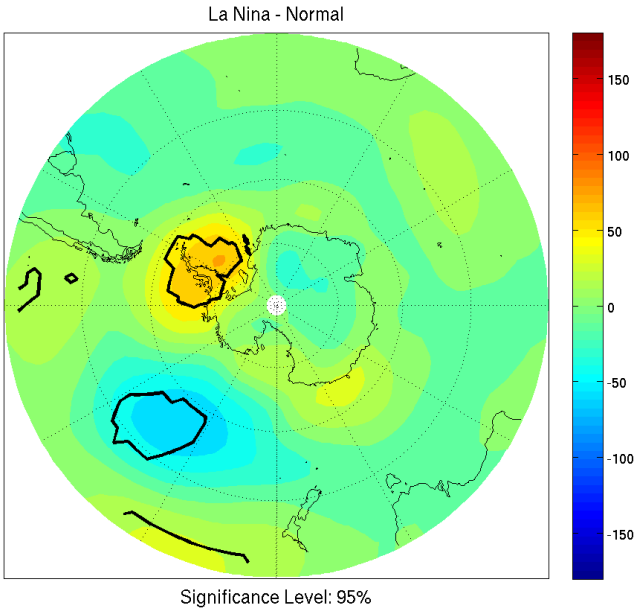

Figure 45: 500 hPa height anomalies for MEI during ON of La Niña.

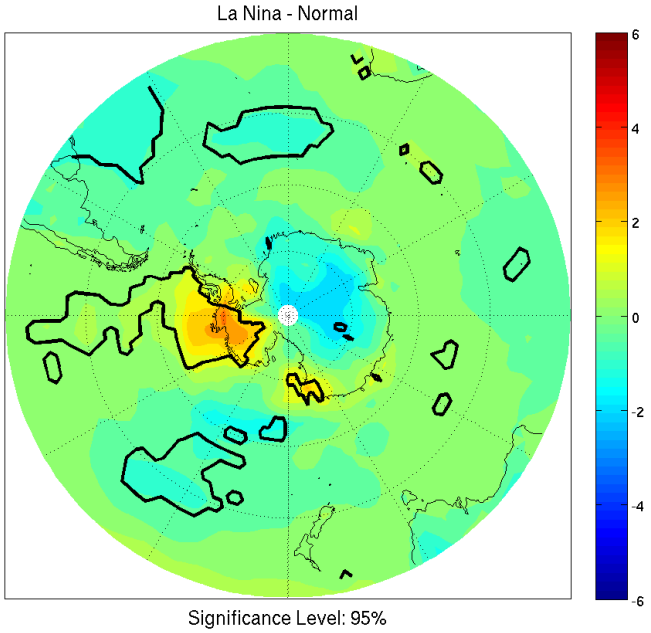

Figure 46: 2 meter temperature anomalies for MEI during ON of La Niña.

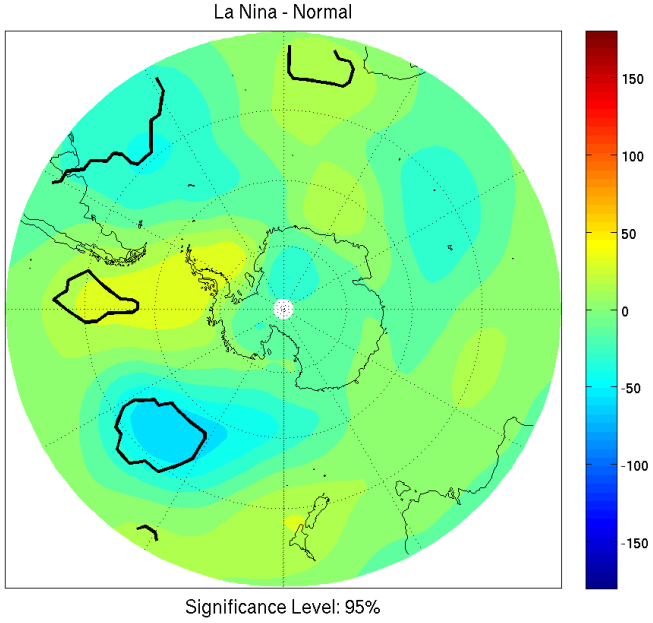

Figure 47: 500 hPa height anomalies for MEI during ND of La Niña.

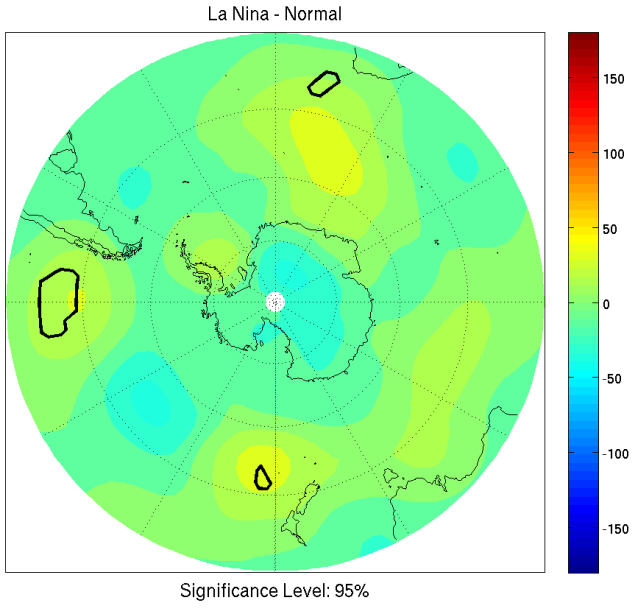

Figure 48: 500 hPa height anomalies for MEI during DJ of La Niña.

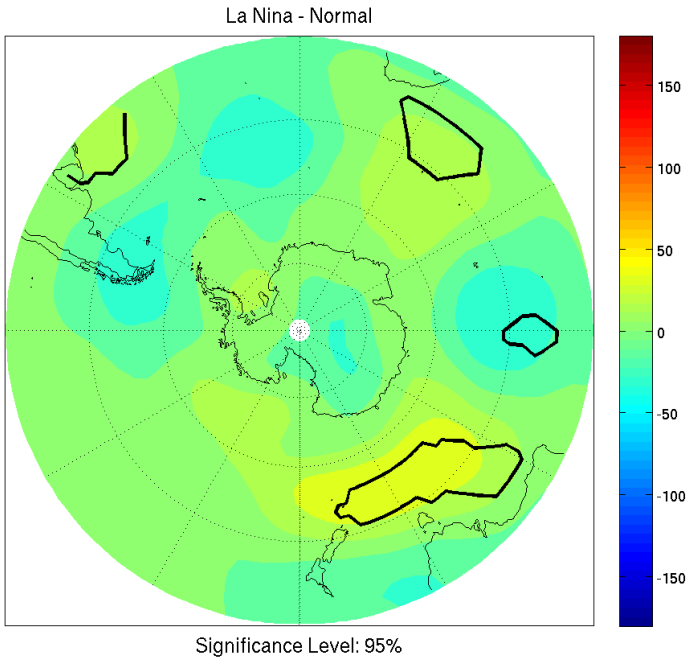

Figure 49: 500 hPa height anomalies for MEI during JF of La Niña.

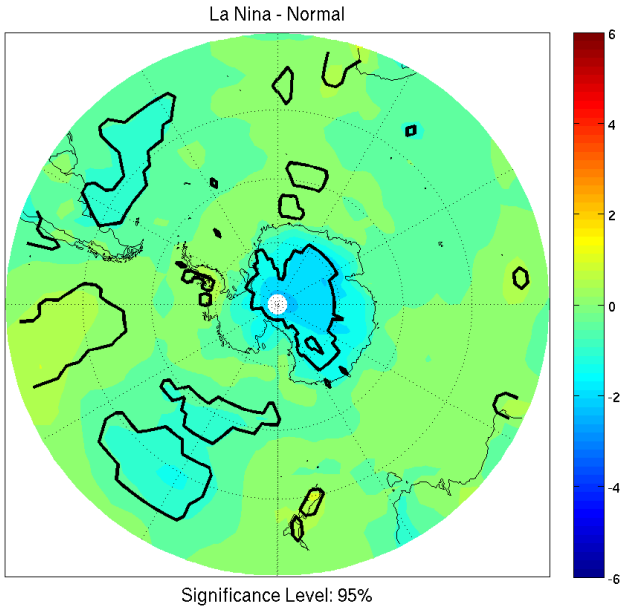

Figure 50: 2 meter temperature anomalies for MEI during DJ of La Niña.

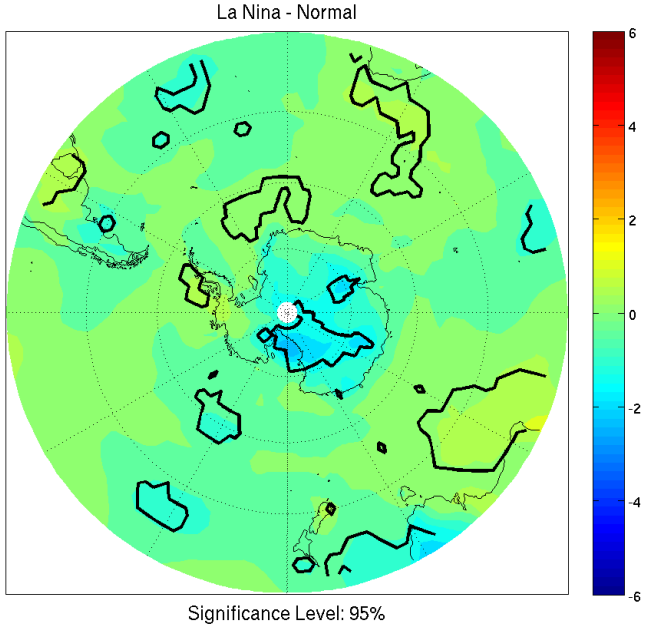

Figure 51: 2 meter temperature anomalies for MEI during JF of La Niña.

4.2.1.B.3 SOI

The SOI composites show considerable differences when compared with the MEI and ONI composites. There are also some interesting similarities between the ONI and MEI composites. During September there is a strong, positive, significant, height anomaly covering much of Antarctica, with only the WS showing the positive anomaly to not be significant (Figure 52). During this period there is little change in surface temperatures seen in West Antarctica, but there is strong, significant

warming seen throughout East Antarctica's coastal region, beneath the regions of the greatest anomaly (Figure 53). This upper level signal is distinctly different from the expectation. Moving forward to October, a drastic change has occurred, as there is now little significance, though the pattern is as expected with an amplification of the ABS low and a weakening of the WS low (Figure 54). The only significant surface anomaly is in Marie Byrd Land in the region between these two upper level features. As expected by advection a warm anomaly is present (Figure 55). In November, the ABS feature has a small region of significance and has shifted toward the Ross Ice Shelf, while the WS low feature remains not significant (Figure 56). Much of the continent experiences a negative height anomaly, though it isn't significant, but there is some significant surface cooling throughout East Antarctica near these regions of negative height anomaly (Figure 57). As the features in the ABS region remain off coast, so does the surface warming.

December again shows no significant height anomaly throughout the continent and is missing the characteristic teleconnection pattern, though the negative anomalies over East Antarctica remain, as do the negative temperature anomalies in the same region (Figure 58 and 59). January

shows a return of the ABS low strengthening generally associated with La Niña, though the weakening of the WS low is not seen. Cooling associated with the enhanced low is also seen, though it remains off-shore, aside from a small region within the Ross Ice Shelf. The negative height anomaly seen over East Antarctica has shifted to the coast and shows significance. Again, negative temperature anomalies are located at the surface in the regions of this anomaly (Figure 60 and 61). February again shows a lack of significant height anomalies, with mild negative anomalies throughout the ABS region and East Antarctica, and mild positive anomalies throughout the WS region (Figure 62). The negative anomaly located in previous periods within East Antarctica is still present, though it has moved further inland, now stretching from bordering the WS to the Transantarctic Mountains (Figure 63). Throughout this analysis, it has become evident that for the single month composites significance is difficult to achieve at upper levels. The same pattern over East Antarctica is present, if not significant, as are the negative temperatures in the same region.

Generally, the pattern seems to indicate La Niña has a greater effect both closer to the Peninsula and throughout East Antarctica, while the ABS region seems to be less affected. This could indicate the expected effect in

the ABS region is focused in El Niño events, or during other seasonal periods than those explored. The pattern seen throughout East Antarctica is of interest primarily as it has not been discussed in prior literature to a large degree. Also of note is that while initially La Niña has an effect on the West Antarctic surface temperatures, as the season progresses this effect diminishes, while the East Antarctic effect increases which indicates a large seasonality to La Niña.

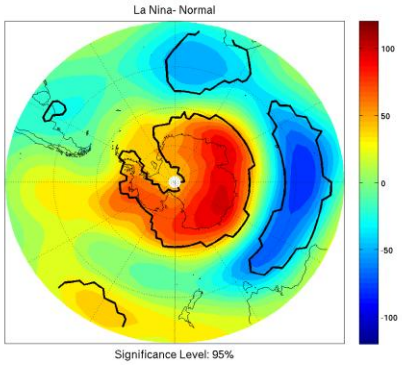

Figure 52: 500 hPa height anomalies for SOI during September of La Niña.

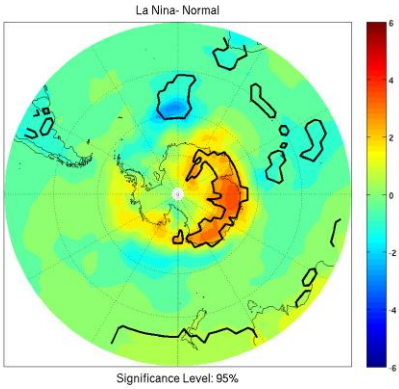

Figure 53: 2 meter temperature anomalies for SOI during September of La Niña.

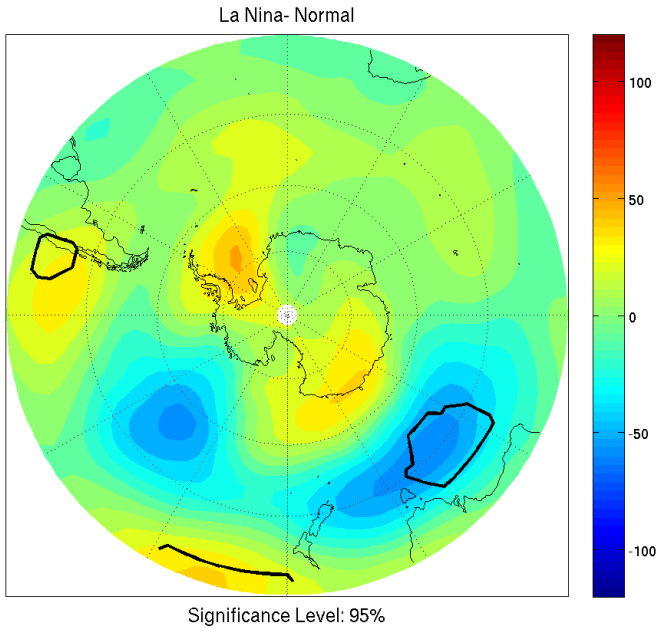

Figure 54: 500 hPa height anomalies for SOI during October of La Niña.

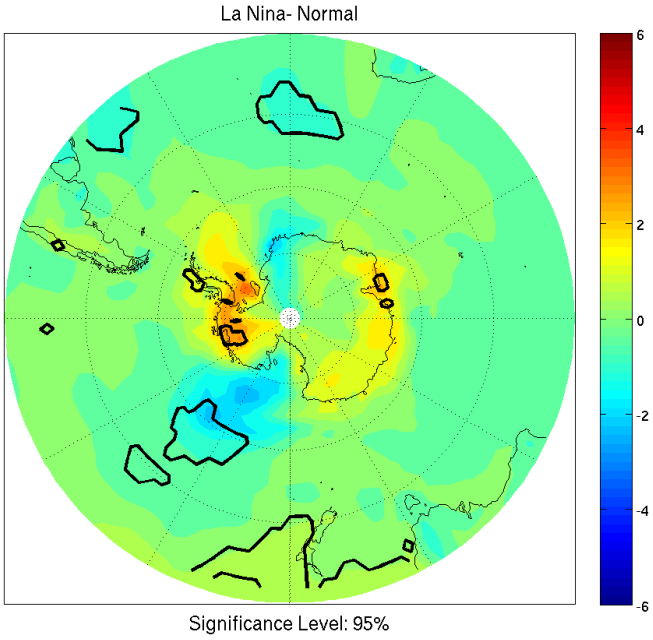

Figure 55: 2 meter temperature anomalies for SOI during October of La Niña.

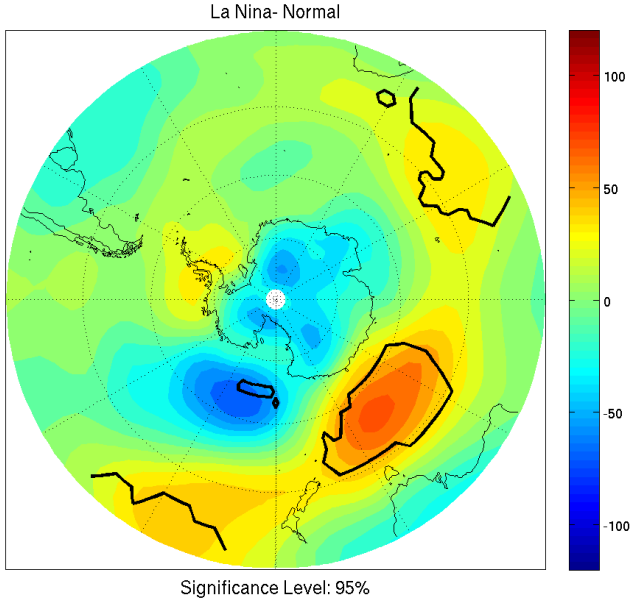

Figure 56: 500 hPa height anomalies for SOI during November of La Niña.

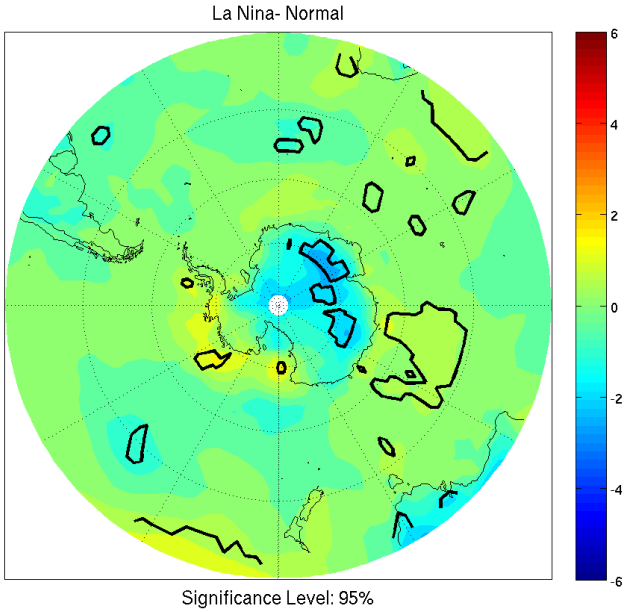

Figure 57: 2 meter temperature anomalies for SOI during November of La Niña.

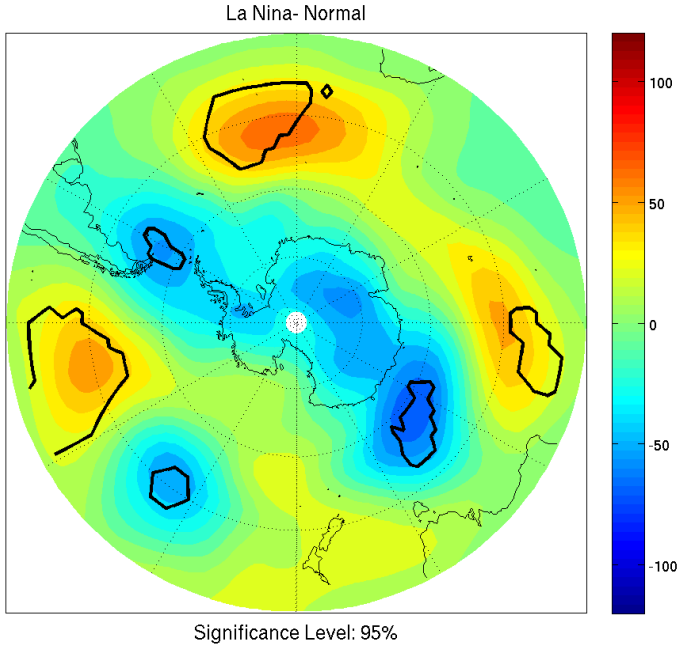

Figure 58: 500 hPa height anomalies for SOI during December of La Niña.

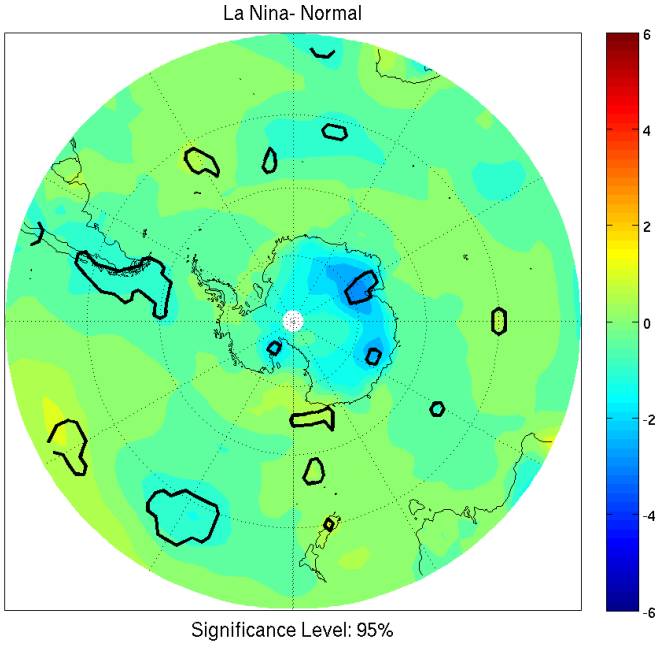

Figure 59: 2 meter temperature anomalies for SOI during December of La Niña.

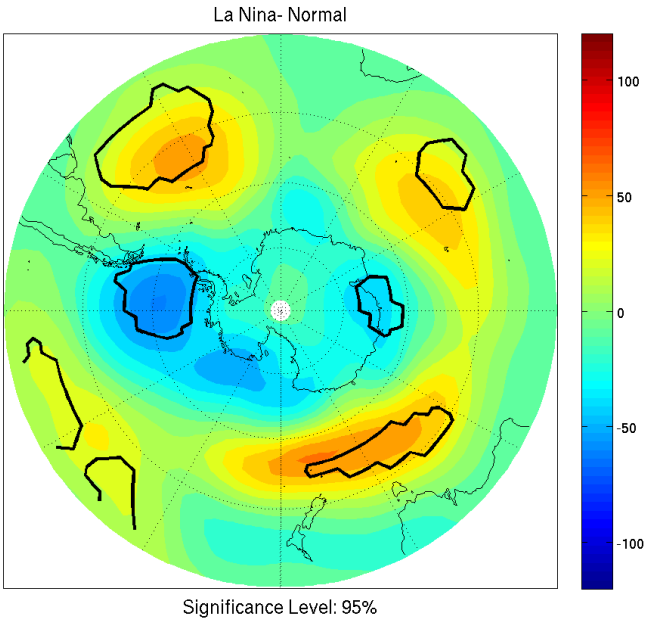

Figure 60: 500 hPa height anomalies for SOI during January of La Niña.

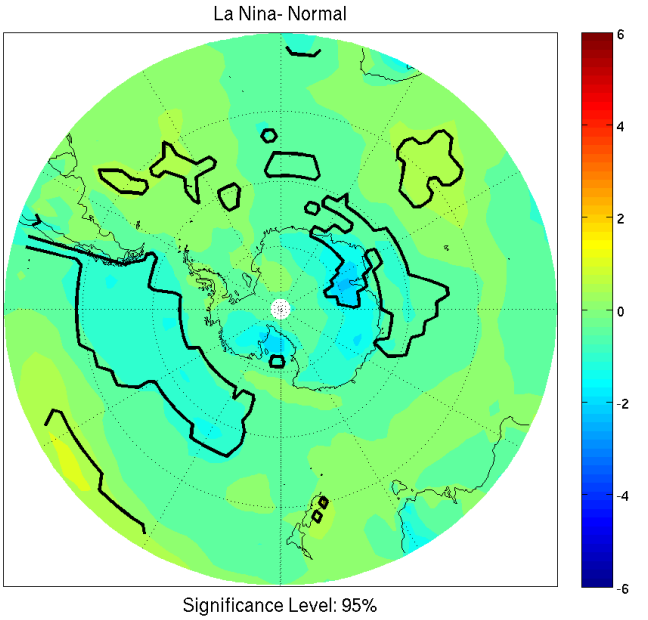

Figure 61: 2 meter temperature anomalies for SOI during January of La Niña.

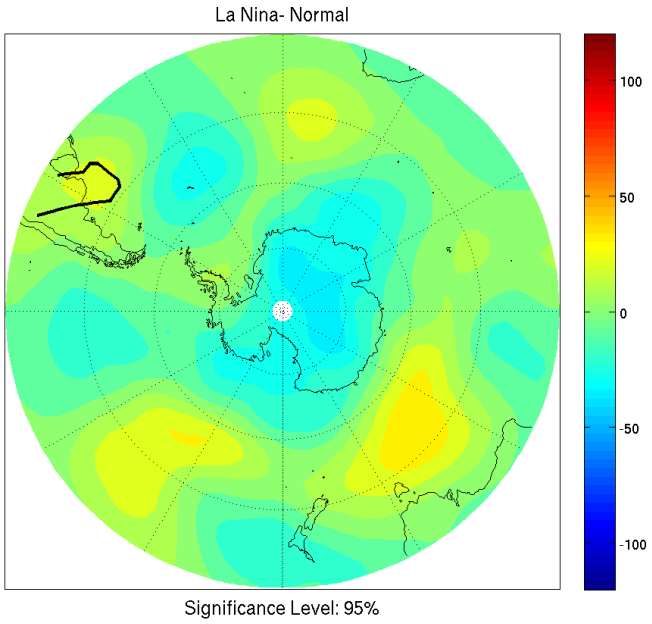

Figure 62: 500 hPa height anomalies for SOI during February of La Niña.

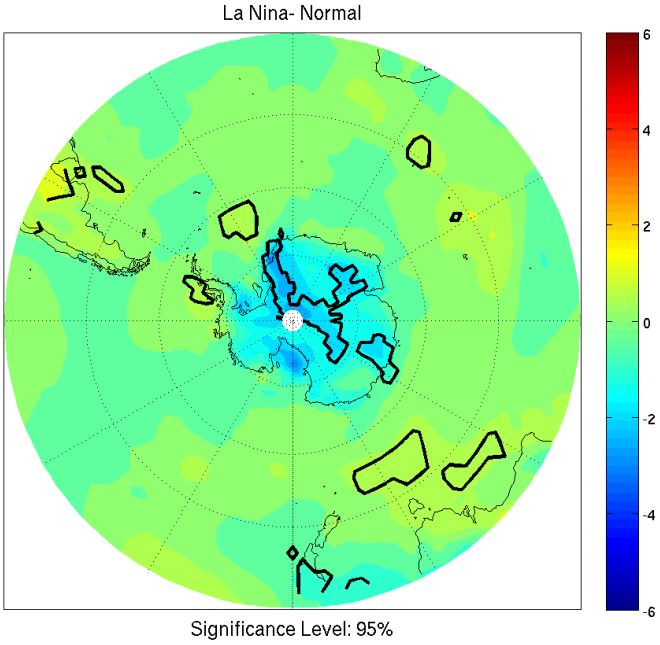

Figure 63: 2 meter temperature anomalies for SOI during February of La Niña.

4.2.2 ERA-Interim

The ERA-Interim composites have been analyzed, and compared with the various indices, as well as to the prior analysis of the ERA-40 composites. It has become evident that the MEI and ONI composites generally agreed more than either index agreed with SOI composites during similar periods. This is likely due to the increased variance in monthly composites and a difference in events chosen between the three different basis techniques used in compositing. Again, mean sea level pressure has not been shown in the interest of space and as it shows similar patterns to those indicated in the upper level composites with minor differences found in regions of significance.

4.2.2.A El Niño

4.2.2.A.1 ONI

As determined in the ERA-40, El Niño seemed to have a predominant effect of weakening the ABS low early in the analyzed period, which decreased as the end of period was approached. The SON to NDJ periods of

the ONI composites all show a distinct weakening of the ABS low with slight variability in the extent and degree of weakening (Figure 64; 65; 66). This is largely in agreement with the ERA-40 composites. The WS low has no significant changes, which slightly differs from the ERA-40 analysis. The DJF analysis differs considerably, as the region of significant upper level anomaly has moved distinctly off shore (Figure 67). This has an effect on the surface of heating the Ross Ice Shelf as well as Marie Byrd Land during the SON, OND, and NDJ periods. The DJF period has small regions of significant warming in the Ross Ice Shelf and Peninsula, but this is well removed from the significant upper level features (Figure 68; 69; 70; 71).

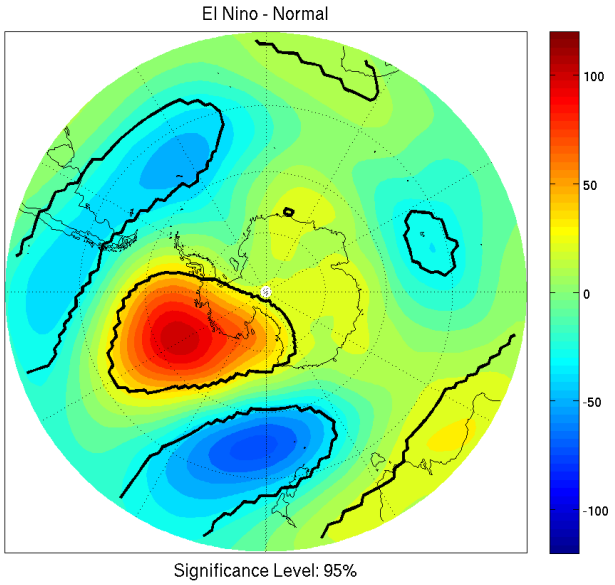

Figure 64: 500 hPa height anomalies for ONI during SON of El Nino.

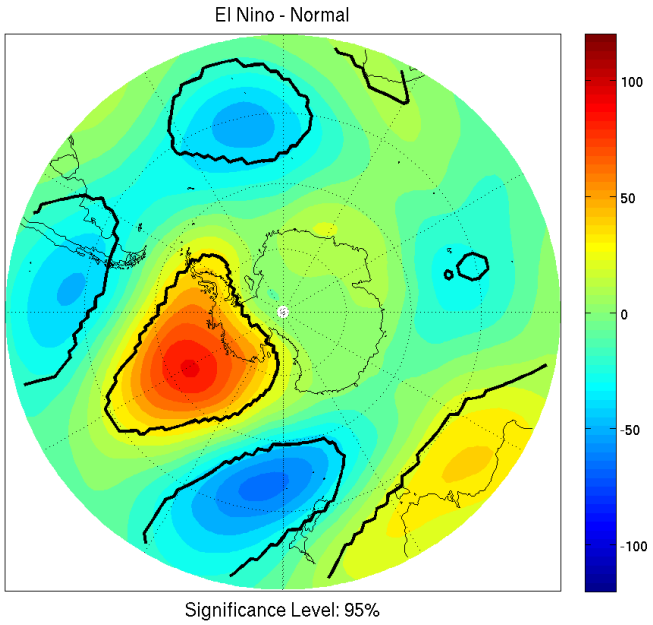

Figure 65: 500 hPa height anomalies for ONI during OND of El Niña.

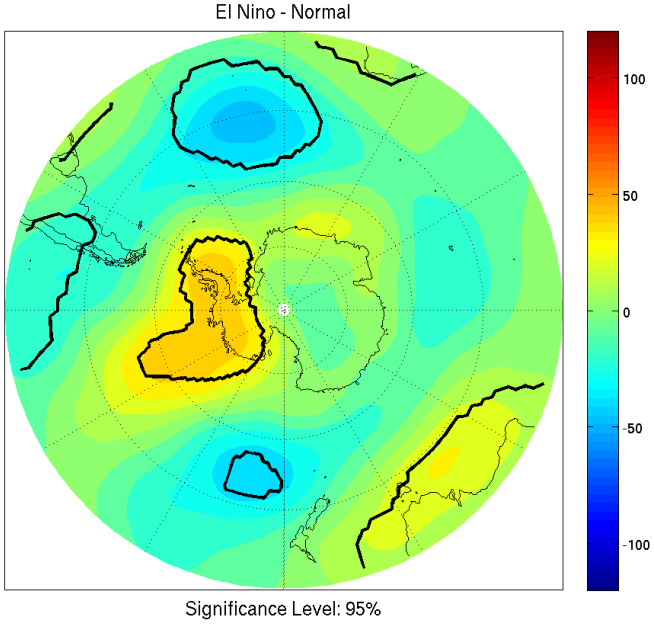

Figure 66: 500 hPa height anomalies for ONI during NDJ of El Niño.

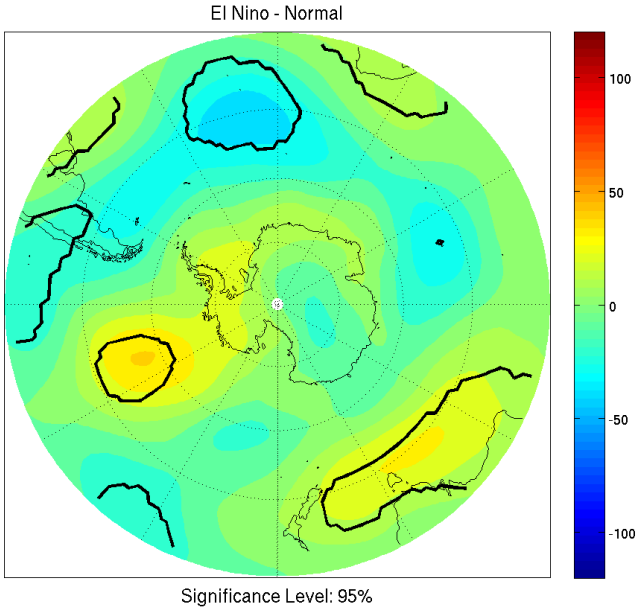

Figure 67: 500 hPa height anomalies for ONI during DJF of El Niño.

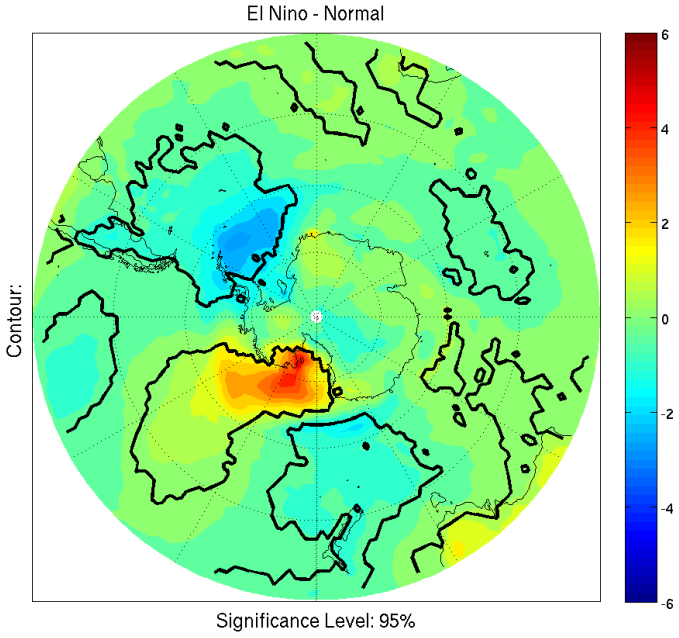

Figure 68: 2 meter temperature anomalies for ONI during SON of El Niño.

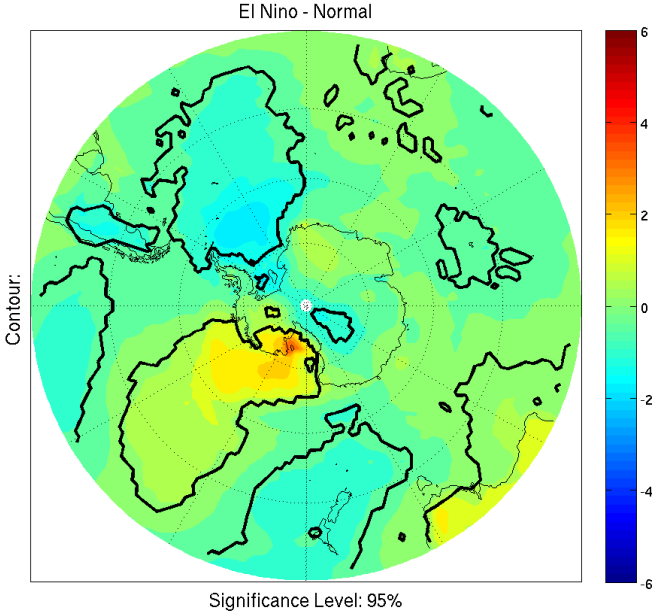

Figure 69: 2 meter temperature anomalies for ONI during OND of El Niño.

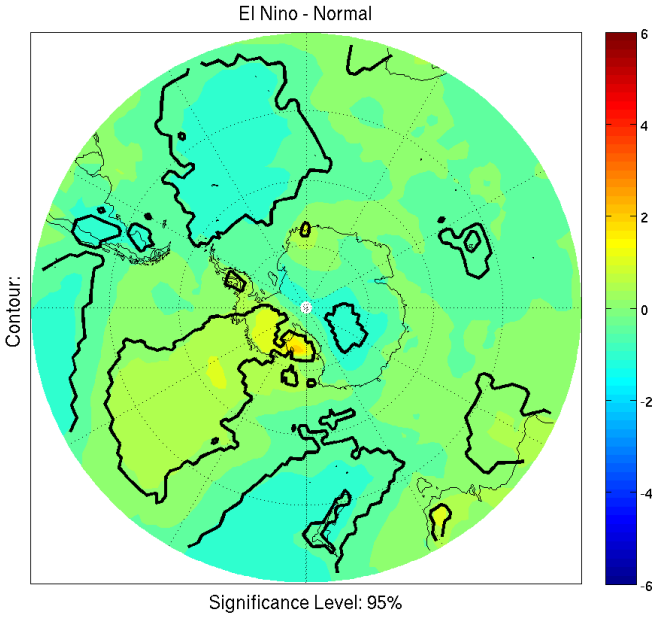

Figure 70: 2 meter temperature anomalies for ONI during NDJ of El Niño.

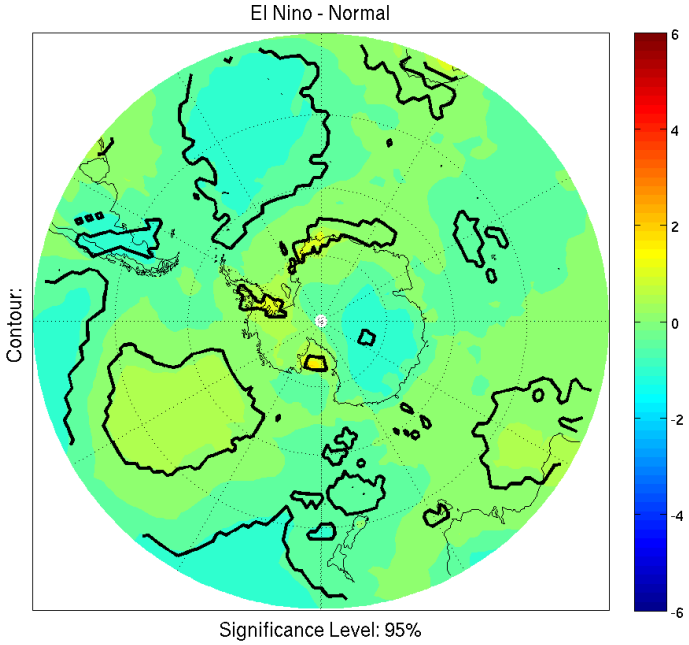

Figure 71: 2 meter temperature anomalies for ONI during DJF of El Niño.

4.2.2.A.2 MEI

The MEI composites generally agree between the ERA-interim and ERA-40 datasets, though the interim potentially shows a weaker signal. The pattern associated with WS low amplification is evident, though not significant, in the SO composite, but not within the ON, ND, DJ, or JF periods, with the JF period indicating mild negative height anomaly. The ABS low weakening is again the predominant feature noticeable within the

composites from SO to ND, while DJ and JF show weak positive height anomalies over the Peninsula (Figure 72; 73; 74; 75; 76). During SO and ON periods, the presence of cooling throughout the Weddell sea is significant, as is the warming within the Ross Ice Shelf associated with the weakened ABS low (Figure 77; 78). The ON and ND periods show distinct warming associated with the weakened ABS low throughout the Ross Ice Shelf and neighboring regions of Marie Byrd Land (Figure 78; and 79). The DJ period shows warming within the Peninsula, which seems to be associated with the small region of weakening in the WS low. There is also a region of significant cooling within Wilkes Land, though this is divorced from any upper level feature (Figure 80). The JF period had no significant temperature effects noticed on the continent (Figure 81).

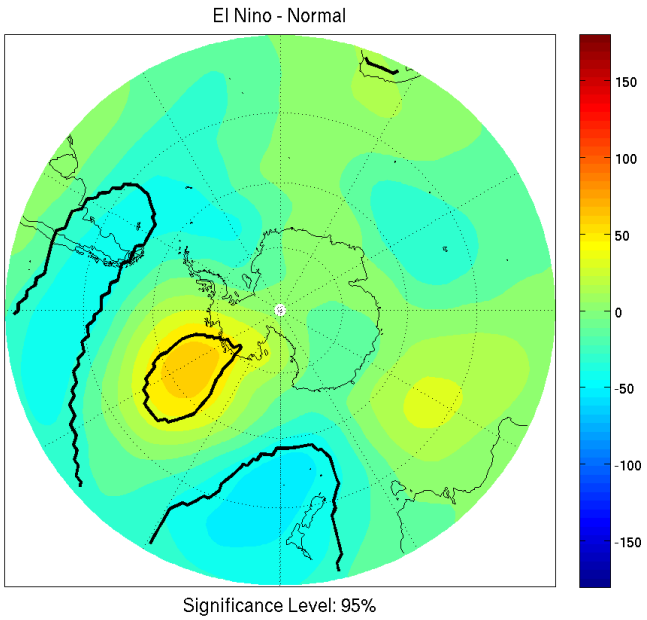

Figure 72: 500 hPa height anomalies for MEI during SO of El Niño.

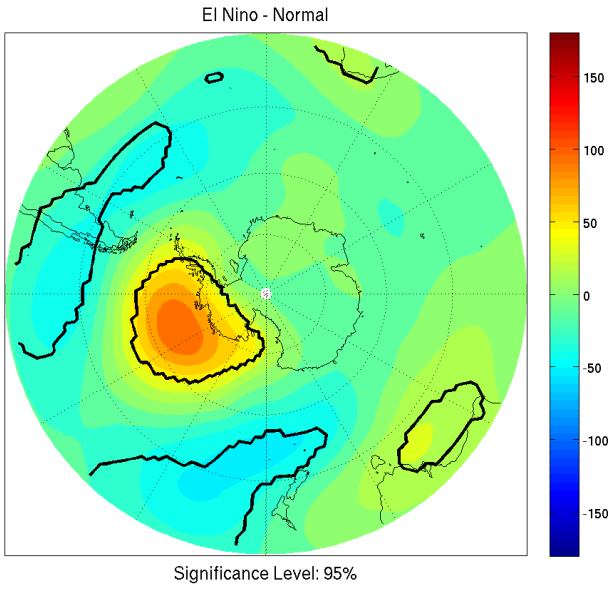

Figure 73: 500 hPa height anomalies for MEI during ON of El Niño.

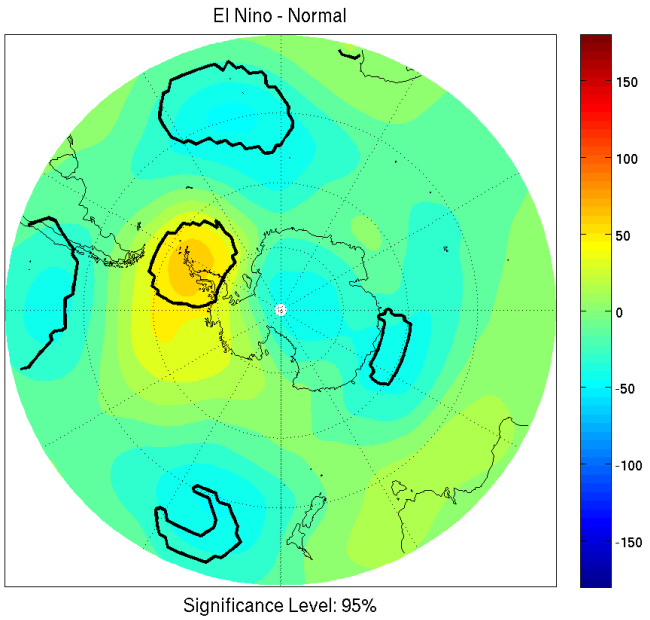

Figure 74: 500 hPa height anomalies for MEI during ND of El Niño.

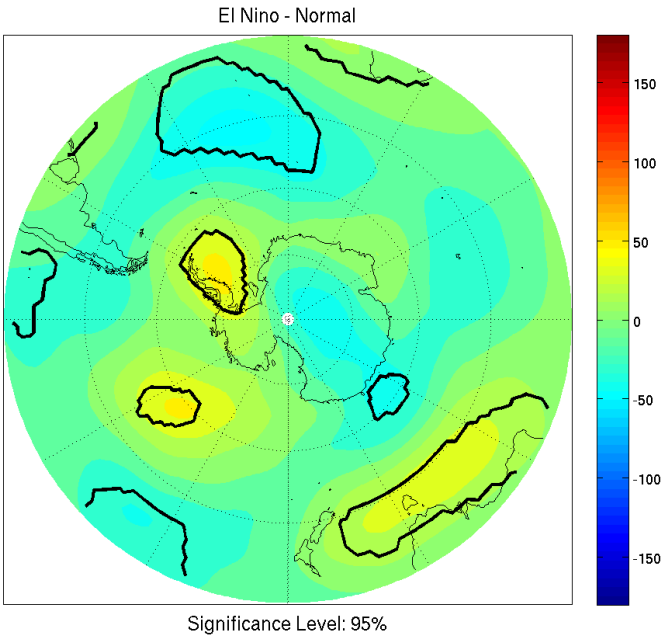

Figure 75: 500 hPa height anomalies for MEI during DJ of El Niño.

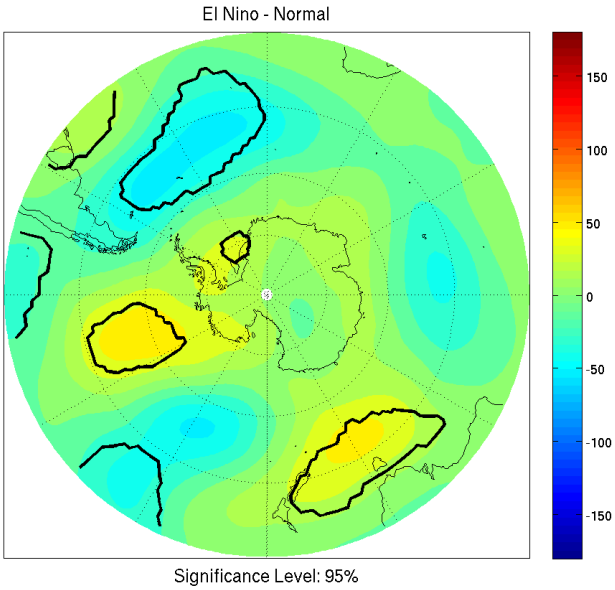

Figure 76: 500 hPa height anomalies for MEI during JF of El Niño.

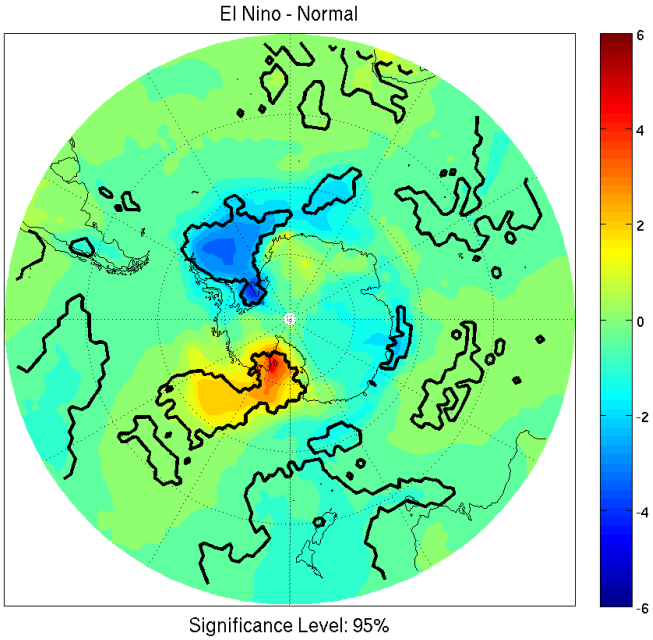

Figure 77: 2 meter temperature anomalies for MEI during SO of El Niño.

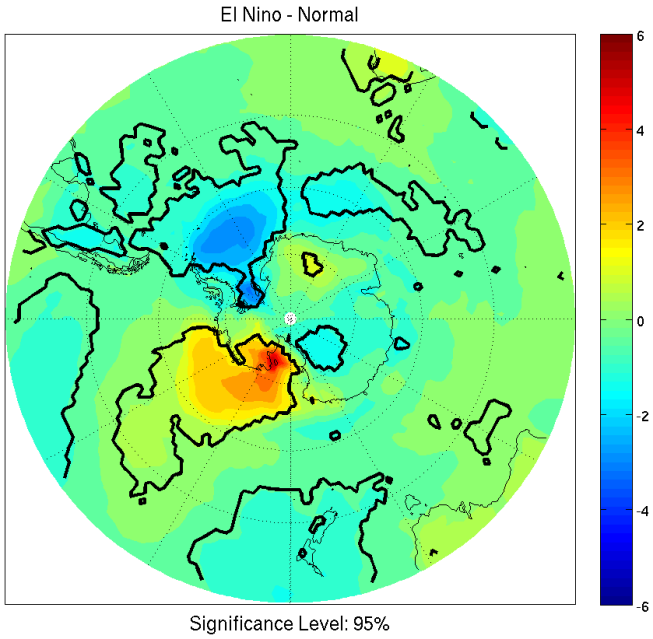

Figure 78: 2 meter temperature anomalies for MEI during ON of El Niño.

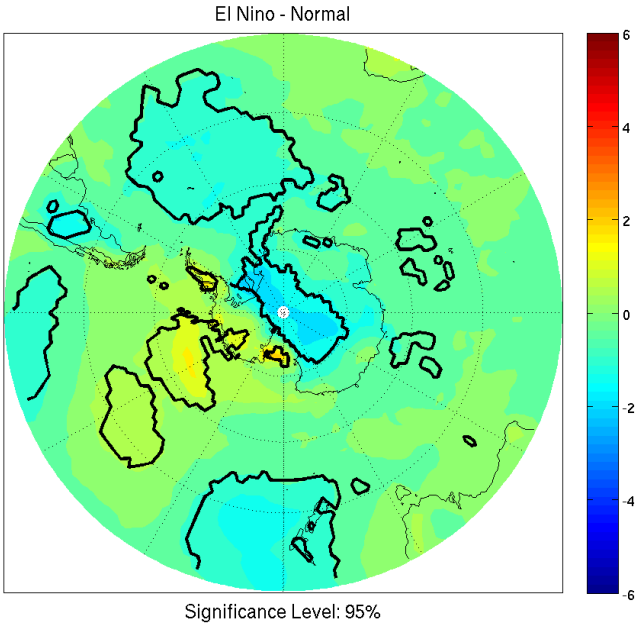

Figure 79: 2 meter temperature anomalies for MEI during ND of El Niño.

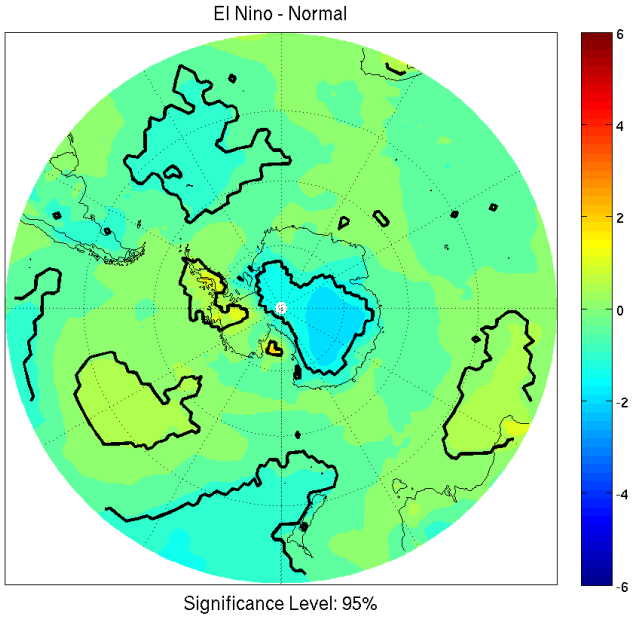

Figure 80: 2 meter temperature anomalies for MEI during DJ of El Niño.

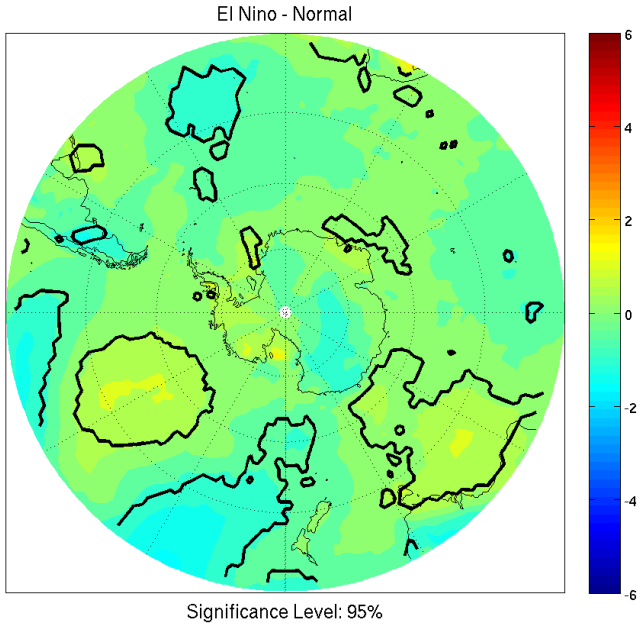

Figure 81: 2 meter temperature anomalies for MEI during JF of El Niño.

4.2.2.A.3 SOI

For the SOI composites, again there is a general lack of significance throughout the anticipated regions during the time period. Throughout the September, October, and November periods the expected pattern of anomalies is present, with a positive height anomaly in the ABS region and a negative height anomaly in the WS (Figure 82; 83; 84). The feature in the ABS region is significant in the November time period. There is also a significant negative height anomaly found throughout much of East Antarctica during the October time period. The East Antarctica features are associated with negative temperature anomalies in Wilkes Land and off the coast of Queen Maud Land (Figure 85; 86; 87). Throughout these three time periods, the ABS (WS) regions experience the expected warming (cooling) during both October and November. Queen Maud Land, directly adjacent to the WS experiences warming during the September period. The November period also indicates warming throughout portions of Wilkes Land and Queen Maud Land. This surface region is directly under a positive height anomaly at upper levels that is not found to be significant. The December, January, and February time periods show distinctly less of the expected

signal, with little effect on Antarctic surface temperature (Figure 88; 89; 90; 91; 92; 93). January shows a weak return of the expected signal in the ABS region, though it is shifted toward the Ross Ice Shelf, and off shore. Other periods lack significance or the expected signal. During these time periods the more significant feature is the weakening of the ABS low, while the WS low amplification is present only a small amount of time, and is distinctly less likely to be significant. This is in general agreement with the ERA-40 analysis, which indicates the WS low is potentially found more predominantly in austral winter, or during La Niña events.

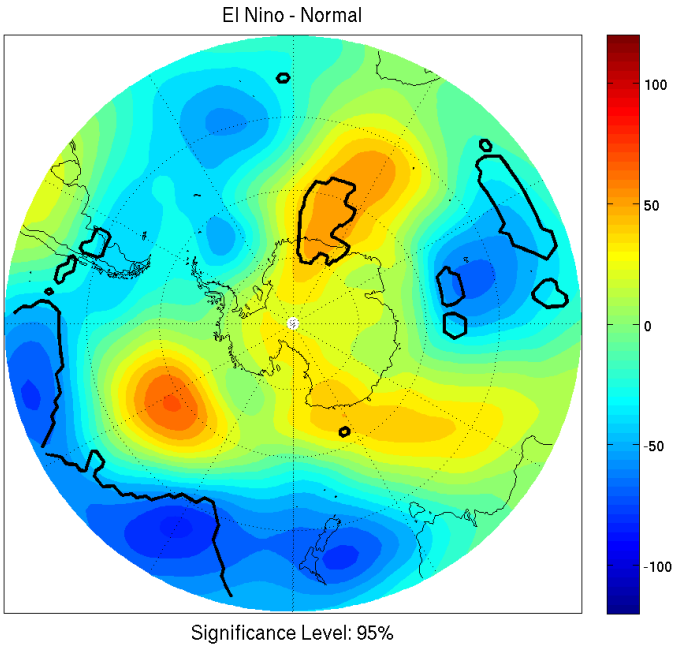

Figure 82: 500 hPa height anomalies for SOI during September of El Niño.

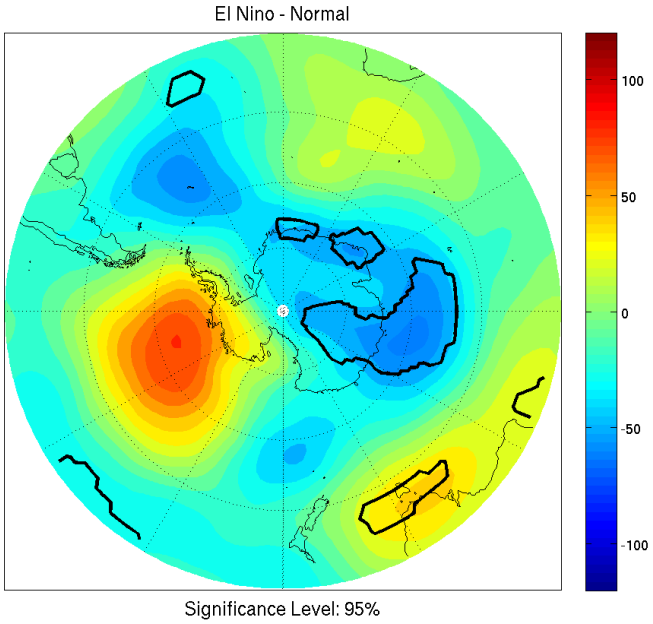

Figure 83: 500 hPa height anomalies for SOI during October of El Niño.

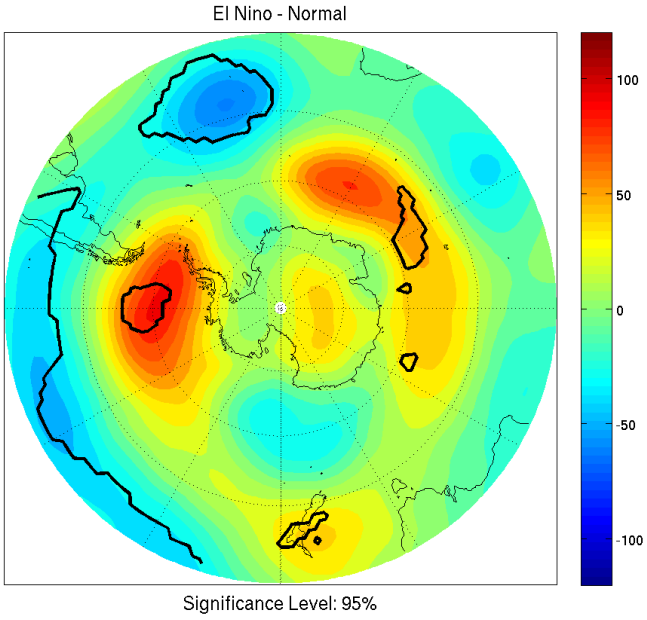

Figure 84: 500 hPa height anomalies for SOI during November of El Niño.

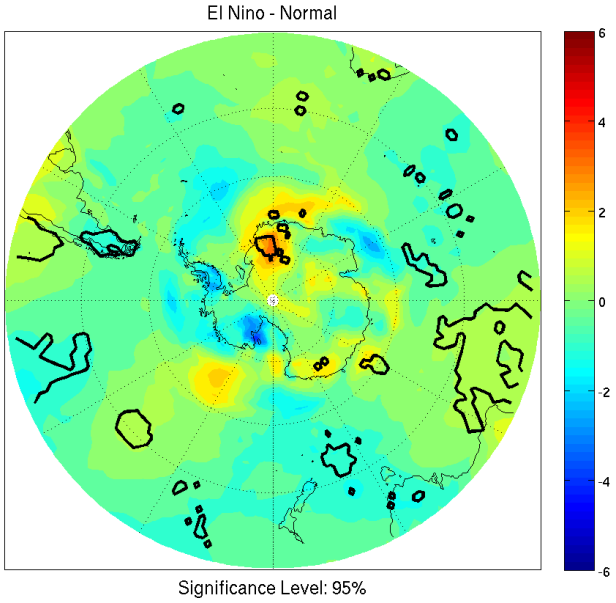

Figure 85: 2 meter temperature anomalies for SOI during September of El Niño.

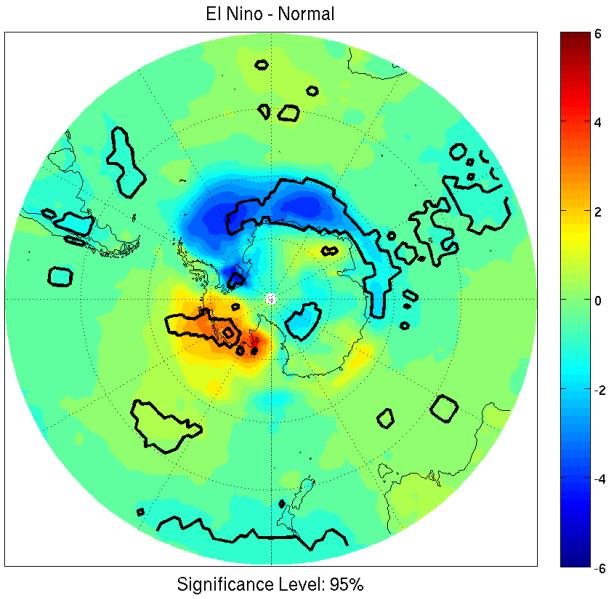

Figure 86: 2 meter temperature anomalies for SOI during October of El Niño.

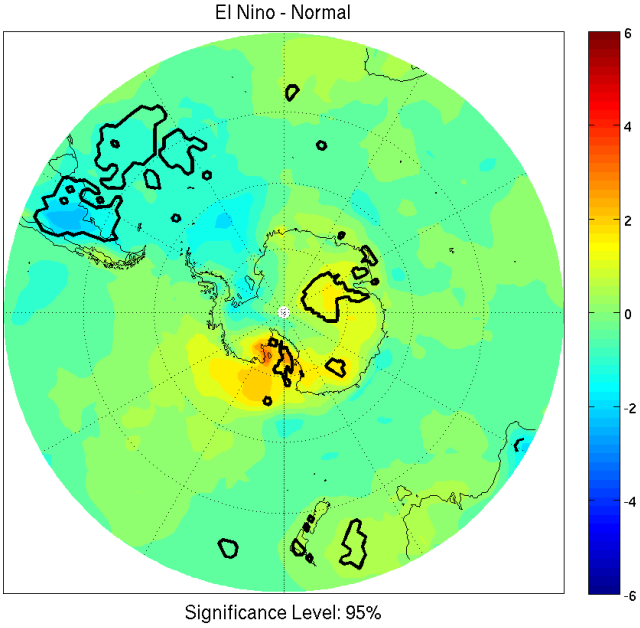

Figure 87: 2 meter temperature anomalies for SOI during November of El Niño.

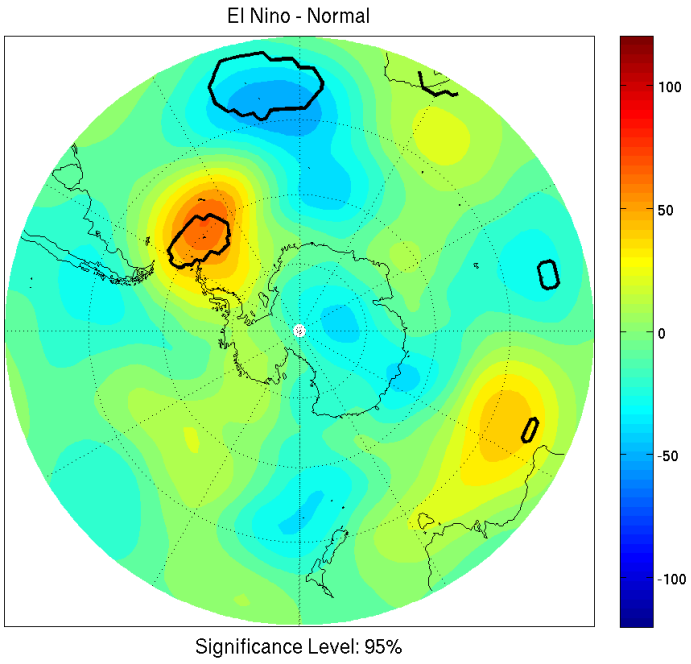

Figure 88: 500 hPa height anomalies for SOI during December of El Niño.

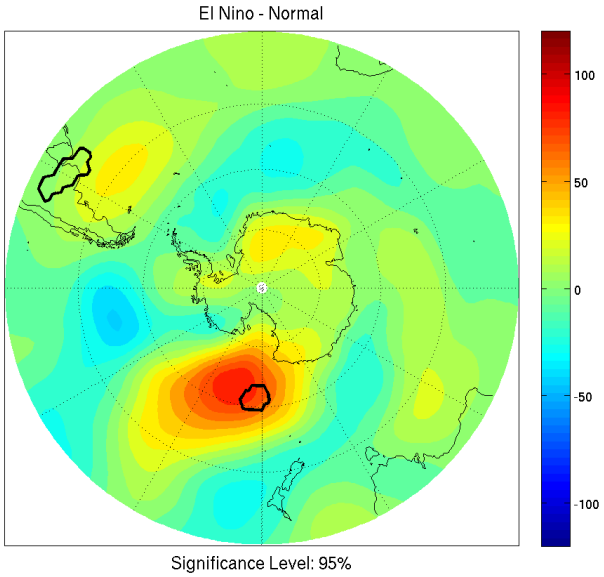

Figure 89: 500 hPa height anomalies for SOI during January of El Niño.

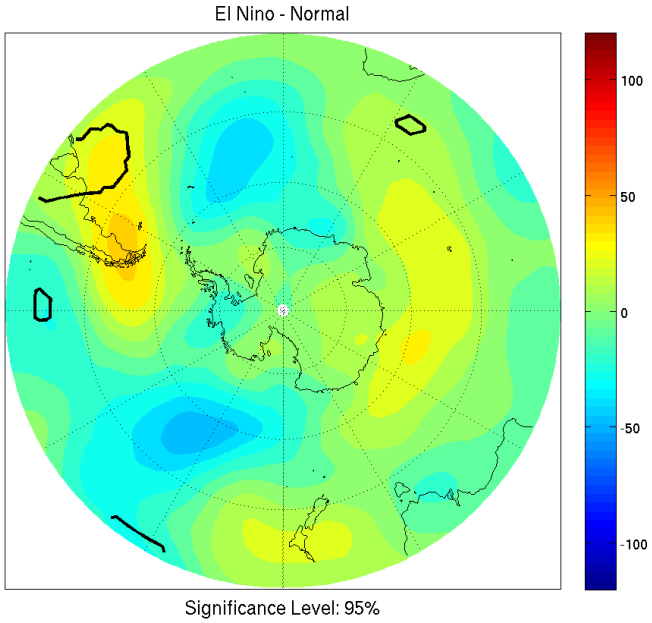

Figure 90: 500 hPa height anomalies for SOI during February of El Niño.

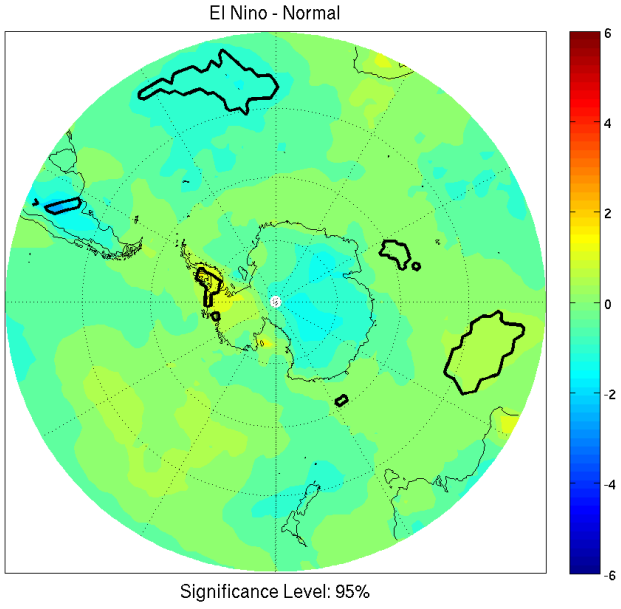

Figure 91: 2 meter temperature anomalies for SOI during December of El Niño.

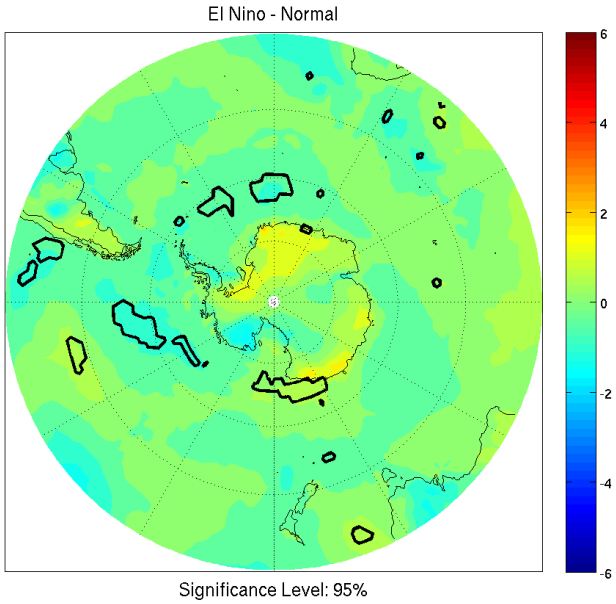

Figure 92: 2 meter temperature anomalies for SOI during January of El Niño.

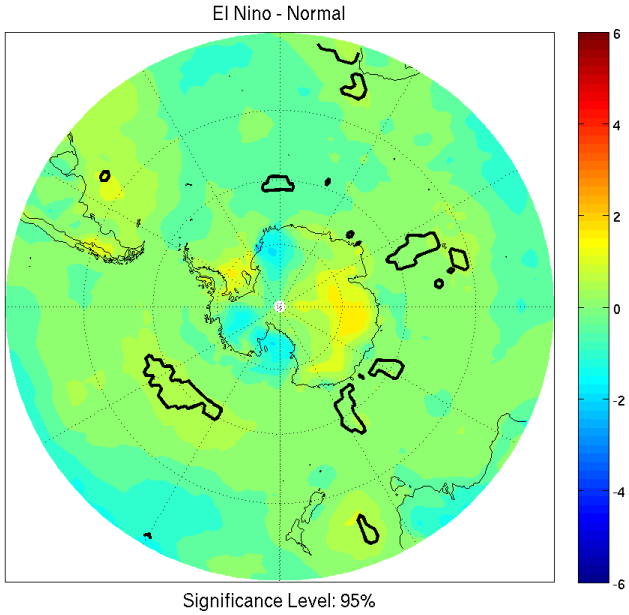

Figure 93: 2 meter temperature anomalies for SOI during February of El Niño.

4.2.2.B La Niña

The ERA-40 indicated the early periods of SON had a lack of distinct teleconnection, and the features gradually moved into the expected regions of ABS and WS before shifting to affect East Antarctica more strongly. This pattern is generally represented again in the ERA-Interim. There is some indication of a stronger and larger significant signal for La Niña, which could be due to differences in the model, or potentially it could be due to interactions with the SAM, which has been trending positive most strongly in austral summer (Marshall 2003).

4.2.2.B.1 ONI

The ONI composite analysis for SON shows much the same pattern as that seen in the ERA-40 with a negative height anomaly situated well off coast and a non-significant positive anomaly located throughout the ABS region. This differs from the ERA-40 in that the positive height anomaly is not significant (Figure 94). The surface temperature shows little effect in these regions, though there is a region of negative anomaly near the South

Pole (Figure 95). The OND time period shows the expected pattern of ABS low amplification and WS low weakening, but there is no significance. Also of note is the negative anomaly that extends from the ABS region throughout much of the continent with two centers of negative anomaly (Figure 96). There is little significant change in the West Antarctic surface temperatures, while East Antarctica indicates weak, but significant, cooling (Figure 97).

The NDJ period again shows the expected pattern, though the negative height anomaly does extend further on coast, as well as into Wilkes Land, and the weakening of the WS low remains not significant (Figure 98). East Antarctic cooling remains the largest surface feature, with regions of significant cooling also appearing in Marie Byrd Land (Figure 99). The DJF period shows a strong two lobed pattern of negative height anomaly, with one lobe situated over East Antarctica, and the other throughout the Ross Ice Shelf and ABS regions, with the Transantarctic Mountains seemingly splitting the two lobes. The positive anomaly remains within the WS region, though again it remains non-significant (Figure 100). The cooling throughout East Antarctica is again the predominant feature, though the presence of significant warming in the WS and in Marie Byrd Land is also of note (Figure 101).

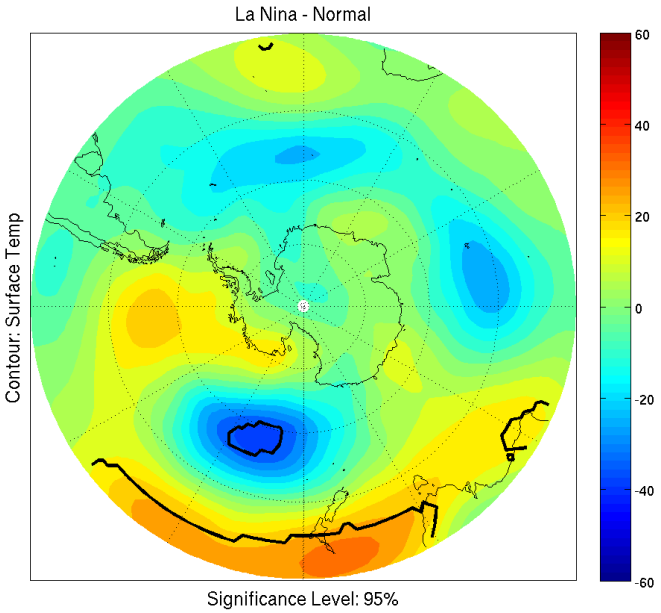

Figure 94: 500 hPa height anomalies for ONI during SON of La Niña.

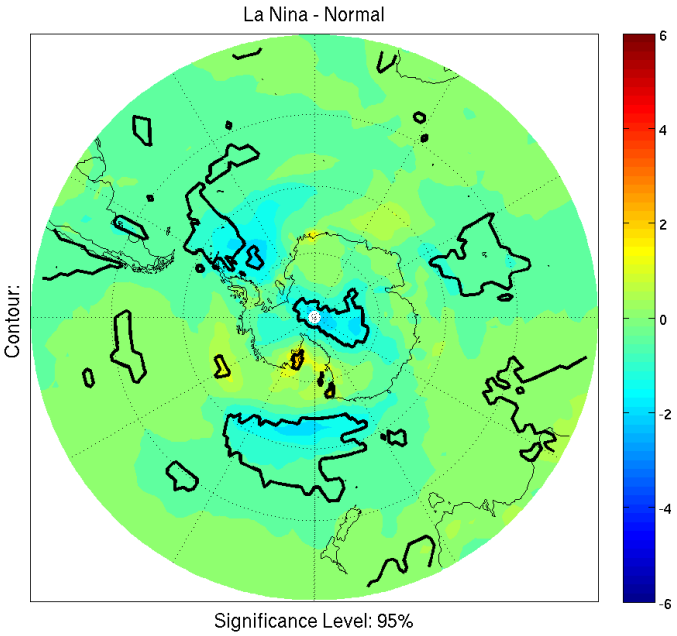

Figure 95: 2 meter temperature anomalies for ONI during SON of La Niña.

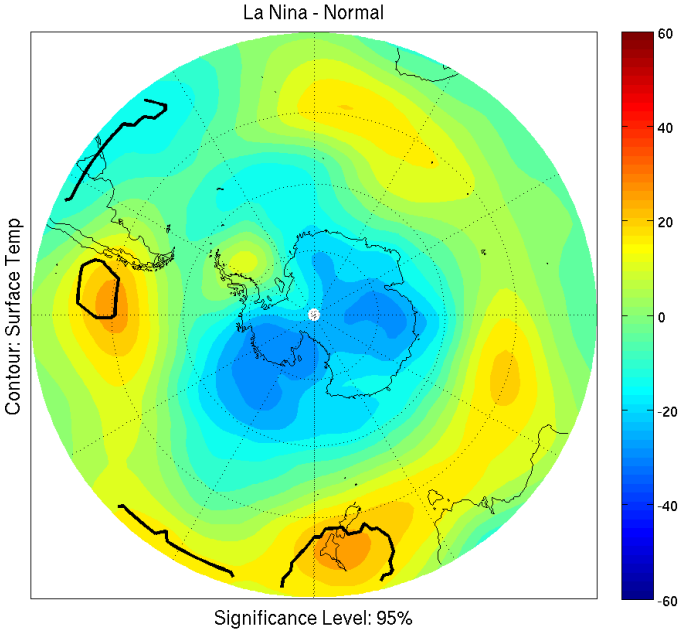

Figure 96: 500 hPa height anomalies for ONI during OND of La Niña.

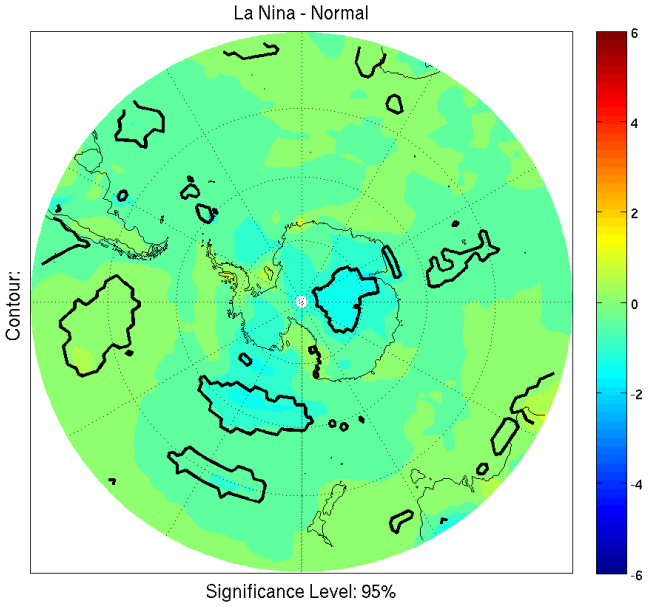

Figure 97: 2 meter temperature anomalies for ONI during OND of La Niña.

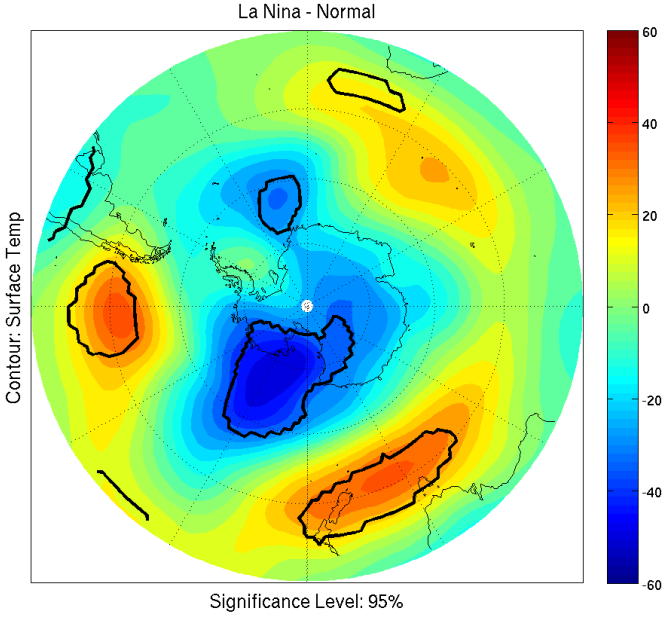

Figure 98: 500 hPa height anomalies for ONI during NDJ of La Niña.

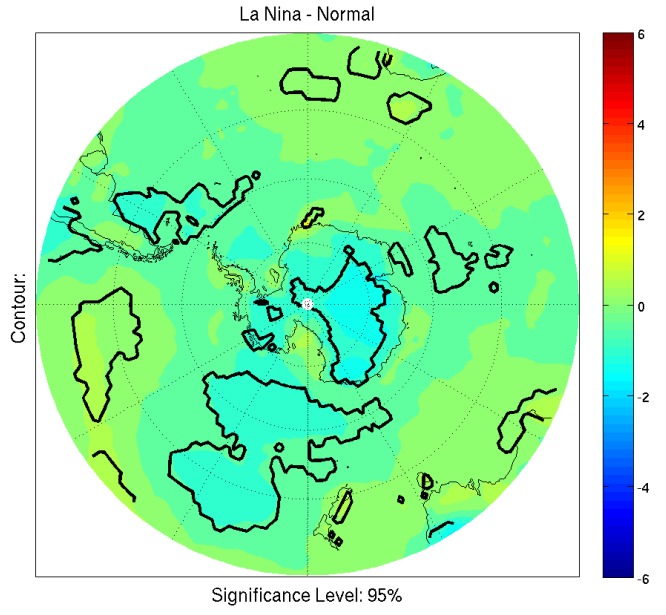

Figure 99: 2 meter temperature anomalies for ONI during NDJ of La Niña.

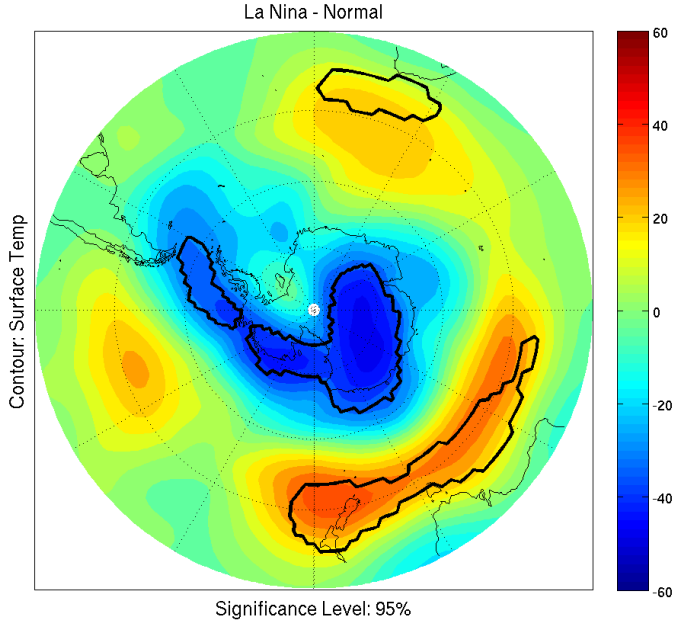

Figure 100: 500 hPa height anomalies for ONI during DJF of La Niña.

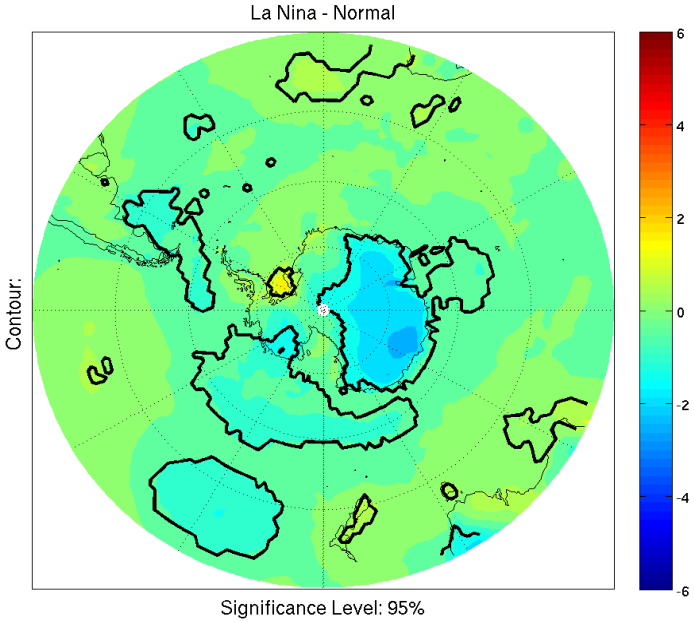

Figure 101: 2 meter temperature anomalies for ONI during DJF of La Niña.

4.2.2.B.2 MEI

The MEI indicates the SO negative height anomaly is closer to the continent than the analysis of the ONI, and it also indicates a less prevalent positive height anomaly, though both are not significant (Figure 102). As there is no significant upper level feature, the expectation is no distinct features, and this is the case with small regions of warming along the Ross Ice Shelf side of the Transantarctic Mountains, and cooling in portions of East Antarctica (Figure 103). The ON period shows the expected pattern lacks significance, though there is a weak negative anomaly located inland in East Antarctica (Figure 104). This feature is directly above a weak negative temperature anomaly at the surface, which is the predominant temperature signal (Figure 105).

The ND period shows a significant amplification of the ABS low, with the negative anomalies also being significant throughout the Ross Ice Shelf, extending through the South Pole and into Queen Maud Land bordering the not significant weakening of the WS low (Figure 106). This lines up with cooling along the Queen Maud Land coast of the WS, though there is no significant signal throughout Marie Byrd Land (Figure 107). During the DJ

period two negative height anomalies are noted, one over East Antarctica and the second over the expected ABS region (Figure 108). Both bring significant cooling throughout East Antarctica as well as Marie Byrd Land (Figure 109). The JF period shows a dramatic drop off in significant signal at upper levels and for surface temperatures (Figure 110). There is a region of negative temperature anomaly throughout Wilkes Land, primarily focused in coastal regions (Figure 111).

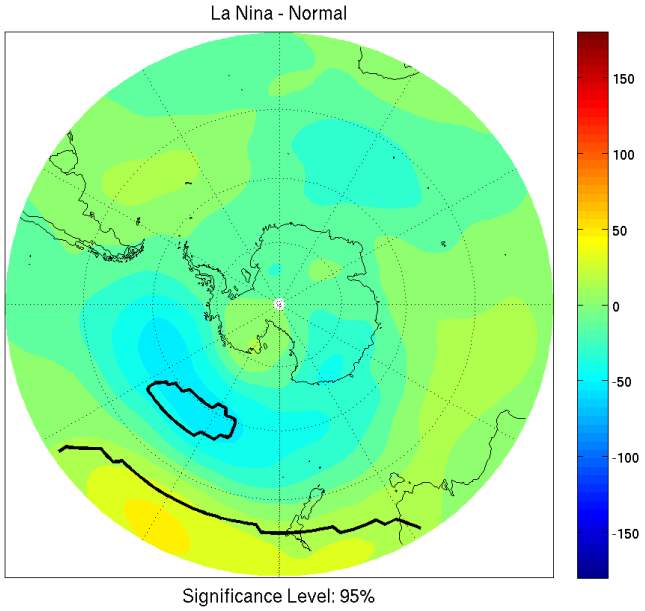

Figure 102: 500 hPa height anomalies for MEI during SO of La Niña.

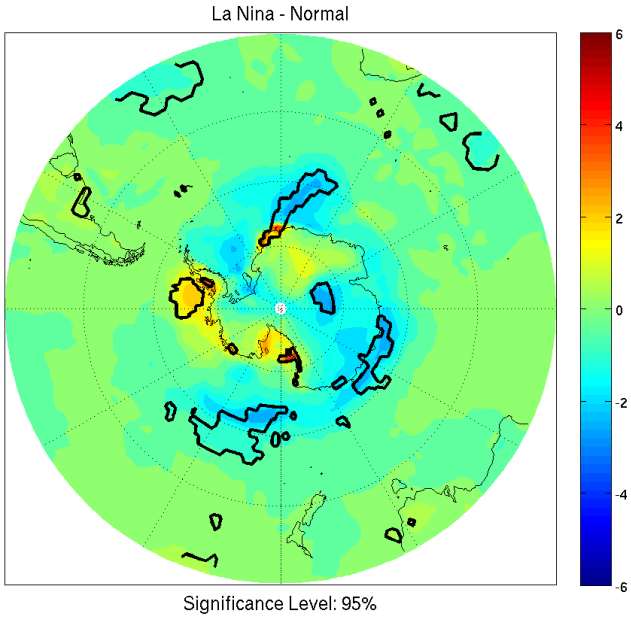

Figure 103: 2 meter temperature anomalies for MEI during SO of La Niña.

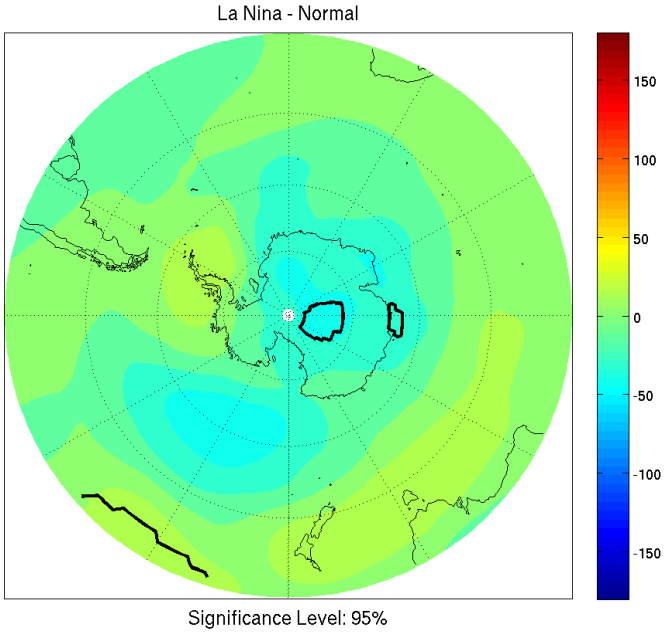

Figure 104: 500 hPa height anomalies for MEI during ON of La Niña.

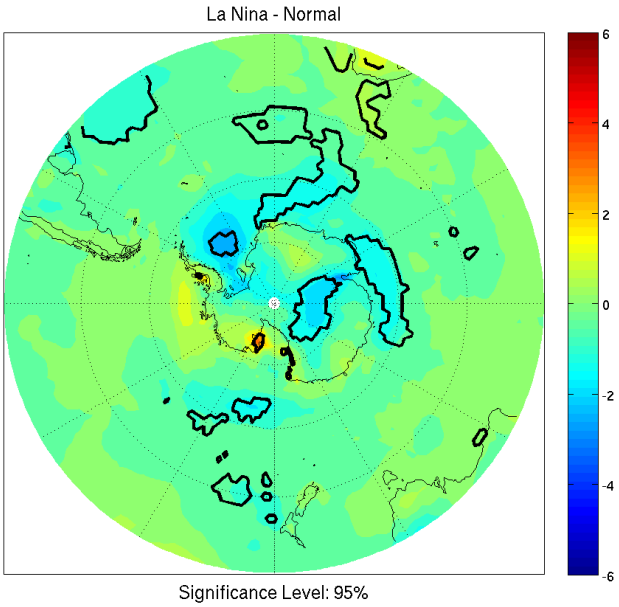

Figure 105: 2 meter temperature anomalies for MEI during ON of La Niña.

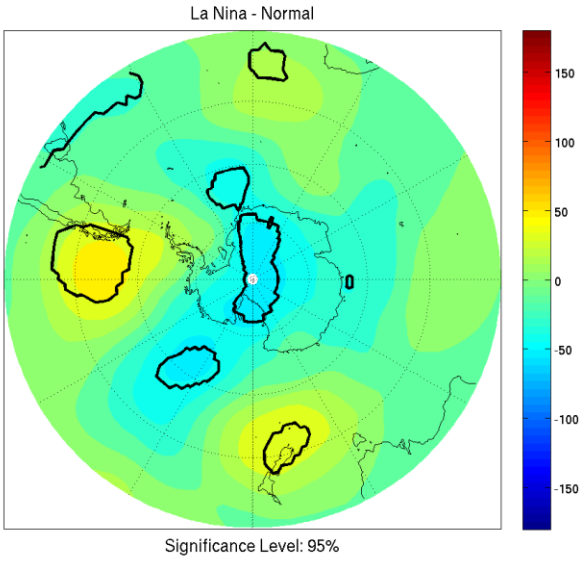

Figure 106: 500 hPa height anomalies for MEI during ND of La Niña.

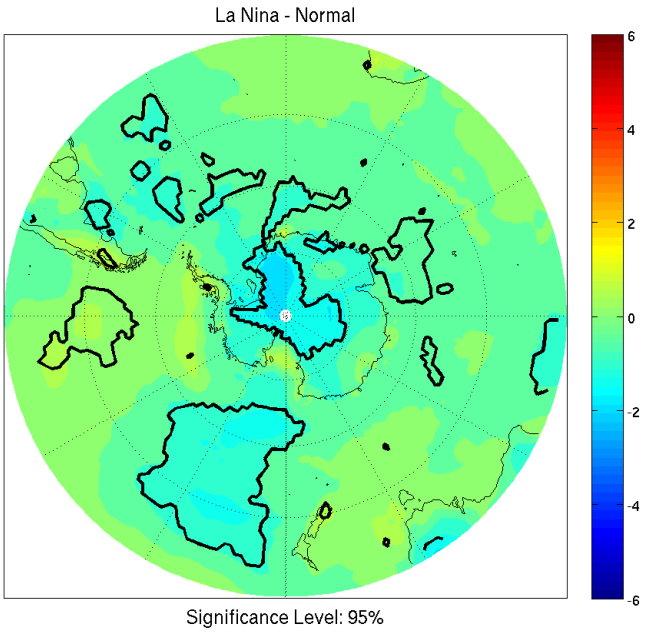

Figure 107: 2 meter temperature anomalies for MEI during ND of La Niña.

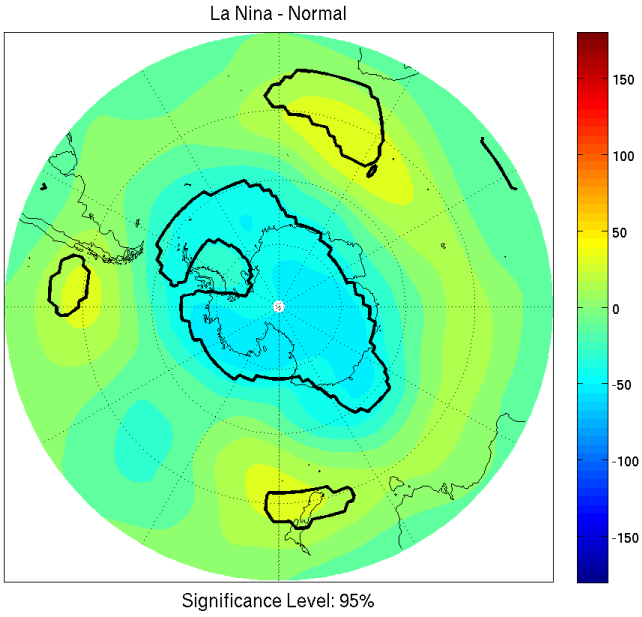

Figure 108: 500 hPa height anomalies for MEI during DJ of La Niña.

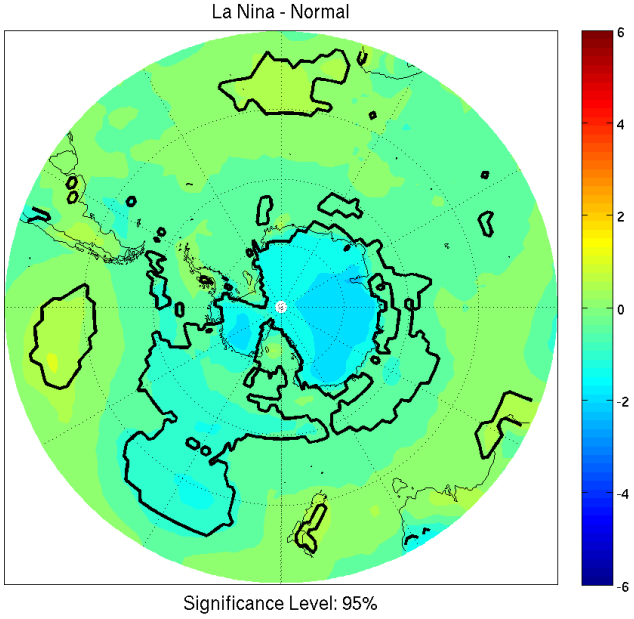

Figure 109: 2 meter temperature anomalies for MEI during DJ of La Niña.

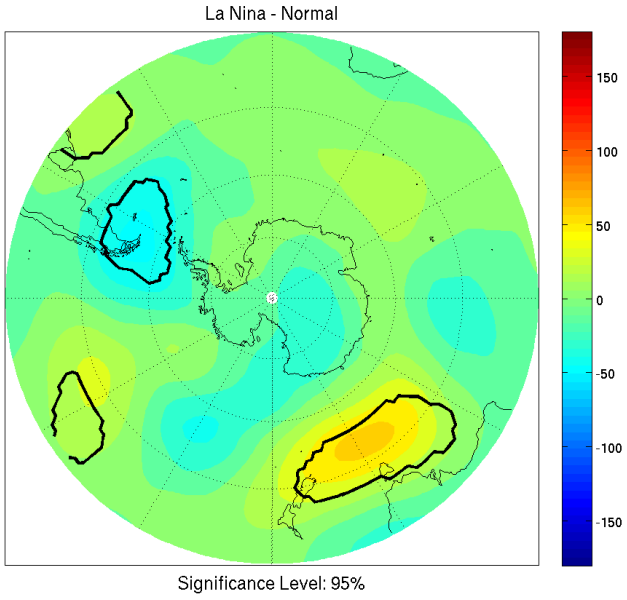

Figure 110: 500 hPa height anomalies for MEI during JF of La Niña.

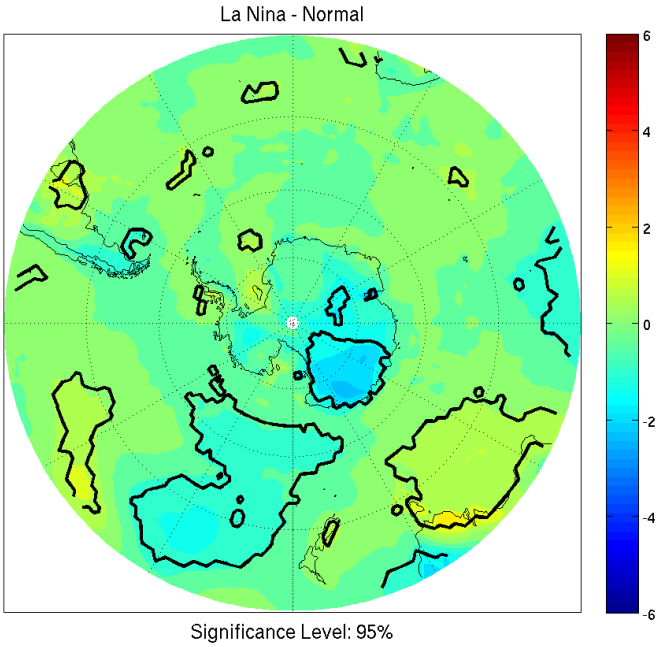

Figure 111: 2 meter temperature anomalies for MEI during JF of La Niña.

4.2.2.B.3 SOI

Unexpectedly, the SOI composites in the earlier portion of the analyzed season show more of the expected pattern than the MEI or ONI, though there still is a lack of consistent significance. In the September time period, there is the expected pattern of alternating highs and lows indicating an amplification of the ABS low, and a weakening of the WS low, but only a small region of the WS region is significant. A much larger region of coastal Queen Maud Land experiences a positive height anomaly during this period (Figure 112). This region of Queen Maud Land also experiences significant warming, while other regions lack significance (Figure 113). During October the ABS region experiences a more prominent, though still not significant negative anomaly, while the WS region positive anomaly is weakened and loses significance. Queen Maud Land and coastal Wilkes Land experience stronger, significant negative height anomalies (Figure 114). The surface shows a less distinct pattern than anticipated, as there is only a small region of warming in coastal Marie Byrd Land, and cooling adjacent to the WS in Queen Maud Land (Figure 115).

November is the first month where the ABS region experiences a

significant negative anomaly. This is also the only distinct anomaly during this period (Figure 116). Despite this upper level feature, there is no discernible pattern in the surface temperatures (Figure 117). December, January and February all indicate weak negative anomalies throughout the ABS region, which generally lack in significance, and no other distinct patterns in high latitudes (Figure 118; 119; 120). Surface temperatures experience only small regions of cooling in Marie Byrd Land and the Ross Ice Shelf during these time periods (Figure 121; 122; 123).

The MEI and ONI composites generally agreed, indicating a progression of the negative height anomaly from far off shore moving onshore, then having an increasing effect in East Antarctica, while remaining strong in West Antarctica. Throughout this progression there is a lack of significance, though a pattern of positive height anomalies is generally found within the WS region. The SOI indicates a more expected pattern throughout the ABS and WS regions, though they lack significance, and a different timing of effects in East Antarctica.

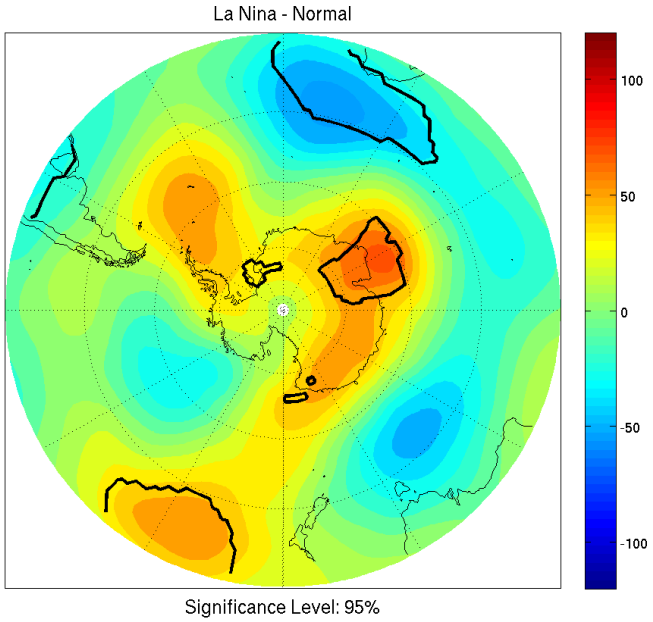

Figure 112: 500 hPa height anomalies for SOI during September of La Niña.

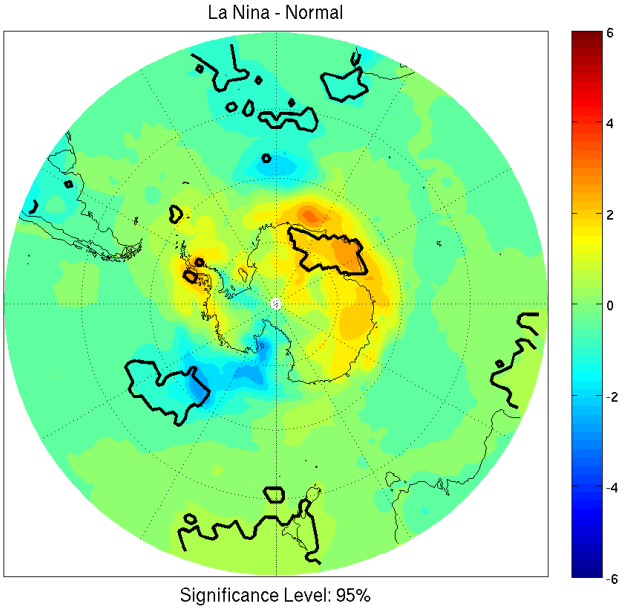

Figure 113: 2 meter temperature anomalies for SOI during September of La Niña.

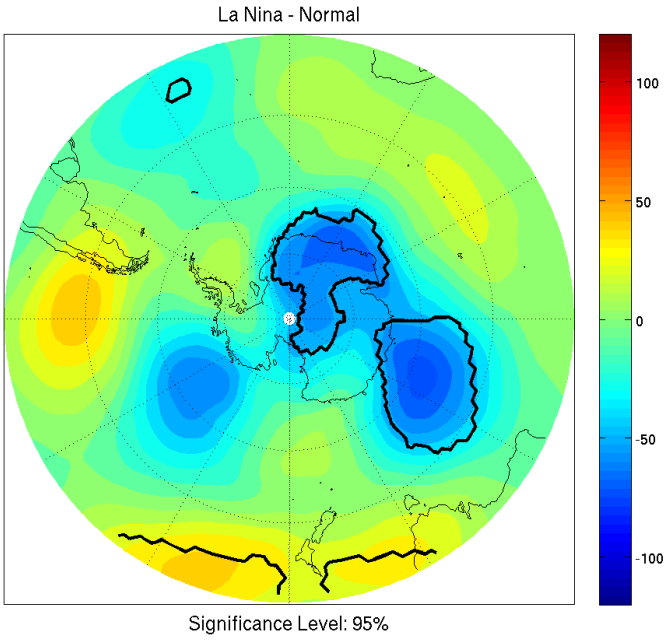

Figure 114: 500 hPa height anomalies for SOI during October of La Niña.

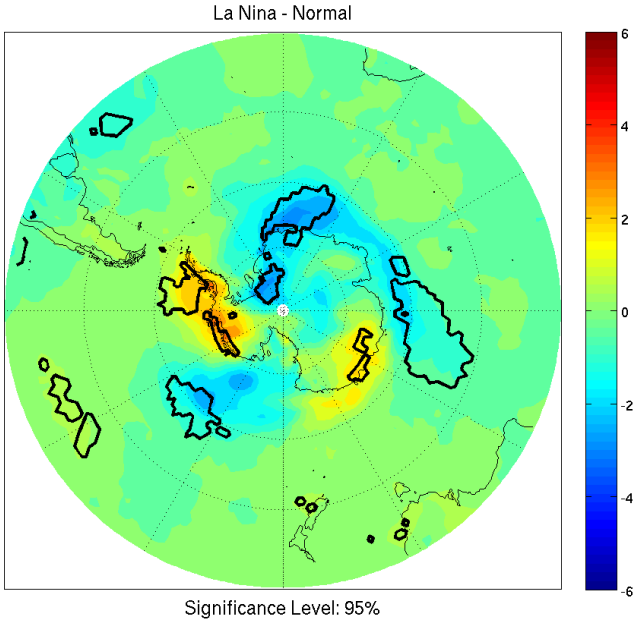

Figure 115: 2 meter temperature anomalies for SOI during October of La Niña.

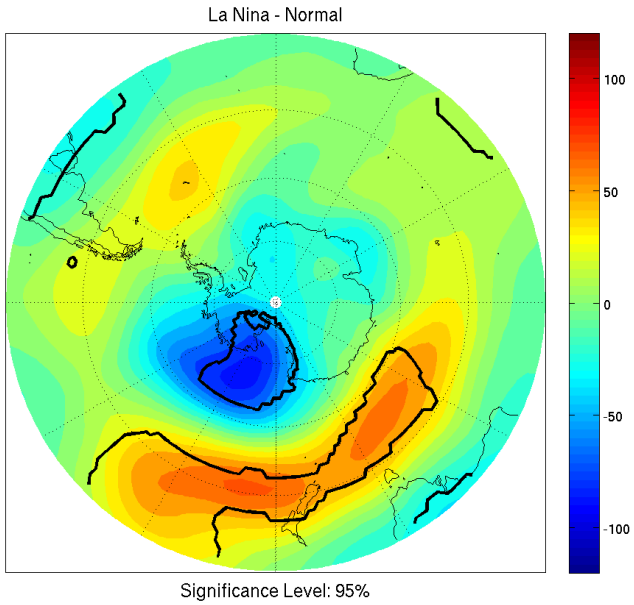

Figure 116: 500 hPa height anomalies for SOI during November of La Niña.

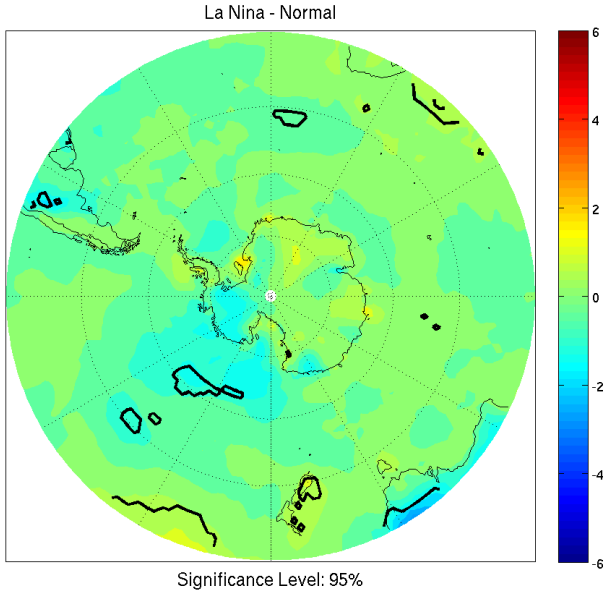

Figure 117: 2 meter temperature anomalies for SOI during November of La Niña.

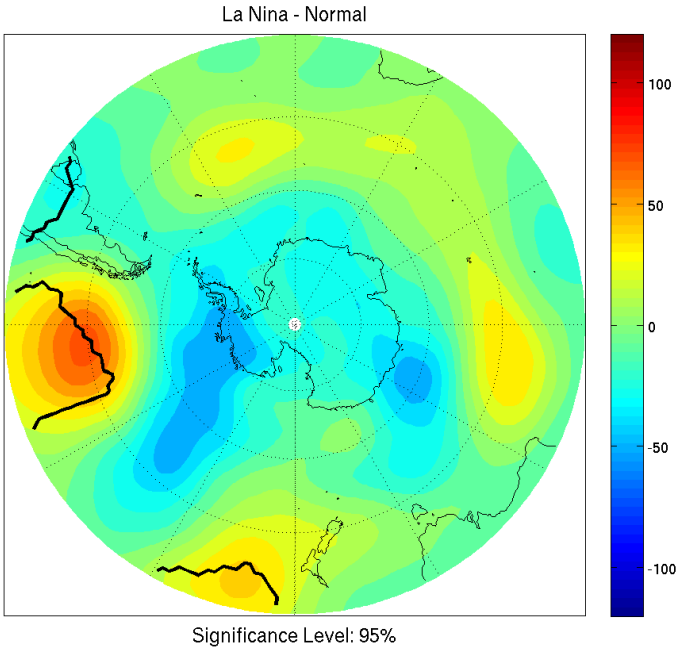

Figure 118: 500 hPa height anomalies for SOI during December of La Niña.

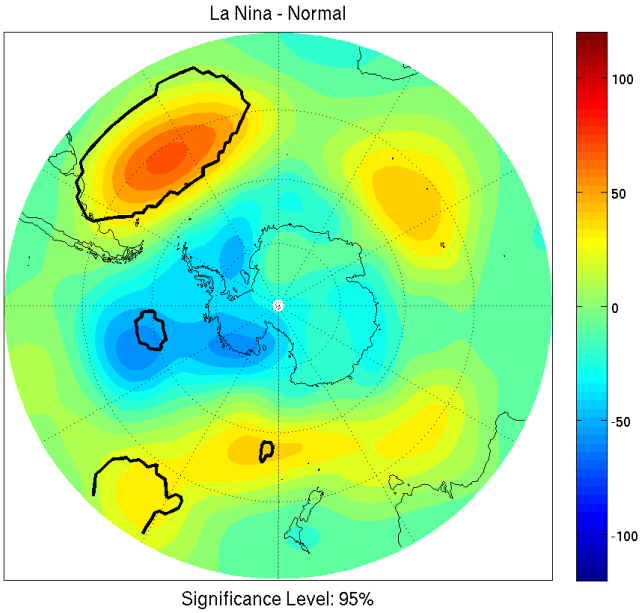

Figure 119: 500 hPa height anomalies for SOI during January of La Niña.

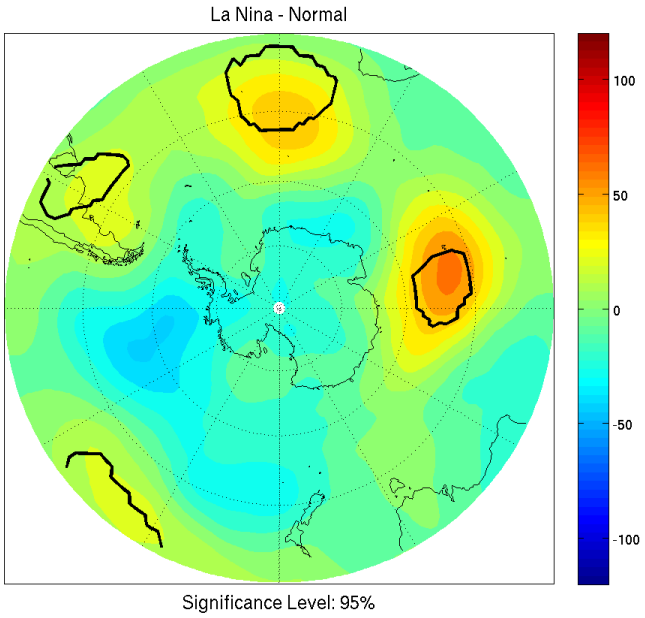

Figure 120: 500 hPa height anomalies for SOI during February of La Niña.

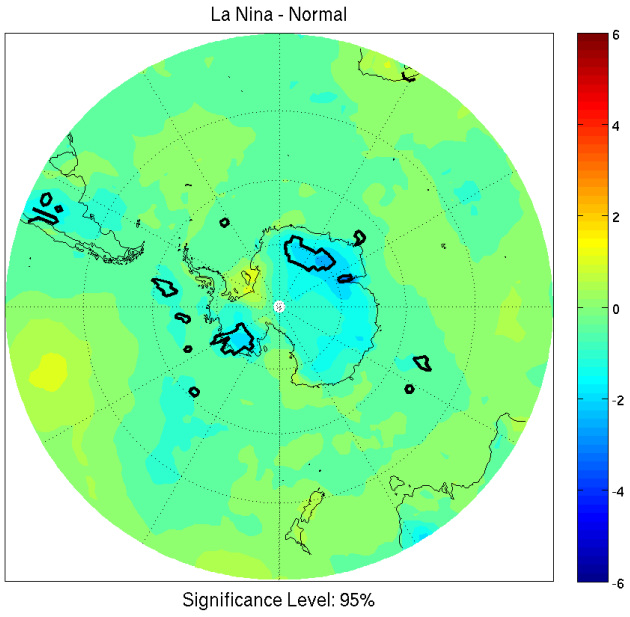

Figure 121: 2 meter temp anomalies for SOI during December of La Niña

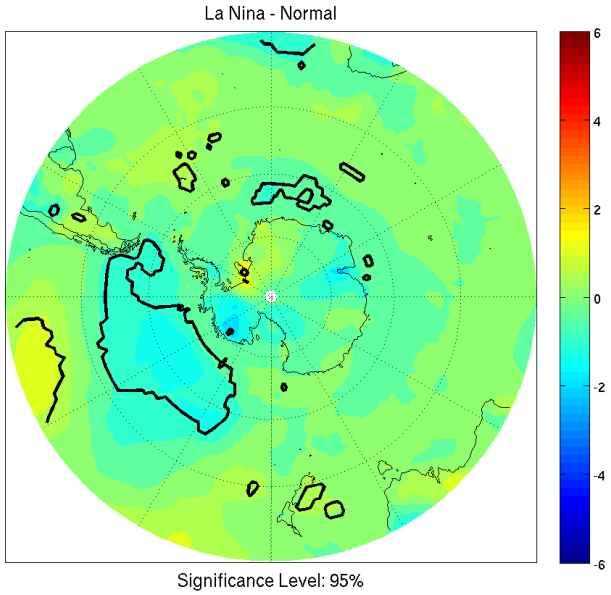

Figure 122: 2 meter temperature anomalies for SOI during January of La Niña.

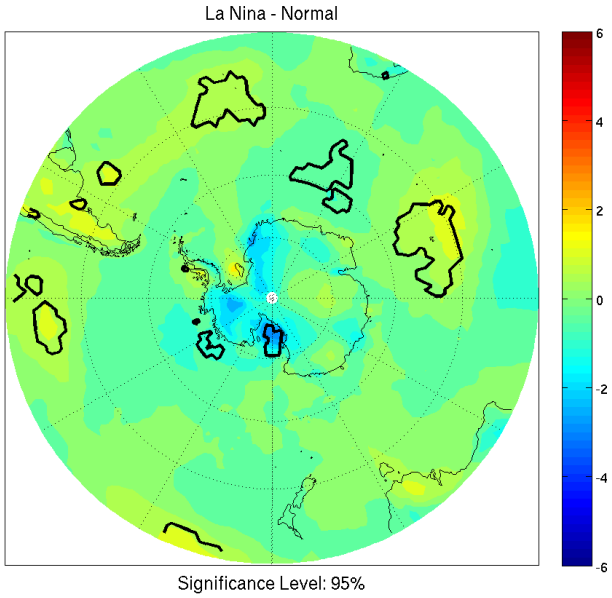

Figure 123: 2 meter temperature anomalies for SOI during February of La Niña.

5 Summary, Conclusions, and Future Work

5.1 Summary

Throughout this analysis a large amount of evidence has been presented regarding both the accuracy of the reanalysis datasets and the aspects of the ENSO signal seen in Antarctica. The reanalysis was interpolated to various points matching the location of AWS. Both the AWS and the reanalysis had their annual cycles removed through fitting three harmonics at 12, 6, and 4 month periods. Both the annual cycles and the anomalies were then compared to determine how well the reanalysis data sets captured the state and variability of the surface. This analysis was performed for surface temperatures, as well as surface pressure.

The composite analysis described a new method in which El Niño and La Niña events were compared with non-events. This method allows how the signals differ between phases of ENSO to be distinguished. Prior literature indicated the primary region of signal during austral spring and summer months would be the ABS region, with the WS region having a secondary signal (Karoly, 1989). It is also expected that austral spring would have a more robust signal than austral summer, as the signal leads by approximately a season (Jin 2008).

Throughout the analysis, austral spring does have a distinctly larger signal than austral summer for El Niño events. El Niño events also show a consistent pattern of weakened ABS low. The WS low amplification is less prevalent during El Niño events during both spring and summer months. These patterns are robust throughout all three indices analyzed as well as throughout both reanalysis datasets. That being said single month composites show considerable more difficulty achieving statistical significance, than either the two month or three month composites. This is primarily due to increased sampling bias in single month composites, which indicates two month, or three month composites are more suited for this analysis.

During La Niña events the characteristic amplification of the ABS region is present, though shifted toward the Antarctic Peninsula, during austral spring. The weakening of the WS low is also more prevalent during austral spring and summer, though this aspect of the signal varies greatly by index, and reanalysis data set analyzed. The MEI and ONI composites agreed more strongly with one another than with the SOI composites. During austral summer a distinct pattern of low heights, and cold temperatures was found throughout East Antarctica. This signal is seen

throughout all indices and reanalysis data sets, indicating a robust signal.

To compare this new method to prior compositing techniques indicates a few things. During austral spring the ABS region is well represented by the prior technique of compositing El Niño against La Niña, though El Niño accounts for more of the signal in this region during this time period. The WS region is relatively well represented. Again, the signal isn't evenly distributed between the phases, with La Niña seemingly providing slightly more of the signal. During austral summer the new method becomes more necessary, as the ABS signal is almost solely due to El Niño events, while La Niña events show a signal in East Antarctica.

5.2 Conclusions

The validation of stations confirms prior literature indicating the ERA-40 and ERA-Interim accurately capture the surface variability for temperature, particularly during the austral summer months when more data is available. Though there may remain a general warm bias that varies based on location, this is not particularly concerning for composite analysis, as the composite technique and analyzing anomalies both act to minimize this bias.

Though not shown the variability of pressure is also adequately captured according to prior validations (Lejiang 2010). According to Kållberg (2004), assimilation of AWS data ceased between 1998 and 1999. Based on correlation remaining high at all locations, and information on the ECMWF website this claim is suspect. While validation of upper level features has not been performed in this analysis. Bromwich (2004) indicates that the ERA-40 adequately captures the variability during the periods analyzed, 1979-2002.

Composite analysis has been shown to be an effective means of analyzing ENSO effects at high latitudes, and the new method of using non-events as one portion of the comparison allows for differences between different phases of ENSO to be distinguished. It is must still be acknowledged that a relatively few number of events have been analyzed due to the quality of reanalysis data prior to 1979 being in question (Bromwich 2004). Despite the small number of events, a number of conclusions can be drawn from the composite analysis performed. A number of consistent patterns became obvious throughout the analysis. First, the ABS region remains the primary location of strong teleconnection, which is to be expected. The seasonality of El Niño and La Niña events

seems to indicate that El Niño plays a larger role within this region than La Niña, though both seem to play a role in this region more strongly in spring than in summer. The WS region is generally a much weaker region during austral summer in both El Niño and La Niña events, though La Niña events seem to have a more consistent effect in the region even though there is a lack of significance. There also seems to be greater seasonal variance in the signal during La Niña events than El Niño events. This is indicated by the consistent late austral summer effect seen in East Antarctica through multiple indices, and reanalysis time periods. This East Antarctica signal warrants further exploration for mechanisms of changes in the location of teleconnections.

5.3 Future Work

This work represents an exploration of potential signals, essentially a step in finding regions of study, and it has determined at least one relatively new region of interest, specifically East Antarctica. Currently only one group of reanalysis data has been used, the ERA datasets, and it is worth exploring other reanalysis products to determine if a similar signal is seen

elsewhere. The next step will be determining potential mechanisms for the signal seen in this region. It is also worth expanding the analysis of the SOI, MEI, and ONI to both two and three month composites to determine which is ideal for this analysis method. Due to the region and timing of the signals seen, there is a potential link with the Walker Circulation, as well as various potential aspects of the Indian and Australian Monsoons that should be explored. Further investigation will also be necessary as more data becomes available, as this work includes a relatively short period of time.

6. References

Bromwich, D. H., and R. L. Fogt, 2004: Strong trends in the skill of the ERA-40 and NCEP-NCAR reanalysis in the high and middle latitudes of the Southern Hemisphere, 1958-2001. *Journal of Climate*, **17**, 4603-4619.

Diaz H., and V. Markgraf, 1992: El Niño. Historical and Palaeoclimatic Aspects of the Southern Oscillation. *Cambridge University Press:* Cambridge.

Fogt R. L., and D. H. Bromwich, 2006: Decadal Variability of the ENSO Teleconnection to the High-Latitude South Pacific Governed by Coupling with the Southern Annular Mode. *Journal of Climate*, **19**, 979-997.

Gong, D., and S. Wang, 1999: Definition of Antarctic oscillation index. *Geophysical Research Letters*, **26**, 459-462.

Kållberg, P., A. Simmons, S. Uppala, and M. Fuentes, 2004: The ERA-40 archive. *ERA-40 Project Report Series No. 17*. ECMWF.

Keller, Linda M., Lazzara, Matthew A., Thom, Jonathan E., Weidner, George A., and Stearns, Charles R., 2010: Antarctic Automatic Weather Station data for the calendar year 2009. Madison, WI, University of Wisconsin-Madison, Space Science and Engineering Center.

Harangozo, S.A., 2000: A search for ENSO teleconnections in the west Antarctic Peninsula climate in Austral winter. *International Journal of Climatology,* **20**, 663-679.

Held I. M., S. W. Lyons, and Nigam S., 1989: Transients and the extratropical response to El Niño. *Journal of the Atmospheric Sciences,* **46,** 163-174

Hoskins B. J., and D. J. Karoly, 1981: The steady linear response of a spherical atmosphere to thermal and orographic forcing. *Journal of the Atmospheric Sciences,* **38**, 1179-1196.

Houseago-Stokes R. E., and G. R. McGregor, 2000: Spatial and temporal

patterns linking southern low and high latitudes during South Pacific warm and cold events. *International Journal of Climatology*, **20**, 793-801.

Jin, D., and B. P. Kirtman. 2009: Why the Southern Hemisphere ENSO responses lead ENSO. *Journal of Geophysical Research*, **114**, D23101.

Karoly D.J. 1989: Southern Hemisphere circulation features associated with El Niño-southern oscillation events. *Journal of Climate*, **2**, 1239-1252.

Lejiang Y., Z. Zhanhai, Z. Mingyu, S. Zhong, D. Lenschow, H. Hsu, W. Huiding, and S. Bo. 2010: Validation of ECMWF and NECEP-NCAR Reanalysis Data in Antarctica. *Advances in Atmospheric Sciences*, **27**, 1151-1168.

Marshall, G. J., 2003: Trends in the Southern Annular Mode from observations and reanalysis. *Journal of Climate*, **16**, 4134-4143.

Mo, K. C., and W. Higgins, 1998: the Pacific-South American modes and tropical convection during the Southern Hemisphere winter. *Monthly Weather Review*, **126**, 1581-1596.

_____, and G. H. White, 1985: Teleconnections in the Southern Hemisphere. *Monthly Weather Review*, **113**, 22-37.

Philander S. G., and E. M. Rasmusson, 1985: The southern oscillation and El Niño. *Advances in Geophysics*, **A28**, 197-215.

Stearns, C. R., and G. Wendler, 1988: Research results from Antarctic automatic weather stations, *Review of Geophysics*, **26,** 45-61.

Thompson, D. W. J., and J. M. Wallace. 2000: Annular modes in the extratropical circulation. Part I: month-to-month variability. *Journal of Climate*, **13,** 1000-1016.

Trenberth K. E. 1975a: A quasi-biennial standing wave in the Southern Hemisphere and interrelations with sea surface temperature.
Quarterly Journal of the Royal Meteorological Society, **101,** 55–74.

_____, 1975b: Reply to comment on ‘A quasi-biennial starting wave in the Southern Hemisphere and interrelations with seasurface temperature’ by K.

E. Trenberth. *Quarterly Journal of the Royal Meteorological Society*, **101,** 174–176.

_____, 1976: Spatial and temporal variations of the southern oscillation. Quarterly Journal of the Royal Meteorological Society 102: 639–653.

Trenberth K.E., 1997: The definition of El Niño. *Bulletin of the American Meteorological Society*, *78*, 2771–2777.

Turner, J., 2004: Review: The El Niño-Southern Oscillation and Antarctica. *International Journal of climatology*, **24**, 1-31

Wolter, K., and M. S. Timlin, 1998: Measuring the strength of ENSO events - how does 1997/98 rank? *Weather*, **53**, 315-324.